Title

SEPARATION AND CHARACTERIZATION OF SUBCLASSES OF HUMAN SERUM HIGH DENSITY LIPOPROTEINS AND THEIR DETERMINATION IN A CALIFORNIA POPULATION SAMPLE

Author

Anderson, David Weston.

Publication Date

1977-05-01

UC-48
LBL-5627

SEPARATION AND CHARACTERIZATION OF SUBCLASSES OF HUMAN SERUM HIGH DENSITY LIPOPROTEINS AND THEIR DETERMINATION IN A CALIFORNIA POPULATION SAMPLE

David Weston Anderson
(Ph. D. thesis)

DONNER LABORATORY

May 1977

Prepared for the U. S. Department of Energy
under Contract W-7405-ENG-48

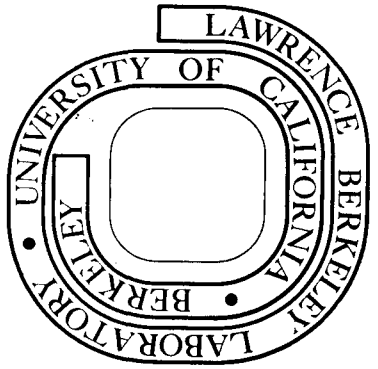

LBL-5627

DISCLAIMER

To my Mother and Father,

..... whose dream it was.

TABLE OF CONTENTS

Separation and Characterization of Subclasses of Human Serum High Density Lipoproteins and Their Determination in a California Population Sample

David Weston Anderson

Lawrence Berkeley Laboratory
University of California
Berkeley, California

ABSTRACT

Density gradient ultracentrifugation of human serum high density lipoproteins (HDL) from both normolipemic males and females resulted in a distribution of HDL concentration versus subfraction hydrated density which has three maxima. Gradient gel electrophoresis of total HDL was characterized by three banding maxima, the positions of which suggest the presence of three particle size ranges: I. 10.8-12.0 nm, II. 9.7-10.7 nm, and III. 8.5-9.6 nm. Gradient gel electrophoresis of density gradient subfractions established an inverse relationsip between particle size and particle hydrated density which was corroborated by electron microscopy and analytic ultracentrifugation. Comparison of male HDL from size ranges I, II, and III with female HDL from the same size ranges showed only small differences in the mean value of the peak $F^{\circ}_{1.20}$ rate, size, molecular weight, protein weight percent, and weight protein/weight phospholipid. Major differences between males and females were seen in the relative amounts of HDL in density gradient subfractions 1-3 (size range I material) and 11-12 (size range III material); the percent total HDL in the group of subfractions 1-3 was greatly increased

in female HDL while that of the group of subfractions 11-12 was increased in the male HDL. These studies indicated the presence of at least three major components in HDL instead of two (HDL_2 and HDL_3) and that peak $F^{\circ}_{1.20}$ rate differences in HDL schlieren patterns between males and females are a function of the relative levels of these three components.

The serum concentrations of the above three components, designated HDL_{2b}, d 1.063-1.100 g/ml; HDL_{2a}, d 1.100-1.125 g/ml; HDL_3, d 1.125-1.200 g/ml, were determined for 160 clinically-screened subjects from a normal population sample. This determination involved computer-fitting of reference schlieren patterns for each of the three components to the subjects' total HDL schlieren patterns. The mean error of fitting all three reference patterns was low (9 ± 8% (S.D.) of total area). Mean serum levels of HDL_{2b} and HDL_{2a} were significantly higher in females than in males for each of the four age decades surveyed (27-36, 37-46, 47-56 and 57-66 years). Mean HDL_3 serum levels were slightly higher in males than in females for the population as a whole. Regression of HDL_{2b}, HDL_{2a}, and HDL_3 levels on each other and on total HDL serum concentration revealed two sex-independent trends: (1) HDL_3 levels are negatively correlated ($r = -0.315$) with HDL_{2b} levels, uncorrelated with HDL_{2a} levels, and are relatively constant (mean level 158 ± 30 mg/dl (S.D.)); (2) HDL_{2b} and HDL_{2a} levels are highly correlated ($r = 0.725$) and display a progressive build up with increasing total HDL levels. Since HDL_{2b} and HDL_{2a} levels account in major part for the differences in total HDL levels observed, the present work indicates that they may be the critical HDL components determining the reported inverse correlation of HDL cholesterol with coronary heart disease.

MOTIVATION

The first part of this thesis deals with the development of methods for separation and characterization of major components of the human serum high density lipoprotein (HDL) particle distribution. Relationships between the properties of such components and the distribution of the components in fresh serum were investigated. These studies developed from an observation that small differences in the solution density during preparative ultracentrifugation of HDL gave rise to: (1) noticeable differences in the flotation rate distribution of fractions isolated at slightly different densities, (2) differences in composition of these fractions, and (3) particle size differences when the fractions are examined in the electron microscope. By pooling certain of these fractions it was possible to identify three major components of the HDL particle size distribution. It was felt that an understanding of the interrelationships among the components of the HDL particle distribution might help to explain the variation of their serum levels in males and females. Furthermore, such an understanding could shed light upon the integrated role of HDL in lipoprotein metabolism.

The identification of three major HDL components (HDL_{2b}, HDL_{2a}, and HDL_3), as developed in the initial section of the thesis, led to a second, fundamental observation. The contours of total flotation rate distributions could be accurately reconstructed by the summation of the separate contours of the HDL_{2b}, HDL_{2a}, and HDL_3 flotation rate distributions after adjusting the latter to an appropriate concentration. This observation allowed the development of a three component analysis scheme whereby the

flotation rate distributions (schlieren patterns) of HDL from 160 individuals surveyed in a normal population study were analyzed for the serum concentration of each HDL component. Statistical analysis of HDL component levels within this population sample provides the basis for a proposal describing possible metabolic interrelationships among the three HDL components.

INTRODUCTION

I. Human Serum Lipoproteins and their Role in Lipid Transport

A. Occurrence and classification

In the serum of human blood, the bulk of the macromolecular components is comprised of the lipoproteins and the serum proteins. The lipoproteins are normally spherical complexes of protein and lipid (unesterified cholesterol, cholesteryl ester, glycerides, phospholipids, low amounts of unesterified fatty acids), vary in molecular weight from approximately 200,000 to 10^{11} daltons, and total approximately 1% by weight of serum (1). Since the early 1950's, three methods of lipoprotein measurement have prevailed as accepted classification systems: (1) electrophoresis on agarose or paper defines the electrophoretic mobility, (2) preparative ultracentrifugal flotation defines the hydrated density (g/ml) range, and (3) analytic ultracentrifugal analysis defines a flotation coefficient (S_f^o or $F_{1.20}^o$)* range. Based upon these measurements, the spectrum of lipoprotein particles in normal sera is broadly classified as follows: (1) Chylomicrons - zero mobility, hydrated densities less than 0.95 g/ml, and S_f^o rates greater than 400, (2) Very low density lipoproteins (VLDL) - pre-beta mobility, hydrated densities between 0.95 and 1.006 g/ml, and S_f^o rates between 20 and 400, (3) Low density lipoproteins (LDL) - beta mobility, hydrated densities between 1.006 and 1.063 g/ml, and S_f^o rates between 0 and 20, (4) High density lipoproteins (HDL) -

*S_f^o rate refers to a low density lipoprotein migration rate in a NaCl medium of density 1.063 g/ml at 26 °C (1.748 m NaCl) and $F_{1.20}^o$ refers to a high density lipoprotein migration rate in a NaCl/NaBr medium of density 1.200 g/ml at 26 °C (0.195 m NaCl, 2.762 m NaBr)(both against the centrifugal field). Both flotation rates are expressed as svedbergs (10^{-13} cm/sec/dyne/g) and have been corrected for concentration dependence of flotation rate and the Johnston-Ogston effect.

alpha$_1$ mobility, hydrated densities between 1.063 and 1.200 g/ml, and $F^o_{1.20}$ rates between 0 and 9 (1, 2).

B. Overall structure, composition, and function

Chylomicrons and VLDL have been termed "micellar" lipoproteins by Schumaker and Adams (3). They are thought to consist of roughly spherical particles between 30 (small VLDL) and 100 nm (Chylomicrons) in diameter which are composed of a neutral lipid (triglyceride and cholesteryl ester) core enveloped by a surface monolayer of phospholipids, unesterified cholesterol, and protein. This micellar structure provides for a primary function of lipoproteins in lipid metabolism, namely the stabilization of hydrophobic triglyceride by hydrophilic surface components. The resulting particle is transportable from the site of dietary fat absorption (as chylomicrons from intestinal epithelial cells) or from the site of endogenous triglyceride synthesis (as VLDL from the liver) to peripheral tissues via the aqueous milieu of the blood. In the course of this transport both the chylomicrons and VLDL act as substrates for enzymic hydrolysis of triglyceride by several tissue-bound lipases (4, 5) into di- and monoglycerides and free fatty acids. These molecules can diffuse across the cell membrane and provide nourishment of high caloric content for storage or energy production.

Lipolysis of chylomicrons occurs rapidly in humans (half-lives are typically less than an hour (6)) and converts them into particles with electrophoretic mobilities, hydrated densities, and S^o_f rates characteristic of VLDL. The lipolysis of VLDL (of either hepatic or chylomicron origin) proceeds more slowly, however (half-lives of 2 to 4 hours), and converts them into successively smaller particles with the above-

mentioned characteristics of the larger LDL (hydrated densities of 1.006 to 1.019 g/ml - VLDL remnants). Attending this reduction in particle size and loss of core triglyceride during lipolysis is the loss of phospholipid and protein (the lipase-cofactor apoprotein C-II and non-cofactor apoprotein C-III)* primarily to particles in the HDL density range (7,8, 9). The arginine-rich and C-I apoprotein components of the chylomicron and VLDL protein moiety are lost to a lesser extent while the apoprotein B comes to represent over 90% of the VLDL remnant protein weight (compare: 5-20% in chylomicrons and 40% in VLDL)(7).

LDL and HDL have recently also been termed "micellar" lipoproteins (10,11) although it remains unclear, particularly in the case of LDL (11), whether the protein moiety resides entirely in the surface phospholipid-protein monolayer. While similar in structure, LDL and HDL are quite different in composition and function. The major LDL component (d 1.019-1.063 g/ml) is 21-25 nm in diameter (12) and is comprised of 19-23% phospholipid, 8-9% unesterified cholesterol, 36-40% cholesteryl ester, 7-12% triglyceride, and 20-25% protein by weight (13). Apoprotein B represents more than 95% of LDL protein. This LDL component is thought to be the smallest remnant of chylomicron and VLDL lipolysis (14) and its serum levels have been positively correlated with relative risk of coronary heart disease (15).

The HDL are the smallest of the lipoprotein particles (4-14 nm (12)) and are comprised of 23-25% phospholipid, 2-3% unesterified cholesterol, 15-17% cholesteryl ester, 5-8% triglyceride, and 47-55% protein

---

*In this thesis, the ABC nomenclature (12) for lipoprotein apoproteins will be used.

by weight (13). The apoproteins A-I and A-II represent 90% and arginine-rich, C-I, C-II, and C-III 10% of HDL protein (16). The composition of HDL has been described as constantly undergoing changes in the circulation (7) which may result from its role in interactions with VLDL as a "reservoir for the C apoproteins" (17) and from structural and compositional changes brought about through the action of lecithin:cholesterol acyltransferase (LCAT)(18). LCAT catalyzes the conversion of lecithin and unesterified cholesterol to cholesteryl ester and lysolecithin and requires the cofactor proteins A-I (19) or C-I (20).

The investigation into the structure, composition, and metabolic function of human serum lipoproteins constantly encounters complications due to the heterogeneity of particle size, hydrated density, and composition which characterizes their in vivo state. Yet inherent in a particular distribution of finite lipoprotein particles is information reflecting metabolism on a molecular scale. The research presented in this thesis will focus on the HDL particle distribution as it is measured in normolipemic, healthy individuals. The description of this distribution on a molecular scale will be of primary concern.

II. Quantitative Aspects of the HDL Distribution

A. HDL subclass characterization

The apparent bimodal distribution of ultracentrifugal flotation rates versus concentration for human serum HDL has long been interpreted in terms of two major HDL subclasses, HDL_2 and HDL_3. The particle hydrated density ranges for these subclasses were defined by preparative

ultracentrifugation procedures which presumably achieved the best division of the HDL flotation rate distribution into the above two components. DeLalla and Gofman (21) reported these density ranges as 1.063-1.125 g/ml for HDL_2 and 1.125-1.200 g/ml for HDL_3. Somewhat later, Lindgren (22) defined two major HDL components in terms of their associated flotation rate intervals, the $F^o_{1.20}$ 3.5-9.0 and $F^o_{1.20}$ 0-3.5 components. These correspond to but are not exactly equivalent to the HDL components, HDL_2 and HDL_3, which have generally been defined in terms of the density intervals used in their ultracentrifugal isolation. Because of these differing definitions, HDL component analysis of ultracentrifugal schlieren patterns as usually performed results in an overestimation (HDL_3) and underestimation (HDL_2) of serum concentrations of the density-defined components.

Recently Kostner and Alaupovic (23) used a density of 1.105 g/ml to achieve a separation of HDL_2 from HDL_3, but did not report analytic ultracentrifugal data describing the flotation rate intervals of these preparations. Other investigators (24,25) however, have continued to use a density of 1.125 g/ml for the separation. When HDL_2 and HDL_3 within the density ranges defined by DeLalla and Gofman (21) are investigated by equilibrium density gradient ultracentrifugation (26) and by successive ultracentrifugal flotation procedures (27), there is evidence of considerable particle density heterogeneity with both subclasses. Thus, the total HDL distribution may consist of more than two components whose characterization and quantitation might contribute to a better understanding of the role of HDL in health and disease.

B. The distribution of HDL subclass levels in populations

1. HDL subclass levels in relation to sex and age

In a study of 1961 males, ages 17-65 years, and 336 females, ages 17-65 years, DeLalla and Gofman (28) first demonstrated statistically significant positive correlations between HDL_2 and HDL_3 serum levels. In addition, their data indicated that HDL_2 levels are significantly increased (about two-fold) and HDL_3 levels slightly increased in premenopausal females as compared to males, regardless of age. Barclay et al. (29) later confirmed the higher HDL_2 levels in premenopausal females but found slightly higher HDL_3 levels in males. The work of Nichols (2) and Gofman and Tandy (15) on the Lawrence Livermore Laboratory employee population again confirmed the positive correlation between HDL_2 and HDL_3 levels and the considerable increase of female mean HDL_2 levels over corresponding male values. Results from this population (15) failed to establish an appreciable age trend for either HDL_2 or HDL_3 serum levels, although the mean levels for each showed a tendency to increase slightly with age.

2. HDL subclass levels in relation to LDL and VLDL levels

A number of studies have presented evidence that an inverse relationship exists between total HDL serum levels and LDL and, more significantly, VLDL levels (30,31). The work of DeLalla and Gofman (28) first demonstrated this effect as arising primarily from an inverse correlation between HDL_2 levels and VLDL (S_f^o 100-400 and S_f^o 20-100) or LDL (S_f^o 12-20 and S_f^o 0-12) component levels. More recently, Nichols (2) and

Gofman and Tandy (15) found the inverse relationship to hold for each of the various ranges (mean minus 1 standard deviation, mean minus 2 standard deviations, etc.) of VLDL or LDL component levels when compared to corresponding HDL_2 levels for males. Comparisons in females showed significant inverse relationships only for the VLDL components. Although a trend in these data toward a similar inverse relationship between HDL_3 levels and VLDL and LDL levels exists, it was not considered significant.

III. The HDL Distribution in Coronary Heart Disease

A. Initial studies

A significant inverse association between HDL cholesterol serum levels and coronary heart disease (CHD) was first reported by Barr et al. (32) in retrospective studies of myocardial infarction. Since then similar associations have been noted by a number of laboratories but were confined to measurement of either total HDL serum concentration or the serum concentrations of a particular compositional component of HDL (i.e. total HDL cholesterol). In a prospective study (15), Gofman and co-workers showed significantly lower HDL_2 and HDL_3 levels in cases of de novo ischemic heart disease than in the base population. Since they had shown, however, that both HDL_2 and HDL_3 are inversely correlated with levels of the low density lipoproteins, S_f^o 0-400 (see section II.B. 2. above), it was not possible to establish whether low HDL_2 and HDL_3 levels in ischemic heart disease were in excess of those anticipated from known increased VLDL and LDL levels in these cases. Although other laboratories have continued to report lower HDL levels in cases of

coronary heart disease, it is only recently that a mechanism for this effect has been proposed by Miller and Miller (33).

B. Current ideas on HDL metabolism and the development of coronary heart disease

There are at present two hypotheses to explain how HDL might exert a negative effect on the development of CHD: (1) HDL may enhance the efflux of cholesterol from vascular endothelial cells by acting as the site for its esterification by LCAT (34). The cholesteryl ester thus formed would then be transported by HDL to the liver for catabolism (33). (2) HDL may inhibit the uptake of LDL by smooth muscle cells of the arterial wall (35). The first of these hypotheses has the most support at the present time. For example, recent work by Hamilton et al. (36) in the rat suggests that the HDL are secreted by the liver as discoidal bilayer structures. As cholesterol is esterified by LCAT and collects in the hydrophobic region of these structures, the discs undergo a transition to a spherical shape (37). In patients with a congenital absence of the LCAT enzyme (38), cholesterol and phospholipid deposits tend to accumulate in certain tissue cells. Cholesteryl esters accumulate in tissue cells of the reticuloendothelial system in patients with familial HDL deficiency (Tangier's disease)(39). It is precisely such accumulations of cholesteryl esters and cholesterol which play a significant role in the pathogenesis of coronary heart disease (40). If hypothesis (1) were correct, the amount of cholesterol contained in the HDL may be an indication of the extent to which such accumulation is being retarded. Experimental support for hypothesis (2) comes principally

from tissue culture work, most of which is in progress at the present time.

C. Current studies on the epidemiology of HDL in coronary heart disease

To qualify as a (negative) risk factor, HDL levels are examined for four criteria in relation to the development of CHD (41): (1) Reproducibility, (2) Generality - demonstrable in different age-race-sex groups, (3) Independence - independent of other known risk factors, and (4) Strength - account for a substantial risk differential. In three separate studies, evidence has accumulated (42,43,44) to suggest that HDL levels do indeed qualify as a negative risk factor. In these studies, HDL levels were estimated by measuring the cholesterol content of sera after heparin-manganese precipitation of the VLDL and LDL (45). As regards criterion (4), it has yet to be established whether this cholesterol measurement provides the strongest or (criterion (1)) most reproducible measure of the inverse correlation between HDL and CHD discussed above. By more closely examining the variation of the major components of the HDL distribution with increasing HDL serum concentrations, the work presented in this thesis allows important insight into this question.

STATEMENT OF PURPOSE

These studies were undertaken to:

1) Achieve a better resolution of the heterogeneity of particle hydrated density and size present in human serum high density lipoproteins (HDL) (i.e. resolution of the major components),

2) Test the effects of ultracentrifugation, in solutions of high salt concentration (approximately 2M), on the molecular properties of HDL and to relate the particle distribution of HDL obtained via ultracentrifugation to that present in fresh serum,

3) Examine how small differences in particle hydrated density and size correlate with differences in the composition of a specific HDL component,

4) Characterize differences in the distribution of these HDL components among normolipemic men and normolipenic women,

5) Develop a method for the simultaneous measurement of the three major HDL component concentrations from total HDL analysis of ultracentrifugal schlieren patterns, and

6) Apply the method developed in 5) to the schlieren patterns of 160 males and females from a normal population survey conducted by the Stanford Heart Disease Prevention Program in Modesto, California.

MATERIALS AND METHODS

I. HDL Isolation According to Techniques Developed in Donner Laboratory

Disodium ethylene diamine tetraacetate (EDTA, 100 mg/100 ml plasma) plasma was prepared from fresh blood samples obtained from eight normolipemic subjects after an overnight fast and an essentially fat-free breakfast. The subjects* were comprised of four males and four females, all students at the University of California and between 25-34 years old. They were judged normolipemic according to their normal VLDL, LDL, and HDL serum concentrations (all lipoprotein concentrations fell within one standard deviation of the mean value of a normal population sample, i.e. 16th-84th percentile ranking) as determined by an automated agarose gel electrophoresis procedure (46). HDL (d 1.063 - 1.210 g/ml fraction) were then isolated from the plasma of each subject by sequential preparative ultracentrifugation under standard conditions (Beckman 40.3 rotor, 114,000 X g, 24 hr, 17°C, at background solution (NaBr-NaCl) densities of 1.063 and 1.210 g/ml)(47). The HDL fraction was subjected to an additional ultracentrifugation at d 1.210 g/ml to reduce possible contamination by plasma proteins. This washed HDL fraction was then dialyzed against a 0.196 m NaCl, 1.390 m NaBr solution (d_{20^oC} 1.110 g/ml) for application to Density Gradient A (see below). All salt solutions used in this study contained 0.5 g/l NaN_3, 0.06 g/l

---

*Each subject signed a consent form in accord with human use protocol of the Program Project (supported by the National Heart, Lung and Blood Institute, HL-18574-01) before the blood sample was taken.

Merthiolate (Eli Lilly Co.) and 0.1 g/l ethylene diamine tetraacetic acid (EDTA). The densities of all solutions were monitored by refractometry (47).

II. Density Gradient Ultracentrifugation Methods Developed in the Thesis Research

A. Density Gradient A: Gradient density range d 1.09 to d 1.14 g/ml

In a 0.5" × 3.5" Beckman cellulose nitrate centrifuge tube the following solutions were layered in a manner similar to the technique of Lindgren et al. (22,47): 1.37 ml of 0.196 m NaCl, 1.964 m NaBr (d_{20^oC} 1.150 g/ml); 1.37 ml 0.196 m NaCl, 1.531 m NaBr (d_{20^oC} 1.120 g/ml); 1.00 ml HDL sample in 0.196 m NaCl, 1.390 m NaBr solution (d_{20^oC} 1.110 g/ml); 1.37 ml of 0.196 m NaCl, 1.250 m NaBr (d_{20^oC} 1.100 g/ml); and 1.37 ml of 0.196 m NaCl, 0.973 m NaBr (d_{20^oC} 1.080 g/ml). The prepared gradient was spun in a Beckman 50.3 rotor for 48 hr at 50,000 rpm (178,125 × g) at 17°C. After centrifugation, the material in the gradient tube was fractionated into twelve subfractions by pipetting 0.54 ml sequentially down the tube. The subfractions were numbered 1-12 in order of their removal. Salt redistribution was monitored by refractometry and is plotted versus subfraction number in Figure 1a. Except for subfractions subjected to analytical ultracentrifugal analysis, all subfractions were immediately dialyzed to 11.3 g/l NaCl, 0.5 g/l NaN_3, 0.06 g/l Merthiolate, and 0.1 g/l EDTA adjusted to pH 8.6 and stored at 4°C.

B. Density Gradient B: Gradient density range d 1.075 to d 1.105 g/ml

In a 0.5" X 3.5" Beckman cellulose nitrate centrifuge tube the following solutions were layered in the manner described for Density Gradient A: 1.37 ml of 0.196 m NaCl, 1.390 m NaBr (d_{20^oC} 1.110 g/ml); 1.37 ml of 0.196 m NaCl, 1.250 m NaBr (d_{20^oC} 1.100 g/ml); 1.00 ml HDL sample in 0.196 m NaCl, 1.111 m NaBr solution (d_{20^oC} 1.090 g/ml); 1.37 ml of 0.196 m NaCl, 0.973 m NaBr (d_{20^oC} 1.080 g/ml); and 1.37 ml of 0.196 m NaCl, 0.702 m NaBr (d_{20^oC} 1.060 g/ml). The prepared gradient was spun in a Beckman 50.3 rotor and fractionated as described for Density Gradient A. Salt redistribution was monitored by refractometry and is plotted versus subfraction number in Figure 1b. Dialysis of subfractions was as described for Density Gradient A.

C. Density Gradient C: Gradient density range d 1.110 to 1.150 g/ml

In a 0.5" X 3.5" Beckman cellulose nitrate centrifuge tube the following solutions were layered in the manner described for Density Gradient A: 1.37 ml of 0.196 m NaCl, 1.964 m NaBr (d_{20^oC} 1.150 g/ml); 1.37 ml of 0.196 m NaCl, 1.818 m NaBr (d_{20^oC} 1.140 g/ml); 1.00 ml HDL sample in 0.196 m NaCl, 1.674 m NaBr solution (d_{20^oC} 1.130 g/ml); 1.37 ml of 0.196 m NaCl, 1.531 m NaBr (d_{20^oC} 1.120 g/ml); and 1.37 ml of 0.196 m NaCl, 1.390 m NaBr (d_{20^oC} 1.110 g/ml). The prepared gradient was spun in a Beckman 50.3 rotor and fractionated as described for Density Gradient A.

Figure 1a. Density Gradient A before and after ultracentrifugation (48 hr at 178, 125 X g and 17°C).
Note: For Density Gradients A, B, & C, each subfraction represents a volume of 0.54 ml sequentially pipetted off the meniscus.

1b. Density Gradient B before and after ultracentrifugation.

1c. Density Gradient C before and after ultracentrifugation.

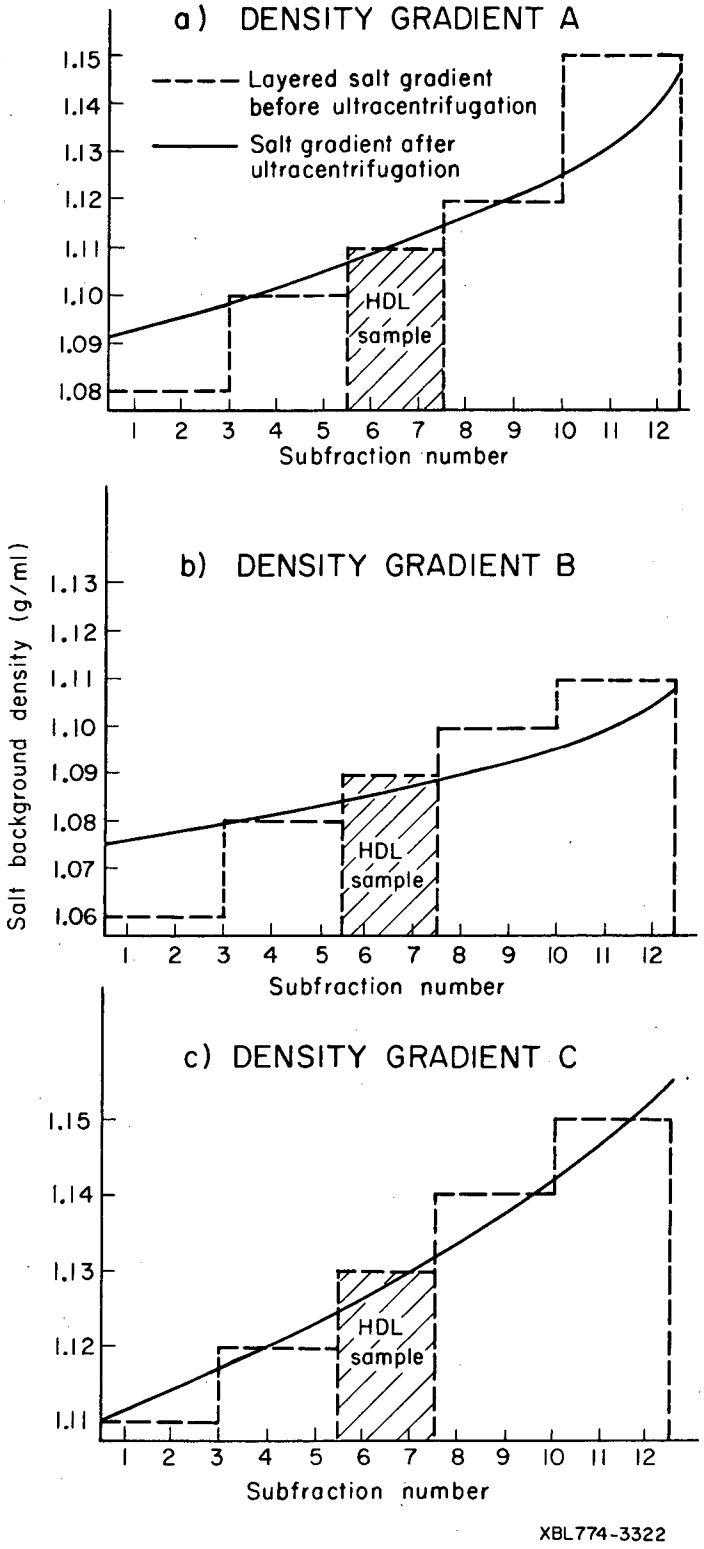

Figure 1

Salt redistribution was monitored by refractometry and is plotted versus subfraction number in Figure 1c. Dialysis of subfractions was as described for Density Gradient A.

III. Characterization of the Molecular Properties of HDL Preparations

A. Analytic ultracentrifugation

Prior to analysis all HDL density gradient subfractions were dialysed to 0.196 m NaCl, 2.762 m NaBr, 0.1 g/l EDTA (d_{26^oC} 1.200 g/ml). Analytic ultracentrifugation was then performed and the computer-derived representation of the schlieren patterns obtained by procedures (48) which corrected for the concentration dependence of $F^o_{1.20}$ rate and the Johnston-Ogston effect. The same parameter (coefficient of $F_{1.20}$ rate concentration dependence = 0.000089 $(mg/100\ ml)^{-1}$)(48) was used in calculating both corrections for all HDL subfractions since both corrections were small (2-3% of the peak $F^o_{1.20}$ rate and 2-3% of the total HDL area) at the low total HDL concentrations (200-300 mg/100 ml) employed.

Since it has been reported (49, 50, 51) that the HDL lose protein-rich lipoprotein complexes as a result of repeated ultracentrifugation in salt solutions, two experiments were designed to assess the magnitude of changes in concentration, peak flotation rate, and shape of the schlieren pattern of a given sample due to ultracentrifugal procedures used. The schlieren pattern of a total HDL preparation previously isolated by the conventional two-step centrifugation process (22) was used as a reference. In the first experiment (Figure 2b) it was found that the schlieren pattern of a pool of all subfractions, isolated via density gradient ultracentrifugation on Density Gradient A, was almost indistinguishable

Figure 2a. Schlieren patterns of subfraction 1, 6, and 12 material from Density Gradient A before and after two consecutive reflotations at d 1.210 g/ml in the preparative ultracentrifuge.

2b. Comparison between the schlieren pattern of a pool of all subfractions (1-12) isolated via density Gradient A ultracentrifugation and the schlieren pattern of the original HDL sample prior to fractionation.

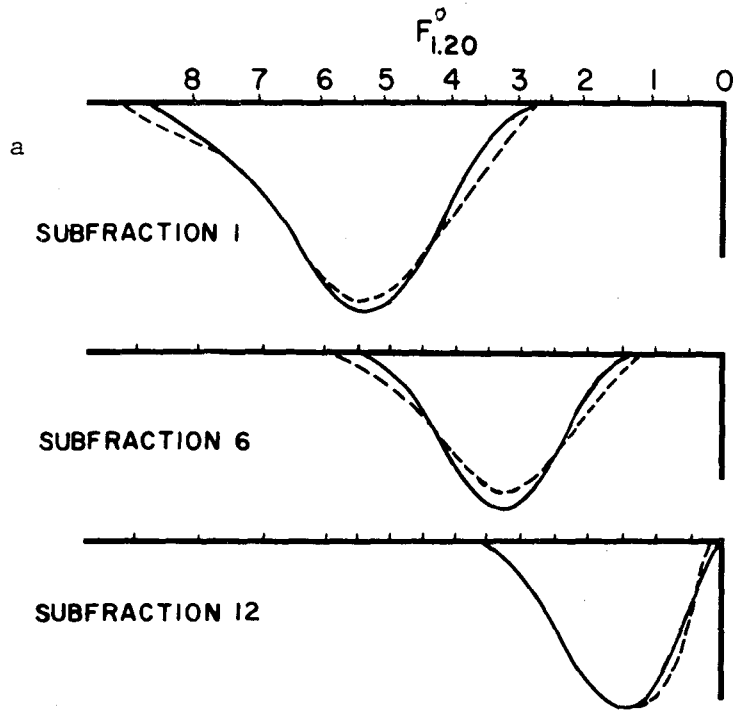

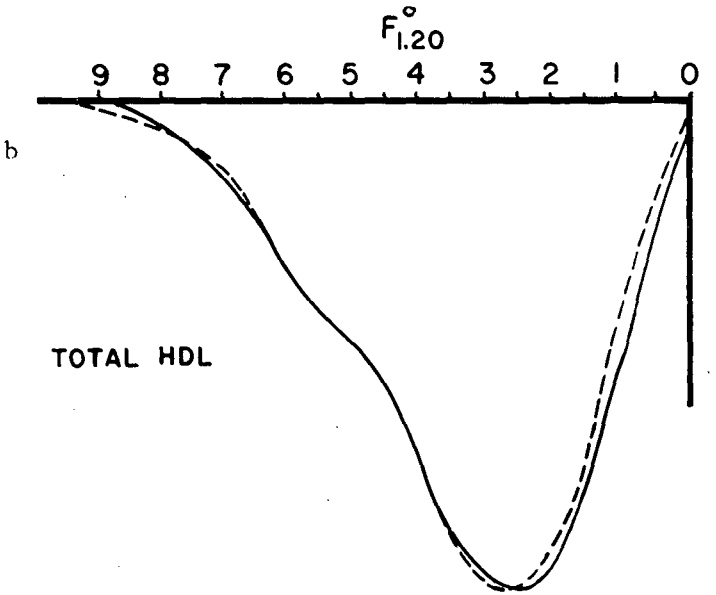

——— Corrected Schlieren Patterns of Isolated Subfractions

- - - - - - - - Corrected Schlieren Patterns of Subfractions after Two Consecutive Reflotations

	SUBFRACT. 1		SUBFRACT. 6		SUBFRACT. 12	
	Before	After	Before	After	Before	After
$F^{\circ}_{1.20}$	5.50	5.44	3.24	3.14	1.56	1.66
AREA (cm^2)	7.59	7.70	4.23	4.32	4.58	4.58

——— Corrected Schlieren Pattern of Original HDL

- - - - - - - Corrected Schlieren Pattern of Recombined Subfractions 1-12

	Original	Recombined
$F^{\circ}_{1.20}$	2.57	2.73
AREA (cm^2)	29.43	28.15

XBL774-3308

Figure 2

from that of the original sample prior to fractionation (total area: 28.15 vs 29.43 cm^2, peak flotation rate: $F^o_{1.20}$ 2.73 vs 2.57, for the subfraction pool and original sample, respectively). In a second experiment, little change was observed in the shapes and area of schlieren patterns for subfractions 1, 6, and 12 (see Materials and Methods section on Density Gradient A) after two consecutive reflotations at d 1.210 g/ml (average area loss: 4%, average peak $F^o_{1.20}$ rate shift: +0.09 svedbergs) in Figure 2a. These results indicate that if lipoprotein degradation occurs as a result of ultracentrifugation, it is minimal after the initial isolation of HDL from normolipemic subjects and of the order of the uncertainty of the measurement (±5% of area, ±0.10 svedbergs in $F^o_{1.20}$ rate) (52). Determination of lipoprotein degradation during the initial two-step ultracentrifugal isolation of HDL is complicated by the presence of the plasma proteins, and was therefore not attempted.

B. Porosity gradient electrophoresis

Gradient gel electrophoresis was carried out on a Pharmacia Electrophoresis Apparatus GE-4 loaded with four gradient gels PAA 4/30 (Pharmacia Fine Chemicals, Uppsala, Sweden). Approximately 100 µg total protein of each HDL density gradient subfraction from Density Gradient A was applied to the gel. Electrophoresis was carried out at 150 volts for 24 hr at 10°C in a Tris-borate buffer (0.09 M Tris HCl, 0.08 M borate, 0.1 g/l EDTA, 0.5 g/l NaN_3, and pH 8.35). Gels were stained with 1% Amido Schwartz (Bio-Rad, Richmond, CA.) and electrophoretically destained. Thyroglobulin (Schwarz/Mann, Orangeburg, NY.), apoferritin (Grand Island Biological Co., Grand Island, NY.), catalase (Worthington, Freehold, NJ.), human serum albumin (Pentex Inc., Kankakee, IL.), and ovalbumin

(Schwarz/Mann, Orangeburg, NY.) were used as the standard proteins with 50 µg of each protein applied to sample lanes 1 and 6 on opposite ends of the gel. The Stokes' diameter of each protein was calculated from its diffusion coefficient $D_{20,W}$ (53) according to the Stokes-Einstein relationship (54). Since migration distance of such globular proteins on a gel with a continuous linear pore-gradient is inversely proportional to the logarithm of their diameter (55), a calibration of the migration distance in terms of Stokes' diameter is possible. The migration distance was measured from the top of the gel to the middle of the stained band. A typical calibration curve of Stokes' diameter versus migration distance is shown in Figure 3. A separate calibration curve was plotted for each gel and the values of the Stokes' diameter $(d_o)_{gg}$*, for the density gradient subfractions were determined according to their migration distance. Scanning of the gels was performed on a model #2950 RFT densitometer (Transidyne Corp., Ann Arbor, MI.).

C. Electron Microscopy

HDL density gradient subfractions were dialysed against 1% ammonium acetate buffer (pH 7.4) containing 5 mg/l EDTA and diluted with the same buffer to approximately 2 mg total HDL/ml. An aliquot of diluted HDL was mixed with an equal volume of 2% sodium phosphotungstate (pH 7.4). A small droplet of lipoprotein in sodium phosphotungstate was applied to a Formvar/carbon grid and allowed to remain on the grid for 30 seconds after which time excess fluid was withdrawn with filter paper.

---

*$(d_o)_{gg}$ designates the diameter value derived from the gradient gel, in contrast to other diameter values derived from electron microscopy, $(d)_{em}$, or the Svedberg ultracentrifuge equations $(d_o)_{uc}$.

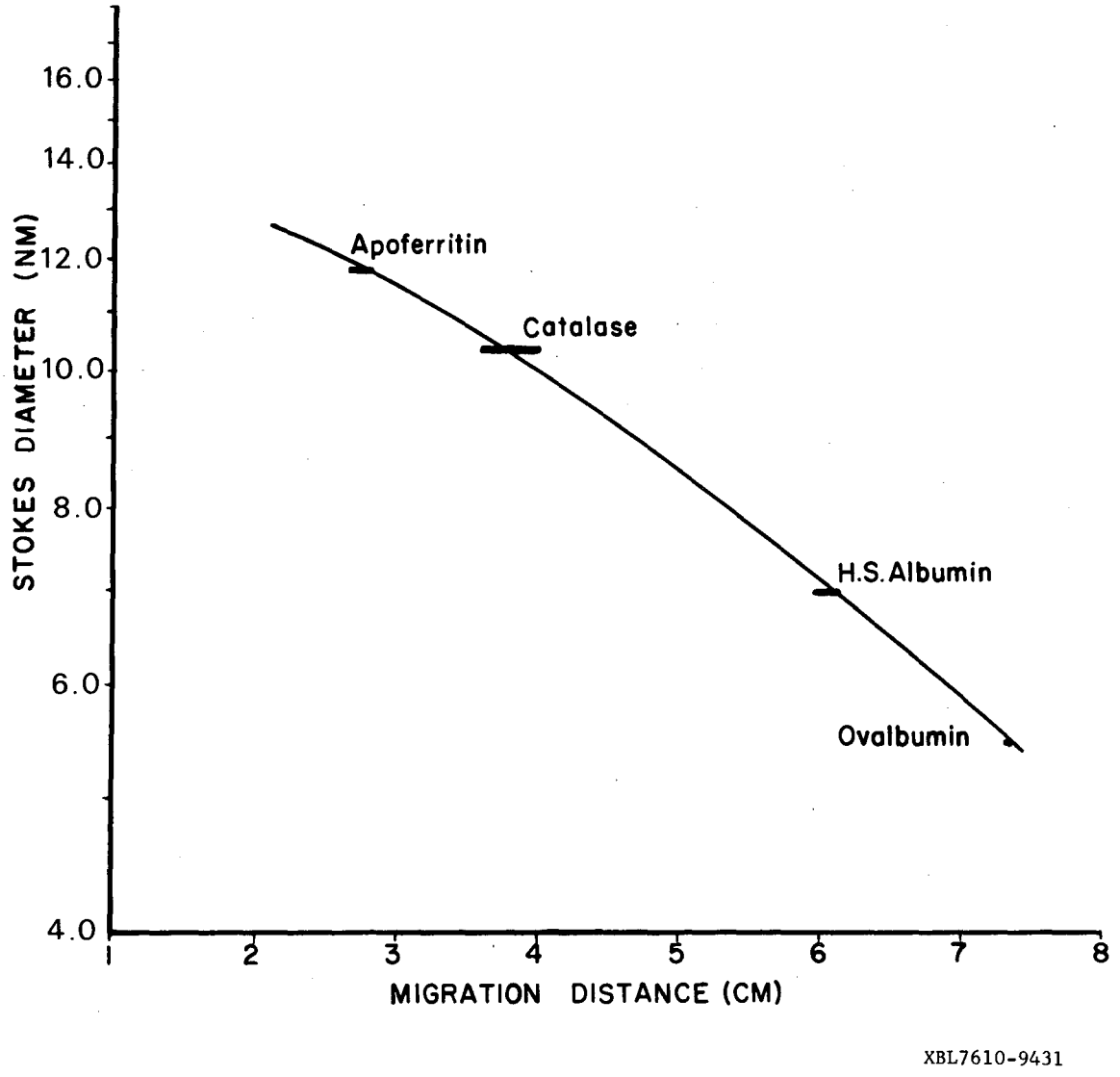

Figure 3. Representative Stokes' diameter calibration curve. The curve was fitted through the midpoint of the band widths for the standard proteins apoferritin, catalase, human serum albumin, and ovalbumin.

Grids were immediately examined in a JEM 100B (JEOLCO. Inc., Tokyo, Japan) electron microscope operating at 100 kV. Micrographs were recorded at instrument magnifications of 40,000-80,000.

IV. Characterization of the Lipid and Protein Compositions of the HDL Preparations

A. Phospholipid determination and elemental NCH analysis

The weight percent protein of a given HDL sample was calculated from N, C, and H values determined by elemental NCH analysis (56). The contribution of phospholipid N to the above values was estimated from phospholipid phosphorus values determined by the method of Barlett (57). The weight percent phospholipid was then calculated from the inorganic phosphorus value using the factor 25.

B. Triglyceride, cholesteryl ester, and unesterified cholesterol analysis

Total cholesterol, unesterified cholesterol, and triglyceride concentrations of a given HDL sample were determined in triplicate on the System 3500 Gilford Computer Directed Analyzer (Gilford Instruments, Oberlin, OH.) and were converted to weight percent values from the weight percent total lipid determined above (elemental NCH analysis). Cholesteryl ester concentrations were taken as (total cholesterol concentration minus unesterified cholesterol concentration) $\times$ 1.68. Assay methods and reagents used were: Worthington-Gilford enzymatic assay for total cholesterol (Worthington Biochemical Corp., Freehold, NJ.), Boehringer-Mannheim enzymatic assay for unesterified cholesterol (Boehringer-Mannheim, Palo Alto, CA.), and Eskalab enzymatic assay for triglyceride (Smith-Kline

Instr. Inc., Sunnyvale, CA.).

C. Estimation of total cholesterol in the supernatant fraction of serum treated with heparin-manganese from the area of the total HDL schlieren pattern.

Treatment of fresh human plasma with heparin and manganese chloride solutions (45) has been shown to quantitatively precipitate apolipoprotein B - containing lipoproteins (VLDL and LDL). The lipoprotein cholesterol remaining in the supernatant fraction after centrifugation of the precipitate has been demonstrated to be associated with the HDL. Thus, Lindgren et al. (58) have correlated the concentration of this heparin-manganese supernatant cholesterol with the serum concentration of total HDL as measured by the analytic ultracentrifugal schlieren pattern. The slope and intercept of the linear regression of total HDL concentration from the analytic ultracentrifuge on supernatant cholesterol ($r = 0.849$) were found to be: 4.684 and 78.9 mg/dl, respectively (58). This regression equation was used to estimate total heparin-manganese supernatant cholesterol values from total HDL concentration values as determined by the analytic ultracentrifugal schlieren patterns of various cases in the Modesto Study (see RESULTS section III.E.).

V. Quantitative Analysis of Three HDL Components from Total HDL Schlieren Patterns

A. The three component approach to HDL schlieren pattern analysis

In the analysis scheme outlined below, standard total HDL ultracentrifugal schlieren patterns are analyzed as a summation of three separate HDL_{2b} (HDL from size range I), HDL_{2a} (HDL from size range II), and

HDL_3 (HDL from size range III) reference schlieren patterns after adjustment of each to an appropriate concentration. In particular, the total HDL schlieren patterns of 160 subjects, ages 27-66 years, surveyed in a normal population study (Modesto Study) conducted in Modesto, California by Lindgren et al. (59) were analyzed. In this study a random subpopulation of 20 subjects in each decade of each sex was selected from 774 clinically screened normal volunteers. All schlieren patterns in this thesis were obtained by procedures (48) which corrected for the concentration dependence of $F^o_{1.20}$ rate and the Johnston-Ogston effect. Final computer-derived patterns were plotted in terms of 173 heights, which are represented by the array of heights, $[H_i]$, $i = 1,2,\ldots,173$, at corresponding values of $F^o_{1.20}$ rates, which are represented by the array of $F^o_{1.20}$ rates $[F_i]$, $i = 1,2,\ldots,173$ (Figure 4b). This representation of the corrected schlieren pattern in terms of 173 heights along the $F^o_{1.20}$ rate scale is employed in this thesis to describe the operations involved in the three component analysis. A description of the reference HDL_{2b}, HDL_{2a}, and HDL_3 schlieren patterns and their application to the three component analysis of the total HDL pattern follows.

B. Reference HDL_{2b}, HDL_{2a}, and HDL_3 schlieren patterns

Reference schlieren patterns of the HDL_{2b}, HDL_{2a}, and HDL_3 components are used in the present analysis to reconstruct the standard total HDL pattern. The reference patterns are the mean corrected schlieren patterns obtained by separately averaging the HDL_{2b}, HDL_{2a}, and HDL_3 patterns from the four normolipemic males and four normolipemic females (see RESULTS section III.A.), and are shown in Figure 5. The reference

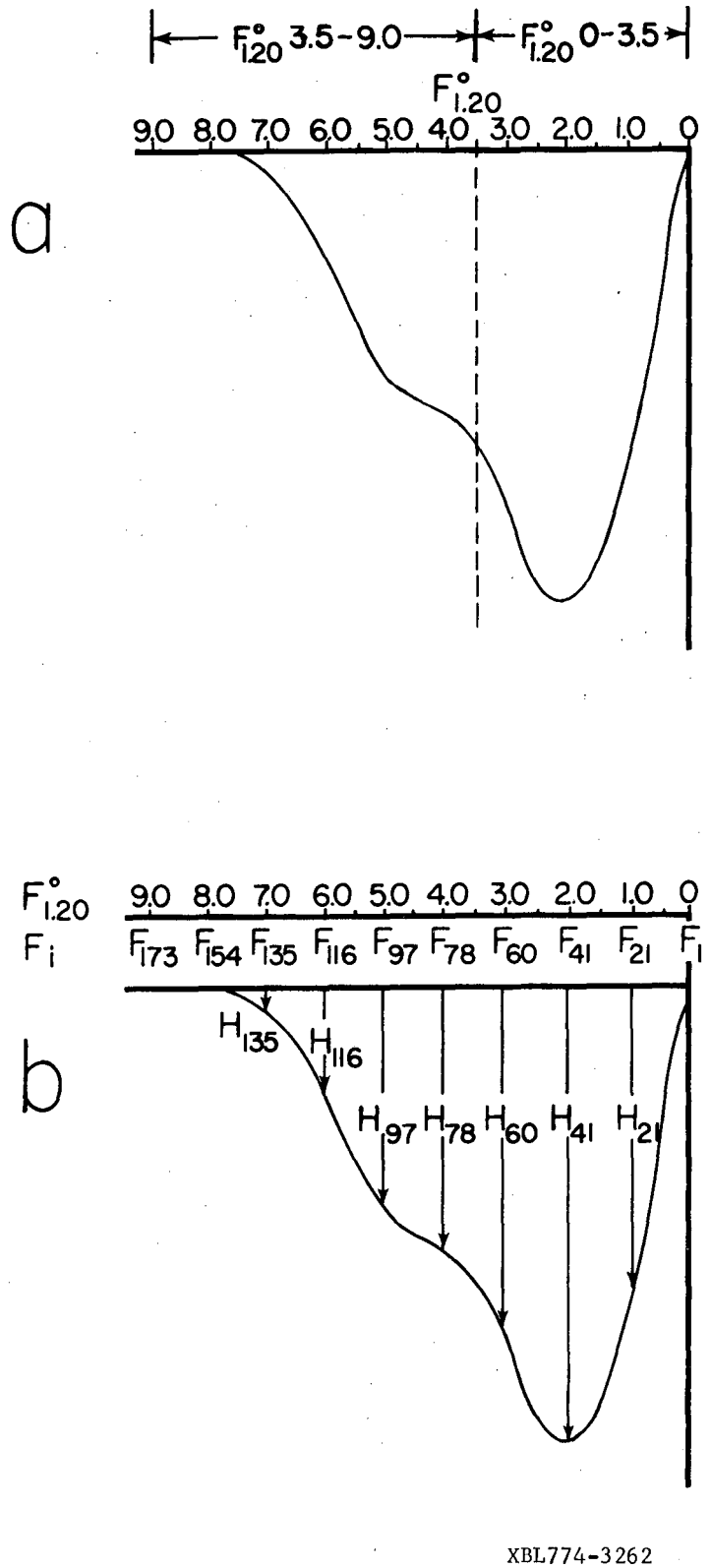

XBL774-3262

Figure 4a. Representation of a total HDL schlieren pattern and indication of $F^{\circ}_{1.20}$ 3.5-9.0 and $F^{\circ}_{1.20}$ 0-3.5 components.

4b. Representation of a total HDL schlieren pattern as an array of heights, $[H_i]$, i=1,2,...,173 at corresponding $F^{\circ}_{1.20}$ rates, $[F_i]$, i=1,2,...,173.

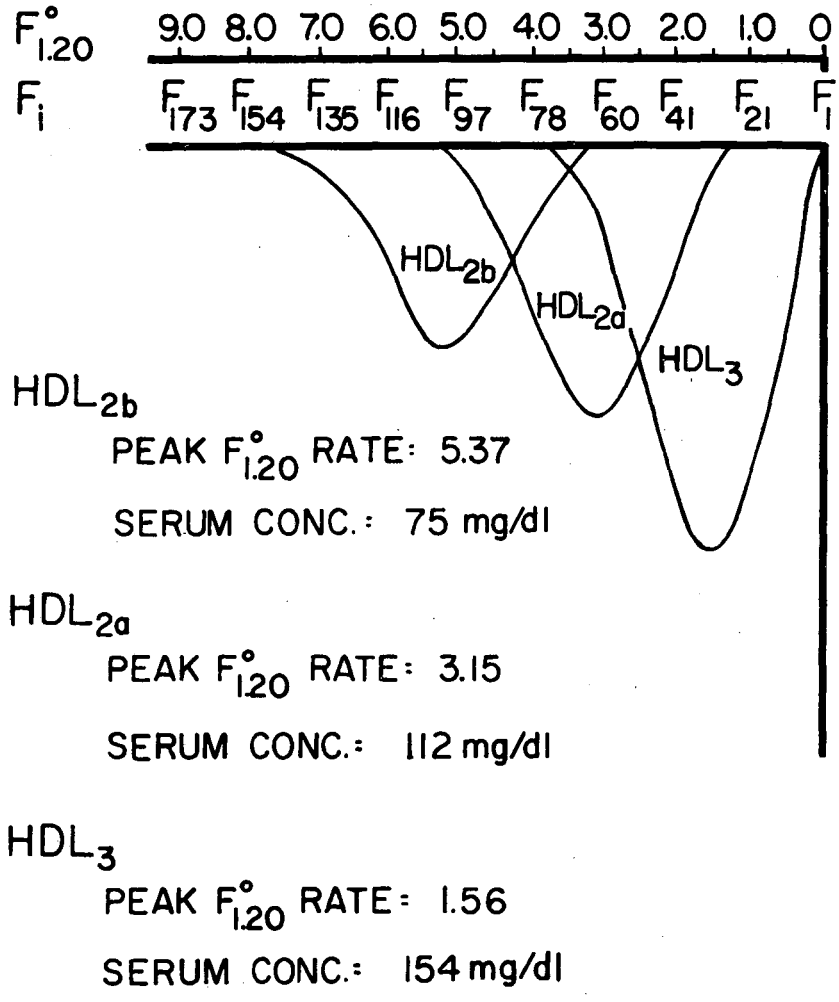

XBL774-3261

Figure 5. HDL_{2b}, HDL_{2a}, and HDL_3 reference schlieren patterns. Each pattern is the mean of corresponding component patterns from four normolipemic males and four normolipemic females.

patterns in Figure 5 represent the average of the serum concentrations of the three components from the four males and four females.

C. Quantitative analysis of total HDL schlieren patterns from the Modesto Study in terms of three components

The design of this analysis is to successively fit the contours of each of the three reference patterns to that of the total HDL pattern. The successive fitting procedure is based on the fact that in a system of more than one component undergoing ultracentrifugal flotation, the contour of the corrected schlieren pattern will be the sum of the contours of the component corrected patterns. In Figure 6 a description of the analysis scheme is given. The first step is to fit the HDL_3 reference pattern to the total HDL pattern. This is done by determining the factor f_3 (see Figure 6 Legend, Step 3), by which every HDL_3 reference pattern height, $(h_i)_3$, in the $F^o_{1.20}$ rate interval 0.50-1.30*, is multiplied to equal the corresponding total HDL pattern height, $(H_i)_T$ in that interval. This particular $F^o_{1.20}$ rate interval (0.50-1.30) is chosen in order to fit the HDL_3 reference pattern to the interval of the total HDL pattern where there are no contributions from the HDL_{2b} or HDL_{2a} reference patterns (both HDL_{2b} and HDL_{2a} have higher flotation rates). Each of the 173 heights of the HDL_3 reference pattern are then multiplied by f_3 to generate an HDL_3 pattern fitted to the total HDL pattern. This fitted pattern is designated by the expression $f_3 \cdot [h_i]_3$ (see Figure 6b). Since both the initial total HDL pattern and the reference

---

*The $F^o_{1.20}$ rates 0.50 and 1.30 correspond to F_{12} and F_{27}, respectively.

THREE COMPONENT ANALYSIS SCHEME

Step 1: a) The corrected schlieren pattern of total HDL is divided into 173 values of the ordinate height. This pattern can then be represented by the array of heights $[H_i]_T$ paired with corresponding values of the $F^{\circ}_{1.20}$ rate scale, $[F_i]$, i = 1,2, . . , 173 (see Figure 3a).
b) The reference corrected schlieren patterns of the three HDL components are likewise divided into 173 values of the ordinate height. These patterns can then be represented by the arrays of heights: $[h_i]_{2b}$, $[h_i]_{2a}$, and $[h_i]_3$ paired with corresponding values of the $F^{\circ}_{1.20}$ rate scale, $[F_i]$, i = 1,2, . . , 173.

NOTE: The corrected schlieren patterns in both a) and b) are obtained by the method of Ewing et al. (1).

Step 2: The fitting factor, f_3, for the component HDL_3 is computed (Figure 3b):

$$f_3 = \frac{\left(\sum_{j=a}^{b} (H_j)_T/(h_j)_3\right)}{(b - a + 1)}$$

where b = 27, a = 12 as seen from Figure 3b.

Step 3: The reference schlieren pattern of HDL_3, $[h_i]_3$, is fitted to the total pattern, $[H_i]_T$, to yield the fitted HDL_3 pattern, $f_3 \cdot [h_i]_3$ (Figure 3b): $f_3 \cdot [h_i]_3 = f_3 \cdot (h_i)_3$ for all i = 1,2, . . , 173.

Step 4: The fitted HDL_3 pattern, $f_3 \cdot [h_i]_3$, is subtracted from the total HDL pattern, $[H_i]_T$, to yield a difference pattern, $[H_i]_T - f_3 \cdot [h_i]_3$ (Figure 3c):
$[H_i]_T - f_3 \cdot [h_i]_3 = (H_i)_T - f_3 \cdot (h_i)_3$ for all i = 1,2, . . , 173.

Step 5: The fitting factor, f_{2a}, for the component HDL_{2a} is computed:

$$f_{2a} = \frac{\left(\sum_{j=a}^{b} \frac{(H_j)_T - f_3 \cdot (h_j)_3}{(h_j)_{2a}}\right)}{(b - a + 1)}$$

where b = 60, a = 28 as seen from Figure 3c.

Step 6: The reference schlieren pattern of HDL_{2a}, $[h_i]_{2a}$, is fitted to the difference pattern $[H_i]_T - f_3[h_i]_3$ to yield the fitted HDL_{2a} pattern, $f_{2a} \cdot [h_i]_{2a}$ (Figure 3c):
$f_{2a} \cdot [h_i]_{2a} = f_{2a} \cdot (h_i)_{2a}$ for all i = 1,2, . . , 173.

Step 7: The fitted HDL_{2a} pattern, $f_{2a} \cdot [h_i]_{2a}$ is subtracted from the difference pattern, $[H_i]_T - f_3 \cdot [h_i]_3$ to yield a second difference pattern, $[H_i]_T - f_3 \cdot [h_i]_3 - f_{2a} \cdot [h_i]_{2a}$ (Figure 3d).

Step 8: The serum concentrations of HDL_{2b}, HDL_{2a}, and HDL_3 are calculated from their respective fitted patterns as:

$$\text{Conc. } HDL_{2b} = A \cdot \Delta F \cdot \sum_{i=60}^{173} (H_i)_T - f_3 \cdot (h_i)_3 - f_{2a} \cdot (h_i)_{2a}, \quad \text{Conc. } HDL_{2a} = A \cdot \Delta F \cdot \sum_{i=1}^{173} f_{2a} \cdot (h_i)_{2a},$$

$$\text{and Conc. } HDL_3 = \sum_{i=1}^{173} f_3 \cdot (h_i)_3.$$

where A = High density lipoprotein concentration/schlieren pattern area and ΔF = 0.05 cm.

XBL 774-8328

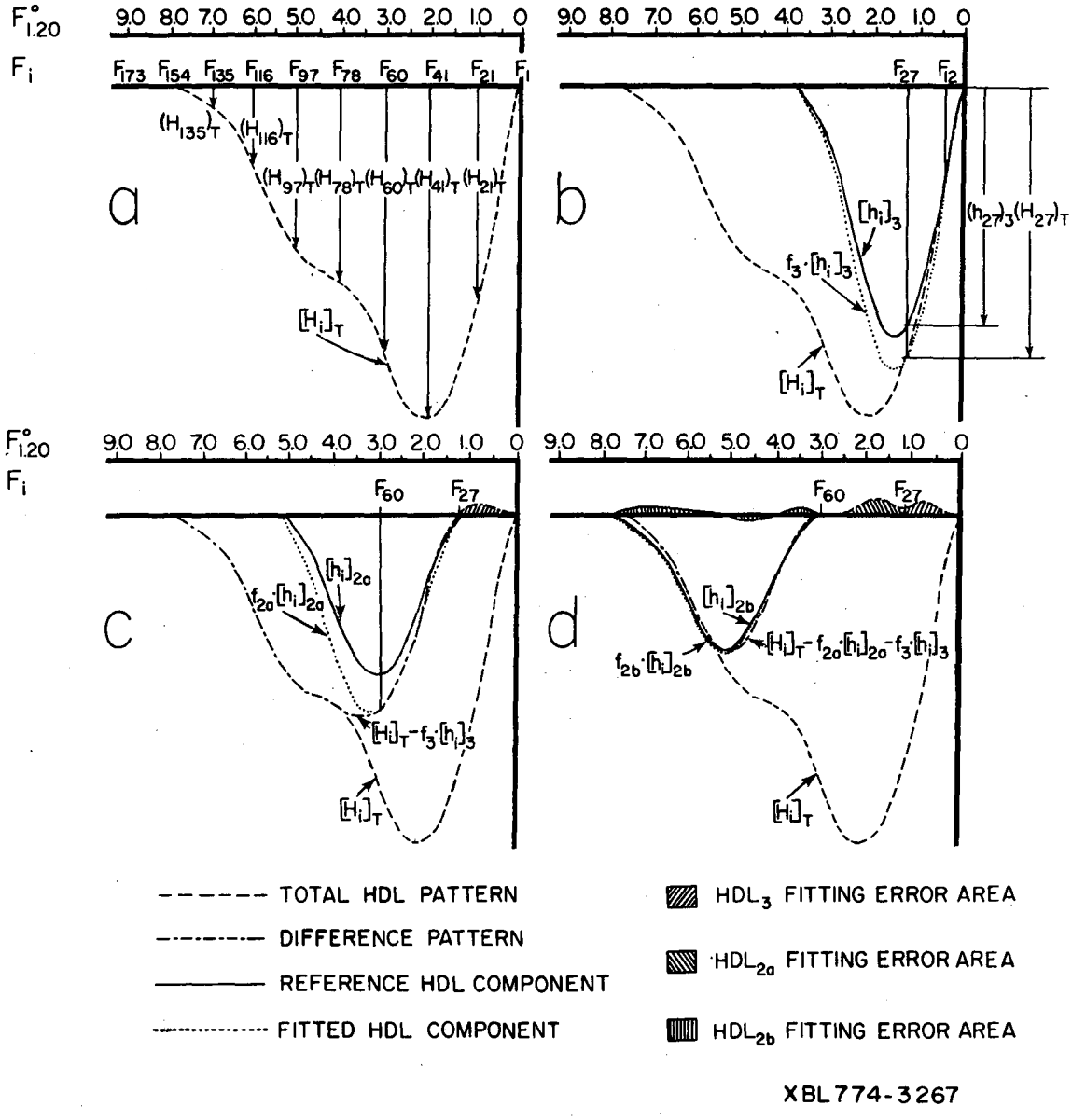

Figure 6

HDL component patterns have been corrected to standard conditions, as described above, their contours are not differentially distorted as a function of lipoprotein concentration. Thus, the multiplication of all 173 heights of a reference HDL component pattern by a single factor to adjust its area to represent a higher or lower serum concentration is justified.

The fitted HDL_3 pattern, $f_3 \cdot [h_i]_3$, is then subtracted from the total HDL pattern, designated as the array $[H_i]_T$, to yield a difference pattern, $([H_i]_T - f_3 \cdot [h_i]_3)$ (Figure 6c). In practice, each of the heights of the fitted HDL_3 pattern is generally not exactly equal to heights at corresponding $F^o_{1.20}$ rate values of the initial total HDL pattern in the $F^o_{1.20}$ 0-1.30 interval. Hence, subtraction of the fitted HDL_3 pattern from the total HDL pattern yields a positive or negative difference which can be used as a measure of the error of fit.

The reference HDL_{2a} pattern, $[h_i]_{2a}$, is then fitted to the difference pattern $([H_i]_T - f_3 \cdot [h_i]_3)$ between the flotation rates $F^o_{1.20}$ 1.35 - 3.00* in the manner described above (see Figure 6 Legend, Step 5). The $F^o_{1.20}$ rate interval (1.35 - 3.00) is chosen in order to fit the HDL_{2a} reference pattern to the interval of the total HDL pattern where there are no contributions from the HDL_{2b} reference pattern (HDL_{2b} has higher flotation rates and the fitted HDL_3 pattern has already been subtracted). This yields the fitted HDL_{2a} pattern designated by the array $f_{2a} \cdot [h_i]_{2a}$ (Figure 6c). The fitted HDL_{2a} pattern is then subtracted from the difference pattern $([H_i]_T - f_3 \cdot [h_i]_3)$ to yield a second difference pattern

---

*The $F^o_{1.20}$ rates 1.35 and 3.00 correspond to F_{28} and F_{60}, respectively.

$([H_i]_T - f_3 \cdot [h_i]_3 - f_{2a} \cdot [h_i]_{2a})$ (Figure 6d). As in the fitting of the HDL_3 pattern, the fitted HDL_{2a} pattern heights will not be exactly equal to the corresponding heights of the difference pattern $([H_i]_T - f_3 \cdot [h_i]_3)$ in the $F^o_{1.20}$ 1.35-3.00 interval and a fitting error (positive or negative area) can be determined from the differences. For the case given in Figure 6d, overfitting occurred and is seen as a negative area in the interval $F^o_{1.20}$ 1.35 - 3.00.

The reference HDL_{2b} pattern, $[h_i]_{2b}$, can now be fitted to the second difference pattern $([H_i]_T - f_3 \cdot [h_i]_3 - f_{2a} \cdot [h_i]_{2a})$, between the flotation rates $F^o_{1.20}$ 3.05 - 5.00* in the same manner as described above (see Figure 6 Legend, Step 8). This yields the fitted HDL_{2b} pattern, designated by the array $f_{2b} \cdot [h_i]_{2b}$ (Figure 6d). Subtracting the fitted HDL_{2b} pattern from the second difference pattern then gives the fitting error for the interval $F^o_{1.20}$ 3.50 - 9.00. At this point, the analysis has been completed and the serum concentrations of each component (HDL_{2b}, HDL_{2a}, and HDL_3) are given by the values of their fitted schlieren patterns. In view of the near identity in most samples between the second difference pattern, $([H_i]_T - f_3 \cdot [h_i]_3 - f_{2a} \cdot [h_i]_{2a})$, and the adjusted HDL_{2b} pattern, $f_{2b} \cdot [h_i]_{2b}$, (Figure 6d), the area under the second difference pattern can be usually taken to represent the serum concentration of the HDL_{2b} component without detailed fitting of the reference HDL_{2b} component pattern. In cases where the HDL_{2b} serum levels are approximately 150 mg/dl or greater, however, the reference HDL_{2b} pattern consistently underfits the

---

*The $F^o_{1.20}$ rates 3.05 and 5.00 correspond to F_{61} and F_{97}, respectively.

the second difference pattern (Figure 7). The positive error area generated increases with increasing HDL_{2b} concentration and will be discussed in the RESULTS section III.B.1.

VI. Statistical Analysis of the Modesto Study Data

A. Second and third degree polynomial regression analysis

Second and third degree polynomial regression analysis of the various regressions performed in the RESULTS section was carried out according to Williams (60). The multiple correlation coefficient was calculated and significance levels estimated from the F values of the polynomial fit to the data.

B. Comparison between mean levels of the various HDL components

The HDL_{2b}, HDL_{2a}, and HDL_3 components for the eighty male and eighty female subjects in the Modesto Study were compared under the assumption that the HDL_{2b}, HDL_{2a}, and HDL_3 values have a multivariate normal distribution with the same unknown covariance matrix.* A test was made of the hypothesis that the two sexes have a common mean vector, i.e., that they arose from the same population. The two sample T^2 statistic had the value 100.772; the associate F was 33.165, with degrees of freedom 3 and 156, respectively. Under the hypothesis of equal mean vector, the probability of exceeding such an F value would be less than 0.005, and there-

---

*It had been shown previously by Ito and Schull (61) that if the sample sizes are equal, the presence of unequal covariance matrices have no effect upon the size of the type 1 error probability or the power function if the sample sizes are large.

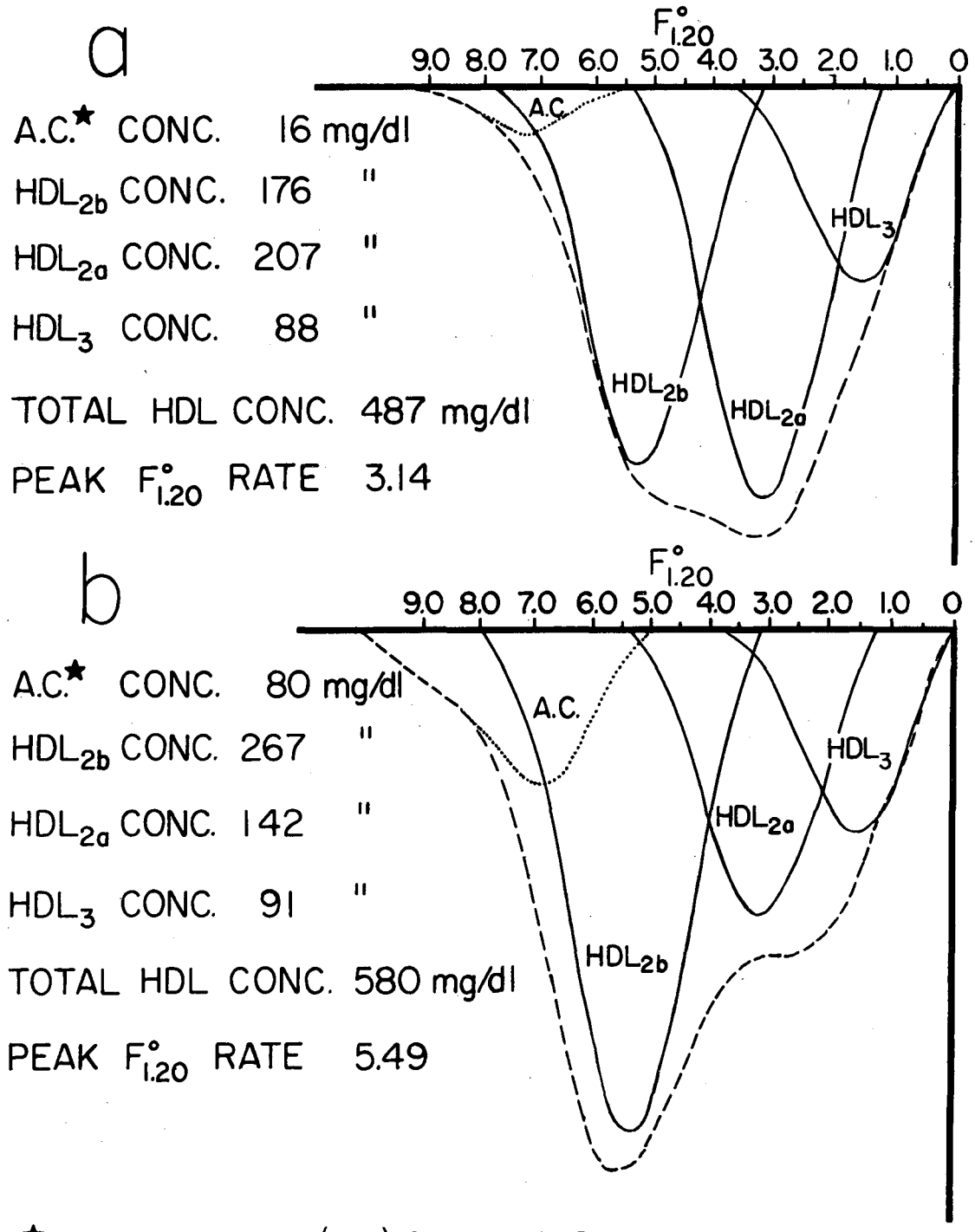

XBL774-3263

Figure 7a. Mean schlieren pattern (two female and two male cases) representative of Modesto Study cases with total HDL concentrations greater than 475 mg/dl.

7b. Total HDL schlieren pattern from subject with highest concentration in Modesto Study of additional components (A.C.) not fitted by the reference HDL_{2b} pattern.

fore we could reject the null hypothesis at the 5% level.

The simultaneous confidence intervals were then used to determine which individual HDL component means were significantly different. The critical value for the confidence intervals with joint confidence coefficient 0.95, obtained from linear interpolation between the reciprocals of the degrees of freedom 150 and 200, was found to be 2.67. The confidence intervals for the difference in the HDL_{2b}, HDL_{2a}, and HDL_3 means of the male and female populations are:

$$HDL_{2b}: \quad -85.25 \leq \mu_{11} - \mu_{12} \leq -36.74$$
$$HDL_{2a}: \quad -87.22 \leq \mu_{21} - \mu_{22} \leq -46.70$$
$$HDL_3: \quad 0.15 \leq \mu_{31} - \mu_{32} \leq 26.74 .$$

Since zero is not included in each of the intervals, it can be concluded that at the 5% joint significance level, all mean values for the three male and female HDL component levels are different.

The critical value for the confidence intervals with a joint confidence coefficient of 0.99 was found to be 3.91. The confidence intervals for the difference in the HDL_{2b}, HDL_{2a}, and HDL_3 means of the eighty males and eighty females from the Modesto population are:

$$HDL_{2b}: \quad -79.56 \leq \mu_{11} - \mu_{12} \leq -42.43$$
$$HDL_{2a}: \quad -82.47 \leq \mu_{21} - \mu_{22} \leq -51.45$$
$$HDL_3: \quad 3.27 \leq \mu_{31} - \mu_{32} \leq 23.62 .$$

The 99% simulataneous confidence intervals indicate that HDL_{2b} and HDL_{2a} mean serum levels are different between the eighty females and eighty males while the HDL_3 mean serum levels are not.

RESULTS

I. Evidence for Three Major Subspecies in the HDL Particle Distribution

A. HDL mass distribution on the density gradient

Figure 8a shows the distributions of percent total HDL mass versus subfraction number on the Density Gradient A for HDL samples of three separate subjects. These distributions are representative of the types of percent total mass profiles encountered in the eight subjects studied. Each of the samples shows to a greater or lesser extent the presence of three maxima, at subfraction numbers 1, 6-8, and 12. HDL obtained from female subjects (e.g., subjects A and B) typically showed elevated mass percent values in subfractions 1-3 compared to HDL from male subjects (e.g., subject C). On the other hand, HDL from male subjects generally showed higher mass percent values for subfractions 6-8 and 11-12 as well as better resolution of the maxima associated with these subfractions. In HDL samples where these maxima were not optimally resolved, such as from subject B, it was possible to obtain a greater resolution of these maxima by recentrifugation (178,125 X g, 48 hr) on a separate Density Gradient C (Figure 8b). By analytic ultracentrifugation, the peak $F^{o}_{1.20}$ rates, as defined by the $F^{o}_{1.20}$ which corresponds to the maximum ordinate of the corrected schlieren pattern, of subfractions 1 (3.20) and 12 (1.60) from sample B on the Density Gradient C (Figure 8b) were shown to be similar to those of subfractions 7 (3.01) and 12 (1.56) from sample B on the Density Gradient A (Figure 8a). These results strongly support the

Figure 8a. Distribution of percent recovered HDL mass versus subfraction number before (---) and after density gradient ultracentrifugation for sample A (••••••), sample B (——), and sample C (-•-•-). Recovery, as measured by NCH elemental analysis, was typically 95%. HDL samples A and B were obtained from two of the four female subjects and sample C from one of the four male subjects; see text for details.

8b. Distribution of percent recovered HDL mass versus subfraction number before (---) and after (——) density gradient ultracentrifugation. This HDL sample was a pool of subfractions 6-12 from sample B as described in Figure 8a.

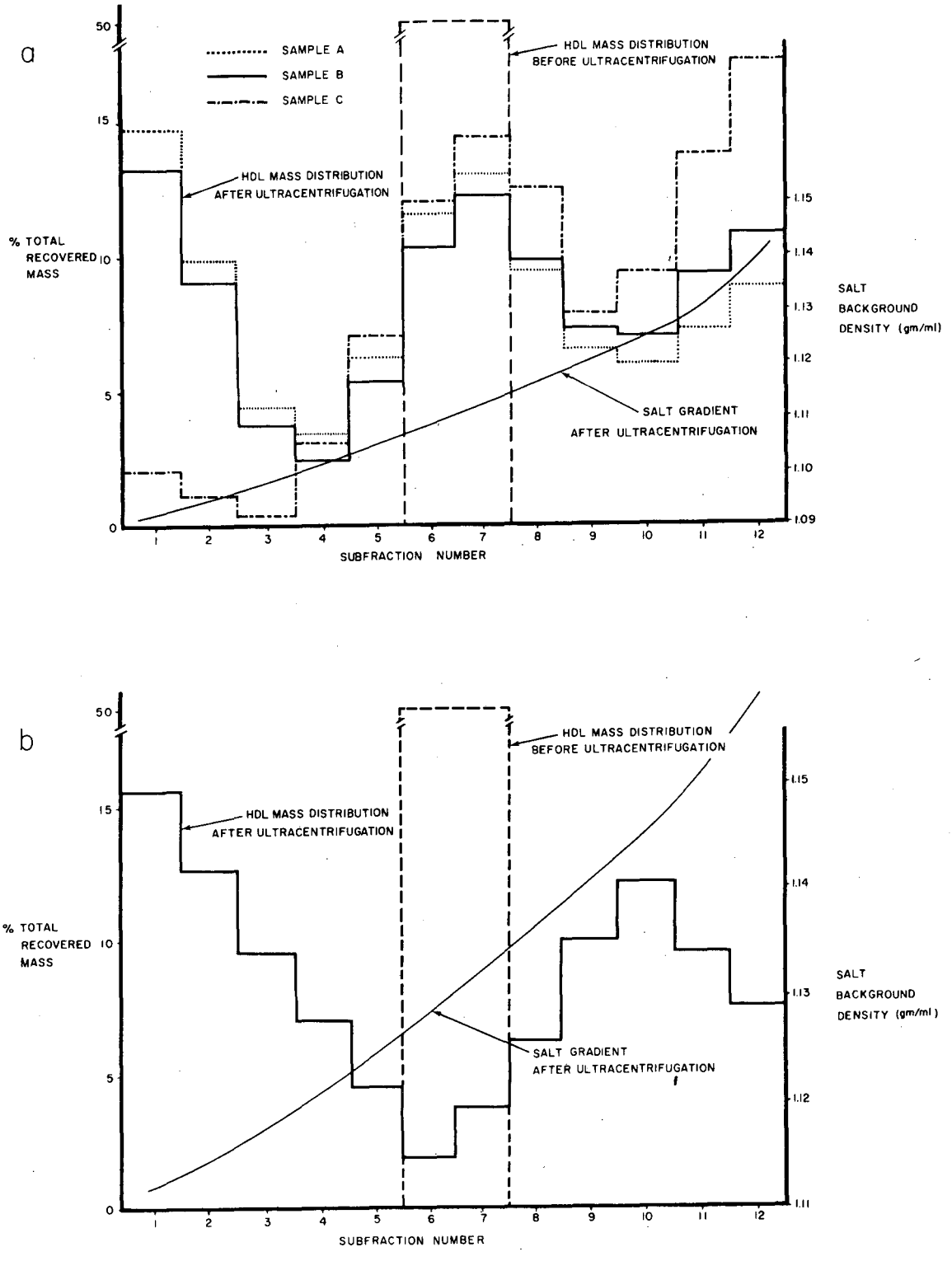

XBL774-3306

Figure 8

interpretation of the two apparent maxima of sample B at subfractions 6-8 and 12 (Figure 8a) as actual maxima of the percent mass versus solution density distribution. The three distributions in Figure 8a, obtained after 48 hr of ultracentrifugation, remained essentially unchanged when the same sample was spun for 54 hr or 60 hr. Hence, except for material at the meniscus and the bottom of the tube, the hydrated density (σ) of each lipoprotein subfraction may be considered equal to its banding position density. The values of σ for subfractions 1 and 12 were determined by recentrifugation (178,125 X g, 48 hr) on Density Gradient B and Density Gradient C, respectively, where each subfraction gave one band near the middle of the tube. The corresponding banding position density was taken as the value of σ (Figure 8a). The value of σ for HDL in NaBr solutions used in forming the density gradients (0.702 - 1.964 m NaBr) is probably slightly smaller (expected variance 1-2%)(62) than the value found in physiological saline (0.186 m NaCl).

B. Gradient gel electrophoresis

Gradient gel electrophoresis of the total HDL sample B described in Figure 8 demonstrates considerable size heterogeneity (Figure 9) with Stokes' diameter $(d_o)_{gg}$ values ranging from 8.5 to 12.0 nm. Densitometric scans of the gradient gels of this sample as well as samples of total HDL from each of the three female and four male subjects studied indicated three definite maxima. The size ranges spanned by these banding regions were approximately 10.8 to 12.0 nm, 9.7 to 10.7 nm, and 8.5 to 9.6 nm. These ranges are designated as size ranges I, II,

Figure 9. Gradient gel electrophoresis of the total HDL sample and of subfractions isolated from it via density gradient ultracentrifugation. Upper: Gradient gel electrophoresis of subfractions: a composite photograph of the stained bands of the total HDL sample and the density gradient subfractions. Lower: Densitometry of gradient gel electrophoretograms: the densitometric scan profiles of the original HDL sample and the density gradient subfraction bands on the gradient gel (Upper). In the upper photograph, the total HDL sample was placed between subfractions 6 and 7 for purposes of comparison.

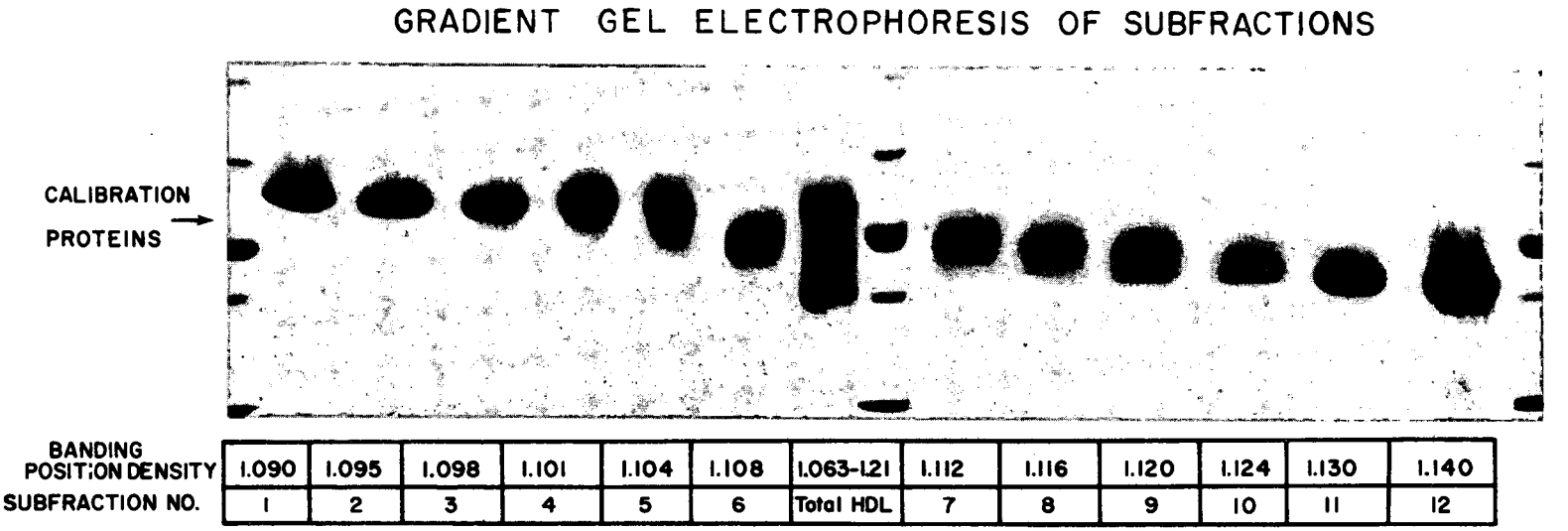

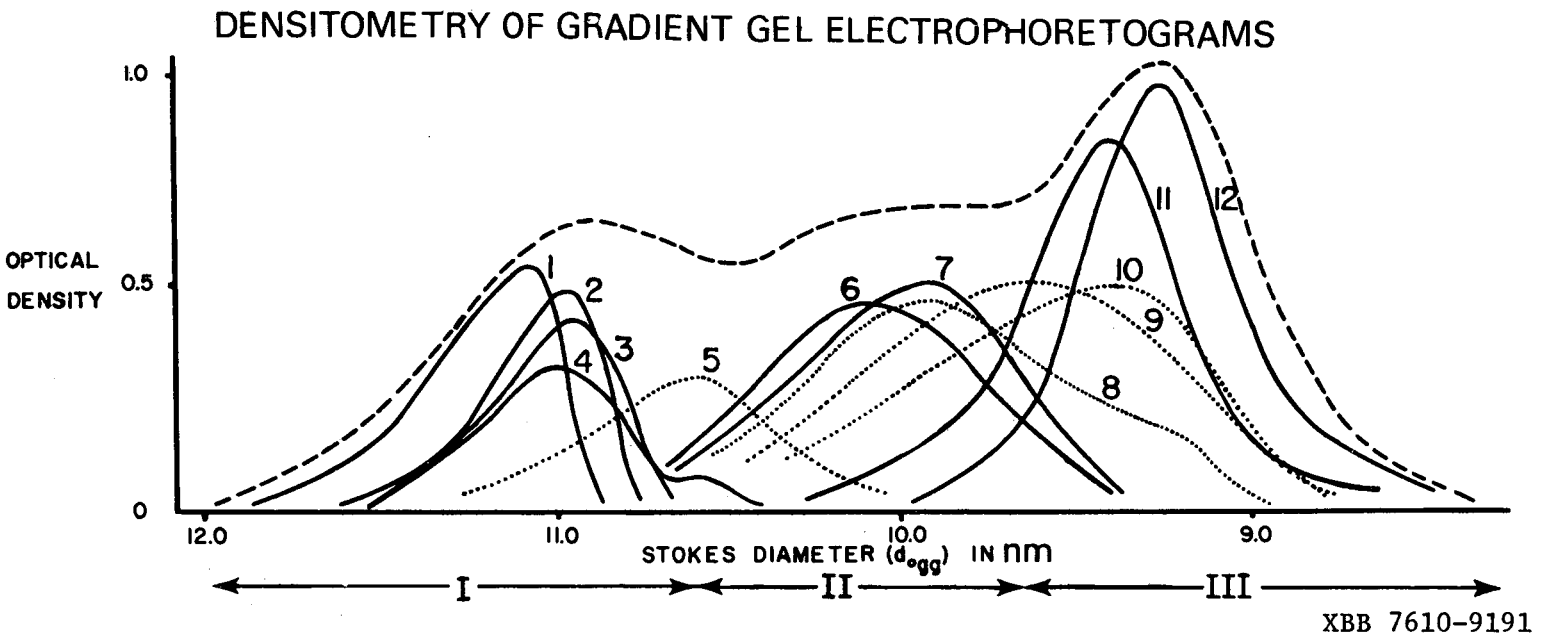

XBB 7610-9191

Figure 9

and III, respectively. Electrophoresis of subfractions obtained from density gradient ultracentrifugation of total HDL showed that all subfractions lie within the three size ranges I, II, and III for each subject. Subfractions which reproducibly banded almost totally in size range I were subfractions 1-3, those in size range II were subfractions 6-7, and those in size range III were subfractions 11-12. Subfractions intermediate to these, particularly subfractions 4 and 8, appeared to overlap two size ranges (i.e., subfraction 4 overlapped size ranges I and II and subfraction 8 overlapped size ranges II and III) in a manner suggesting that these intermediate subfractions consist of mixtures of particles from adjacent size ranges. Thus, for physico-chemical characterization of HDL representative of material falling almost exclusively within each of the three size ranges, only the groups of subfractions 1-3, 6-7, and 11-12 were subjected to the analyses described below. The mean values of $(d_o)_{gg}$ for each of the above subfraction groups were calculated by averaging data for the constituent subfractions and are presented in Figure 10. These data indicate an inverse relationship between particle diameter and banding position density of the HDL subfractions.

C. Analytic ultracentrifugation and electron microscopy

The inverse relationship noted above between particle size and banding position density was corroborated by analytic ultracentrifugation. Particle diameters $(d_o)_{uc}$ were calculated from the peak $F^o_{1.20}$ rate according to the Svedberg equation (Figure 10). The peak $F^o_{1.20}$ rate decreased from 5.50 to 1.56 as the banding position density increased from 1.090 to 1.145 g/ml. Based on the peak $F^o_{1.20}$ rate values and the hydrated densities

determined for each subfraction, values of $(d_o)_{uc}$ were calculated and separately averaged over the three groups of subfractions. The analysis shows a definite inverse relationship between the peak $F^o_{1.20}$ rate of each subfraction and its banding position density. The results are included in Figure 10 together with computer-derived schlieren patterns of the subfractions. To preserve clarity, results for the three groups of subfractions 1-3, 6-7, and 11-12 only are shown.

Electron micrographs of negatively stained subfractions from each size range show particles in two-dimensional hexagonal close packing arrays (Figure 11). Such close packing suggests that the particles are spheres with considerable size uniformity and is in accord with the observation of size homogeneity via gradient gel electrophoresis (Figure 9). In the presence of the two-dimensional hexagonal close packing, the particle diameter $(d)_{em}$ was measured as the center-to-center distance. Values of $(d)_{em}$ determined in this way were approximately 1.6 nm greater than diameters from measurements of the distance between the negatively stained edges of isolated particles. In Figure 10, the mean values and standard errors of $(d)_{em}$ for HDL from the three subfraction groups were determined by measurement of center-to-center distance.

Figure 10. Corrected schlieren patterns and a comparison of size parameters for HDL subfractions in size ranges I, II, and III. Banding position density is given in g/ml and particle diameters from ultracentrifugation, $(d_o)_{uc}$, electron microscopy, $(d_o)_{em}$, and gradient gel electrophoresis, $(d_o)_{gg}$ are given in nanometers. All particle diameter values are the means plus standard error of three separate determinations. The value of $(d_o)_{uc}$ is computed from the Svedberg equation:

$$(d_o)^2_{uc} = \frac{18\ (f/f_o)\ F_{1.20}\eta}{(1.200\ -\sigma)}$$

where σ is assumed equal to the banding position density, η is the bulk solution viscosity at 26°C and the frictional ratio (f/f_o) is taken as 1.187 for HDL from size range I and II, and 1.126 for HDL from size range III [65].

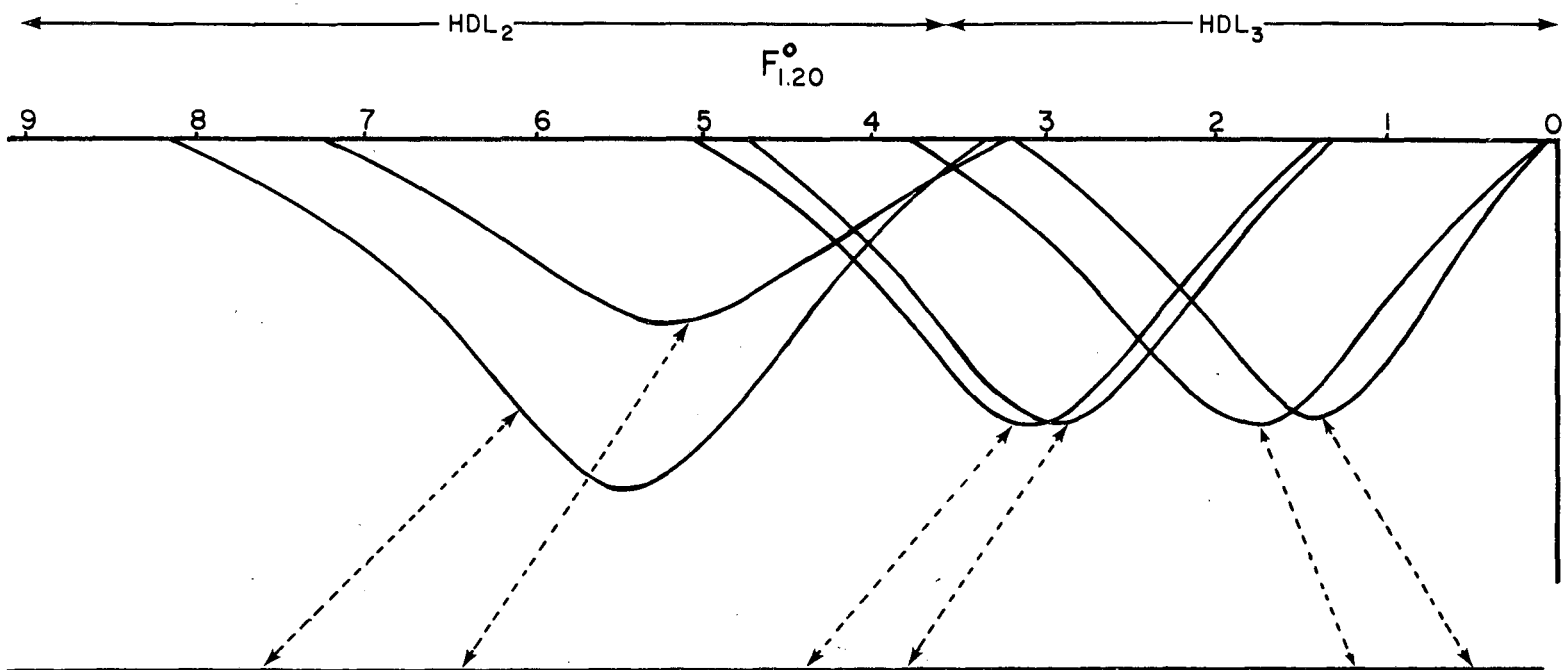

Subfraction Number	1	2	3	4	5	6	7	8	9	10	11	12
Banding * Position Density	1.090	1.095	1.098	1.101	1.104	1.108	1.112	1.116	1.120	1.124	1.130	1.145
Peak $F_{1.20}$	5.50	5.22	5.20	4.64	3.82	3.20	3.01	2.85	2.63	2.24	1.71	1.56
$(d_o)_{uc}$	10.8 ± 0.4					9.1 ± 0.3					7.8 ± 0.3	
$(d)_{em}$	12.0 ± 0.6					10.1 ± 0.7					8.9 ± 0.8	
$(d_o)_{gg}$	11.0 ± 0.8					10.1 ± 0.5					9.3 ± 0.4	

XBL7610-9432

Figure 10

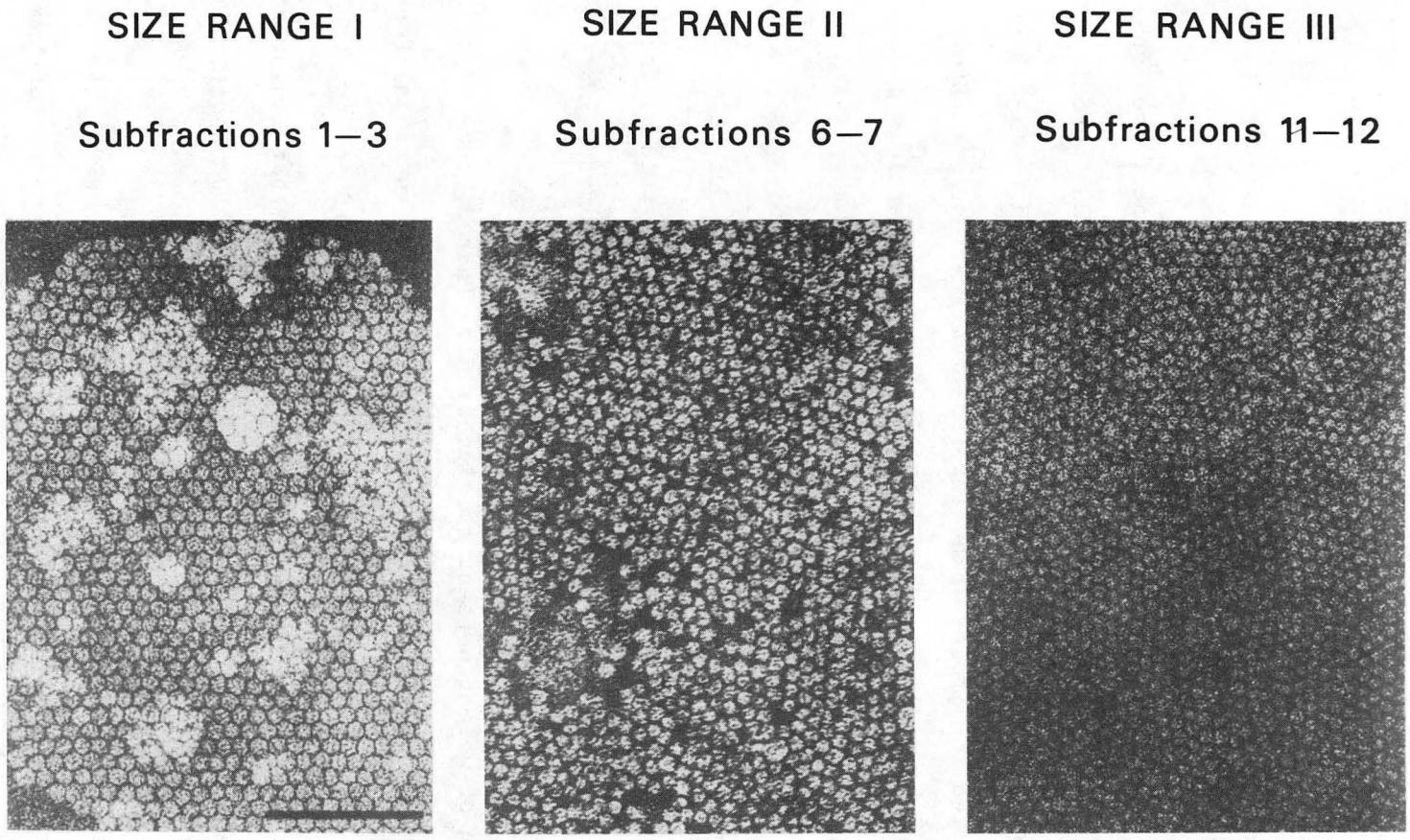

Figure 11. Negatively stained HDL from size ranges I, II, and III. The bar in size range I represents 100 nanometers and is applicable to all three micrographs.

II. Characterization of the Three Groups of Subfractions from Four Males and Four Females

A. Characterization according to molecular and compositional parameters

Density Gradient A subfractionation was also performed separately on total HDL from four normolipemic males and four normolipemic females. Subfractions 1-3, 6-7, and 11-12 were prepared from each subject and evaluated for Stokes' diameter from the gradient gel, Stokes' diameter from the Svedberg equation, peak $F^{o}_{1.20}$ rate, particle molecular weight as calculated from the Svedberg equation, weight percents of protein, phospholipid, unesterified cholesterol, cholesteryl ester, and triglyceride (Table I).

The results of this analysis (Table I) show little difference between males and females in the mean value of each parameter for subfractions falling exclusively within a given size range (with the possible exception of weight percent triglyceride). Indeed, the relatively low values of the standard errors (approximately 10% of the mean) for each parameter indicate considerable homogeneity among HDL subfractions from four male and four female subjects falling within a particular size range. This suggests that, for the subjects studied, the compositional parameters and molecular weight of an HDL particle strongly correlate with its particle size. Furthermore, this relationship appears to be independent of sex, except for small differences in parameters of the group of subfractions 1-3 between males and females.

The sex-independent compositional parameters for HDL from the three size ranges vary according to three distinct trends. As percent

TABLE I. MOLECULAR PARAMETERS AND CHEMISTRIES FOR HDL FROM SIZE RANGES I, II, AND III

Values presented are means and standard errors for four male samples and four female samples. Molecular weights were calculated from the Svedberg equation: molecular weight = $(f/f_o)\ N_o\ (3\ \pi\ \eta\ (d_o)_{uc})\ F^\circ_{1.20}\ /(1-\bar{v}\ \rho)$ where (f/f_o) is the frictional ratio as given in Figure 10 N_o is Avagadro's number, η is the bulk solution viscosity at 26°C, $F^\circ_{1.20}$ is the peak flotation rate, $(d_o)_{uc}$ is the Stokes' diameter value from the Svedberg equation, and ρ is the bulk solution density of 1.200 g/ml at 26°C.

	Size range I		Size range II		Size range III	
Subfractions pooled	1,2,3		6,7		11,12	
Banding position density (g/ml)	1.090		1.110		1.145	
Sex	Male	Female	Male	Female	Male	Female
$(d_o)_{gg}$ (nm)	11.0 ± 0.5	11.1 ± 0.6	10.2 ± 0.3	10.1 ± 0.3	9.2 ± 0.3	9.3 ± 0.2
$(d_o)_{uc}$ (nm)	10.5 ± 0.4	10.7 ± 0.5	9.2 ± 0.1	9.2 ± 0.1	7.9 ± 0.1	7.9 ± 0.1
Peak $F^\circ_{1.20}$ rate	5.34 ± 0.17	5.50 ± 0.25	3.14 ± 0.04	3.16 ± 0.05	1.56 ± 0.11	1.56 ± 0.07
10^{-5} x molecular weight (daltons)	4.10 ± 0.20	4.29 ± 0.21	2.62 ± 0.10	2.64 ± 0.10	1.77 ± 0.09	1.77 ± 0.09
% Protein*	37.8 ± 1.6	36.3 ± 2.9	47.9 ± 0.5	47.6 ± 0.7	54.4 ± 1.6	54.7 ± 1.2
% Phospholipid	39.8 ± 2.1	39.5 ± 3.6	36.5 ± 3.3	36.6 ± 3.0	23.1 ± 2.3	22.8 ± 2.1
% Unesterified cholesterol	6.0 ± 0.3	7.8 ± 0.6	3.0 ± 0.2	3.3 ± 0.2	2.8 ± 0.1	3.2 ± 0.2
% Cholesteryl ester	14.1 ± 1.3	15.1 ± 1.5	11.1 ± 0.5	11.7 ± 0.6	17.7 ± 0.4	18.1 ± 0.5
% Triglyceride	2.6 ± 0.2	1.5 ± 0.1	1.5 ± 0.1	0.7 ± 0.1	2.0 ± 0.2	1.1 ± 0.1

* % denotes percent of total lipoprotein weight.

protein decreases from 54.6 ± 1.0% (mean ± S.E. of male and female values) for HDL in size range I, percent phospholipid increases from 23.0 ± 1.6% (III) to 36.6 ± 2.2% (II) to 39.7 ± 2.1% (I), and the weight:weight ratio of cholesteryl ester to unesterified cholesterol decreases from 5.97 ± 0.32 (III) to 3.62 ± 0.23 (II) to 2.12 ± 0.18 (I).

B. Significant differences in the distribution of HDL mass among males and females

While the results of the above section suggest that for HDL of a given size range the compositional parameters and molecular weight differ little as a function of sex, the relative amounts of HDL in size ranges I, II, and III may be significantly different in males and females. Figure 12b presents the average distributions of the percent total HDL mass versus subfraction number for four male and four female subjects, respectively. The percent of total HDL mass in the group of subfractions 1-3 is considerably increased in the average female distribution (22%) as compared to the average male distribution (7%). The percent of total HDL mass in the group of subfractions 6-7 appears similar in both distributions (22% female versus 21% male) while the percent of total HDL mass in the group of subfractions 11-12 is increased in the male (31%) as compared to the female (19%). The percent of total HDL mass in the group of intermediate subfractions 4-5 (11% female versus 10% male) is similar in both distributions whereas the difference is greater for the group of intermediate subfractions 8-10 (21% female versus 26% male). The greatest differences between male and female distributions lie in the values of percent total HDL mass in groups of subfractions 1-3 and 11-12.

Figure 12a. Mean corrected schlieren patterns averaged from HDL patterns of four male subjects (——) and of four female subjects (-----).

12b. Mean distributions of percent total recovered mass versus subfraction number averaged from data on four male (——) and four female (-----) subjects. The subfraction scale in 12b is aligned with the $F^{o}_{1.20}$ rate scale in 12a such that the position of each subfraction corresponds approximately to the peak $F^{o}_{1.20}$ rate of the material in that subfraction. For comparison with reported HDL_2-HDL_3 separation techniques, the positions on the salt background density gradient curve where preparative ultracentrifugation at 178,125 X g for 48 hr at salt solution background densities of 1.100 and 1.125 g/ml would divide the mass versus subfraction number distribution are designated by arrows.

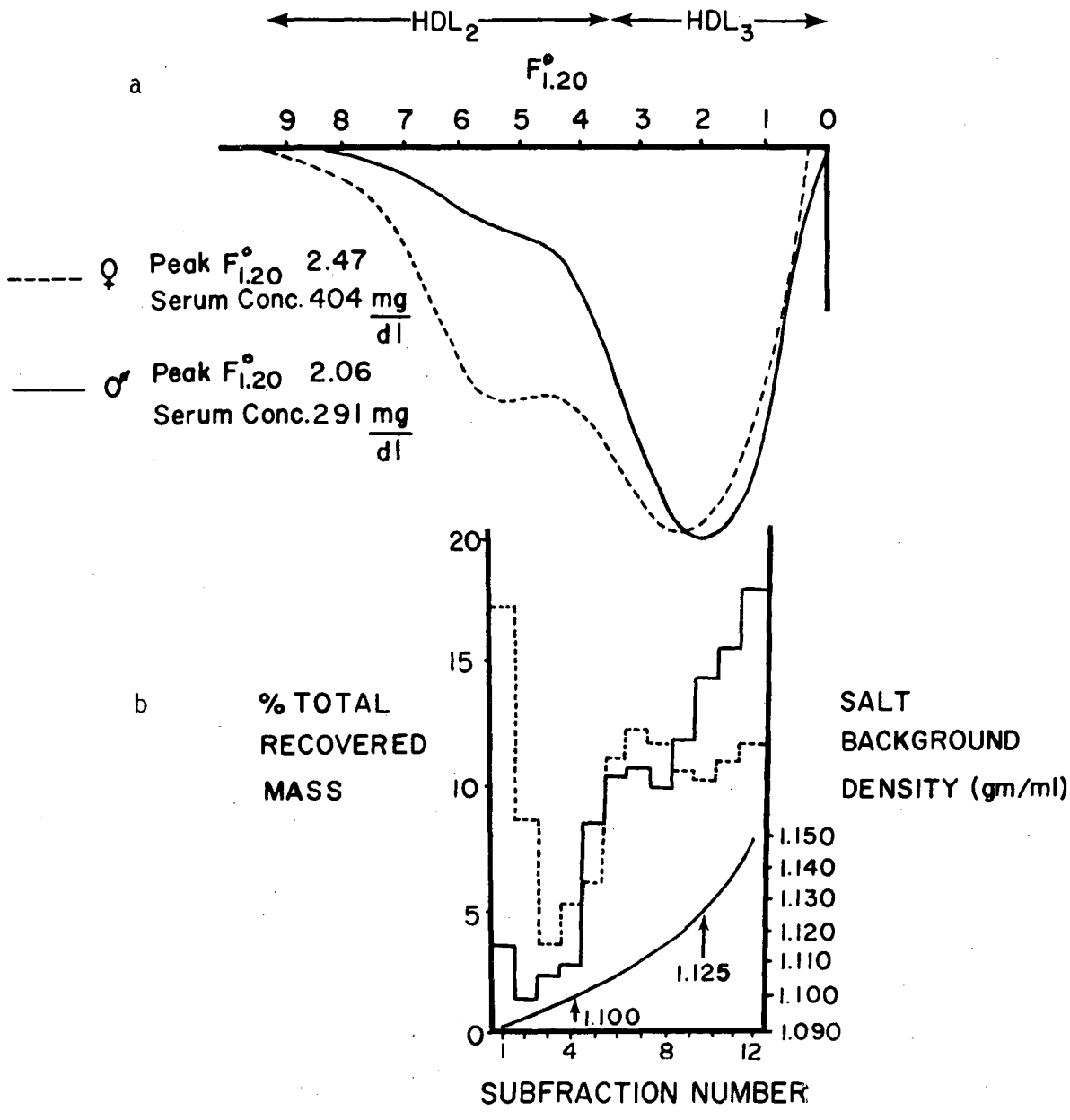

XBL7610-9433

Figure 12

C. Relation of HDL mass versus subfraction number distribution to the total HDL schlieren pattern

The shapes and peak $F^{o}_{1.20}$ rates of the average corrected schlieren patterns (Figure 12a) of the male and female subjects appear to reflect the differences noted above in the values of percent total HDL mass in the groups of subfractions 1-3 and 11-12. The peak $F^{o}_{1.20}$ rate of the average male pattern (2.06) is lower than that of the average female pattern (2.47) and is consistent with a greater percentage of total HDL mass in the group of subfractions 11-12 (mean value of the peak $F^{o}_{1.20}$ rate = 1.56, Table I) in the average male HDL than in the female. Furthermore the fraction of total schlieren pattern area which lies between $F^{o}_{1.20}$ rates 4.00 and 9.00 is considerably increased in the female pattern and reflects the greater percentage of total HDL mass in the group of subfractions 1-3 in the average female HDL than in the male. Thus, the data presented above are suggestive of sex-linked differences in the distribution of total HDL mass among the groups of subfractions 1-3 and 11-12 from the density gradient. Due to the small number (8 subjects) and limited age range (25-34 years) of the subjects tested, such trends are considered preliminary and require further confirmation in a larger group of subjects.

III. Quantitative Analysis of the Three HDL Components from Total HDL Schlieren Patterns

A. Relationship between HDL from size ranges I, II, and III and the reference schlieren patterns of HDL_{2b}, HDL_{2a}, and HDL_3.

Analyses of ultracentrifugal schlieren patterns of lipoproteins in normal sera have generally assumed a continuum of lipoproteins with respect to flotation rate (21). In such analyses, the sum of the concentrations of the lipoprotein continuum between two arbitrary flotation rate limits is determined. For example, the total HDL schlieren pattern area between $F^{o}_{1.20}$ rates 9.0 and 3.5 was taken by Lindgren (22) as representative of the concentration of the HDL_2 density class (d 1.063-1.125 g/ml) while the area between $F^{o}_{1.20}$ rates 3.5 and 0 was considered as representative of the concentration of the HDL_3 density class (d 1.125-1.200 g/ml) (Figure 12a). As was presented above (RESULTS section I.), the results of this study provide evidence for the existence in the HDL distribution of three major HDL components, distinct in particle size, hydrated density, and composition. These HDL components fall within the following size ranges: I (10.8-12.0 nm in diameter), II (9.7-10.7 nm in diameter), and III (8.5-9.6 nm in diameter). Since the particle hydrated density ranges for HDL from size range I (d 1.063-1.100 g/ml) and from size range II (d 1.100-1.125 g/ml) comprise the HDL_2 particle density range (d 1.063-1.125 g/ml), these two components are designated in this thesis as HDL components HDL_{2b} (HDL from size range I) and HDL_{2a} (HDL from size range II). The particle hydrated density range of HDL from size range III (d 1.125-1.200 g/ml) is identical to that of HDL_3 given above.

For the purposes of the three component analysis scheme outlined in MATERIALS AND METHODS section V., corrected schlieren patterns of the three HDL components were obtained from Density Gradient A subfractions of HDL of the eight subjects described above (RESULTS section II.A.) Subfractions 1-3 from a given individual were pooled to determine the HDL_{2b} component schlieren pattern, subfractions 6-7 for the HDL_{2a} component schlieren pattern, and subfractions 11-12 for the HDL_3 component schlieren pattern. The HDL_{2b}, HDL_{2a}, and HDL_3 reference patterns in Figure 5 represent the average of the serum concentrations of the three components from the four males and four females. The molecular properties and composition of the three HDL components are given in Table II.

B. Results of subspecies distribution analysis in a normal population sample

1. Determination of fitting error in three component analysis for serum levels of HDL_{2b}, HDL_{2a}, and HDL_3 in the Modesto Study

The effectiveness of the three component analysis in describing the total HDL pattern was evaluated in terms of its ability to account for the total area of that pattern. As described in MATERIALS AND METHODS, section V. C., fitting errors are encountered during adjustment of each of the reference component patterns to the total HDL pattern. The mean value of the error in fitting the HDL_3 reference pattern was 3.5 ± 1.2 % (S.D.) when expressed as percent of the total HDL serum concentration. In virtually every case, this error was due to an overfitting of the total HDL pattern contour by the HDL_3 reference pattern contour (Figure 6c).

TABLE II.

MOLECULAR PROPERTIES OF HDL FROM SIZE RANGES I, II, AND III.

Values presented are means and standard errors for four male samples and four female samples. Molecular weights were calculated from the Svedberg equation (5) and $(d_o)_{gg}$ represents the Stokes' diameter value of the particle as determined from its migration on porosity gradient polyacrylamide gels (5). The peak $F^{\circ}_{1.20}$ rates of the reference patterns were calculated by averaging over the corrected schlieren patterns of HDL in each size range.

	Size range I (HDL_{2b})		Size range II (HDL_{2a})		Size range III (HDL_3)	
Mean banding position density (g/ml)	1.090		1.110		1.145	
Density range for preparative ultracentrifugal isolation (g/ml)	1.063-1.100		1.100-1.125		1.125-1.200	
Sex	Male	Female	Male	Female	Male	Female
$(d_o)_{gg}$ (nm)	11.0 ± 0.5	11.1 ± 0.6	10.2 ± 0.3	10.1 ± 0.3	9.2 ± 0.3	9.3 ± 0.2
10^{-5} x molecular weight (daltons)	4.10 ± 0.20	4.29 ± 0.21	2.62 ± 0.10	2.64 ± 0.10	1.77 ± 0.09	1.77 ± 0.09
Peak $F^{\circ}_{1.20}$ rate	5.34 ± 0.17	5.50 ± 0.25	3.14 ± 0.04	3.16 ± 0.05	1.56 ± 0.11	1.56 ± 0.07
	Reference pattern		Reference pattern		Reference pattern	
Peak $F^{\circ}_{1.20}$ rate	5.37 ± 0.30		3.15 ± 0.06		1.56 ± 0.13	

Contributing to the overfitting of the HDL_3 reference pattern is a reduction in the total HDL pattern heights in the HDL_3 region due to the presence of a small amount of sedimenting protein remaining in the d < 1.20 g/ml fraction after a 24 hour preparative ultracentrifugation. When total HDL fractions were analyzed after a 48 hour ultracentrifugation at d 1.21 g/ml, no reduction of pattern heights due to sedimenting protein was observed and the fitting error for HDL_3 was smaller (2.0 ± 0.8% of the total HDL concentration, for 10 samples).

The fitting errors in the determination of HDL_{2b} and HDL_{2a} represent both underfitting and overfitting of the total HDL pattern contour by their reference patterns and had mean values of 3.2 ± 6.1% (S.D.) and 2.8 ± 5.2% (S.D.), respectively. Taken together these errors can be used as a measure of the effectiveness of the three component analysis to quantitatively describe the total HDL pattern. For the 160 patterns analyzed, the mean value of the total error in fitting the HDL_{2b}, HDL_{2a}, and HDL_3 reference patterns was 9.5 ± 8.5% (S.D.) when expressed as percent of the total HDL serum concentration. The value of the inherent uncertainty of measurement of the total HDL concentration is ± 5% (52). If the total fitting error is corrected for the estimated contribution due to sedimenting protein, then the fitting error for the total three component analysis would be approximately 7.5 ± 8.1% (S.D.).

Furthermore, it should be noted that in schlieren patterns with high levels of HDL_{2b} (greater than 150 mg/dl), such as those in Figure 7a and 7b, a significant amount of pattern area between $F^{o}_{1.20}$ rates 5.0 and 9.0 cannot be completely fitted by the HDL_{2b} reference pattern. In the

present study, however, only about 18% (14 cases) of the Modesto females and 1% (1 case) of the males showed HDL_{2b} serum levels of 150 mg/dl or greater. In 14 of these cases the area not completely fitted by the reference HDL_{2b} pattern was only 9% or less (Figure 7a) of the fitted HDL_{2b} pattern area. Only one case exhibited a larger discrepancy (30%) in fit and its pattern is shown in Figure 7b. Since insufficient data were available for delineation of the number of contours of possible reference components in this flotation rate region, material with $F^{o}_{1.20}$ rates between 5.0 and 9.0, which was not fitted by the HDL_{2b} reference pattern, was included as part of the HDL_{2b} component concentration. The error in the determination of HDL_{2b} levels due to such pooling was minimal in this population since the fitting error for the reference HDL_{2b} pattern was only $3.2 \pm 6.1\%$ (S.D.).

In studies on specific subpopulations exhibiting elevated levels of HDL_{2b}, such as subjects with hyperalphalipoproteinemia, the amount of this material may be substantial and separate analysis in terms of appropriate reference components would be required. In preliminary studies, material in this flotation range could be isolated by equilibrium Density Gradient B ultracentrifugation. The mean particle hydrated density of this material was determined from its banding position density to be 1.075 g/ml, the particle diameter range as determined by electron microscopy was 13-14 nm, and the mean peak $F^{o}_{1.20}$ rate was 6.87. The total protein to total lipoprotein mass ratio was 0.31 as determined by NCH elemental analysis. Further characterization of this material with respect to particle size and hydrated density distribution will be important in determining the number of components it represents. The establishment of

reference schlieren patterns for each component will then enable the determination of their serum concentrations from total HDL schlieren patterns, in accord with the present three component analysis.

2. Serum levels of the HDL_{2b} , HDL_{2a} , and HDL_3 components as a function of sex and age

The mean serum concentrations of the HDL_{2b}, HDL_{2a}, and HDL_3 components for the Modesto Study population are presented according to age and sex in Table III. For both males and females the progressive increase in mean total HDL concentration from one decade to the next is not statistically significant ($p > 0.05$). However, the mean total HDL concentration increase between the 27-36 and 47-56 or 27-36 and 57-66 year decades is significant ($p < 0.05$). A similar trend is seen in the HDL_3 levels of both males and females. The levels of both HDL_{2b} and HDL_{2a} in female HDL are significantly higher ($p < 0.01$) than in male HDL for each of the four age decades. The mean female HDL_3 levels are actually lower than the mean male value for all corresponding age decades but significant only for the population as a whole ($p < 0.05$).

The fine structure of the differences between female and male patterns of the Modesto Study was also investigated independent of the three component analysis. Difference patterns (female mean total HDL pattern minus male mean total HDL pattern) for each of the four age decades were obtained by computer and are shown in Figure 13. All four patterns clearly demonstrate the presence of peaks in the female minus male difference patterns which are localized within specific flotation regions of the total HDL pattern. As indicated in the figure, these

TABLE III.

MEAN SERUM CONCENTRATIONS OF HDL_{2b}, HDL_{2a}, and HDL_3 COMPONENTS FOR MODESTO STUDY AGE DECADES

Values presented are means and standard errors for male and female samples in each of the four age decades surveyed in the Modesto Study. All concentrations are given in mg/100 ml.

		MALE				FEMALE			
Age decade	n	Total HDL	HDL_{2b}	HDL_{2a}	HDL_3	Total HDL	HDL_{2b}	HDL_{2a}	HDL_3
27-36 years	20	235 ± 55	12 ± 21	70 ± 37	153 ± 26	342 ± 42	63 ± 39	138 ± 28	141 ± 26
37-46 years	20	275 ± 84	29 ± 31	88 ± 52	158 ± 26	382 ± 116	96 ± 90	145 ± 45	141 ± 25
47-56 years	20	283 ± 77	27 ± 37	82 ± 47	174 ± 32	402 ± 104	74 ± 45	164 ± 55	164 ± 26
57-66 years	20	287 ± 81	33 ± 40	82 ± 40	172 ± 26	413 ± 90	108 ± 72	144 ± 47	161 ± 36
27-66 years	80	270 ± 38	25 ± 17	81 ± 22	164 ± 14	385 ± 46	85 ± 34	148 ± 22	152 ± 14

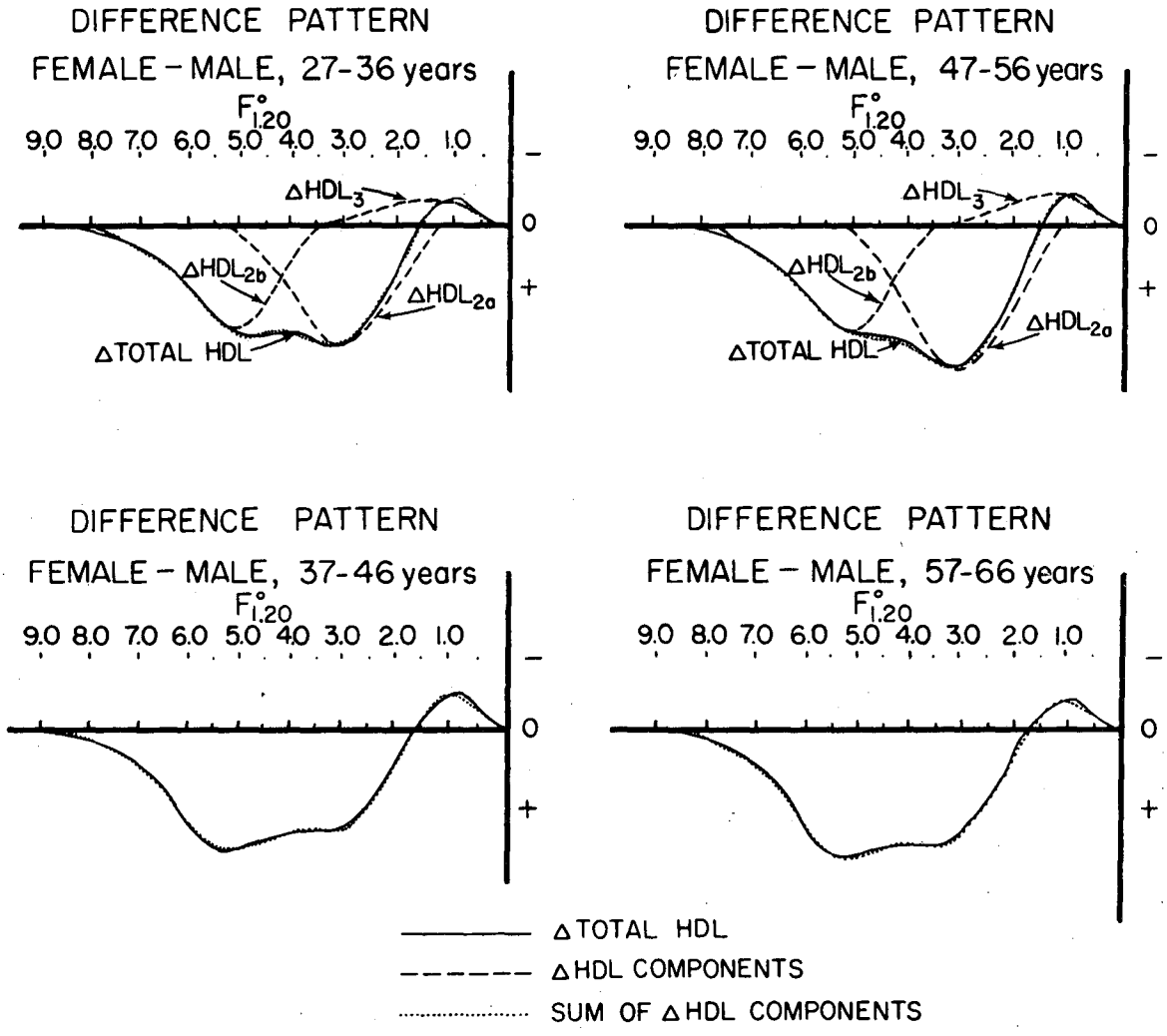

XBL774-3266

Figure 13. Total HDL difference patterns (mean female minus mean male patterns) for the four age decades of the Modesto Study (———). Mean total HDL schlieren patterns of both males and females were fitted by the three component analysis scheme. Separate HDL_{2b}, HDL_{2a}, and HDL_3 fitted patterns of males were subtracted from corresponding female fitted patterns for each age decade to generate the component difference patterns (— — —). The sum of the three separate component difference patterns (••••••) closely approximates the total HDL difference pattern in each age decade.

flotation regions are those that are associated with the major reference components (HDL_{2b}, HDL_{2a}, and HDL_3) used in the present analysis. When the population difference patterns are analyzed via the three component fitting procedure, the fit of the three reference patterns to the difference pattern contour is excellent, strongly suggesting that the reference patterns are representative of subspecies within the HDL distribution whose serum levels may reflect component-specific metabolic control.

The relationship between HDL_{2b} and HDL_{2a} levels among the 160 cases is shown in Figure 14a. A polynomial regression curve of the data shows a nearly linear relationship ($r = 0.725$, $p < 0.001$) between both male and female levels of these components. Based on values of the slope and intercept of the regression curve, the average mole ratio of HDL_{2a} to HDL_{2b} in HDL from this population is approximately 2:1. In addition, at HDL_{2a} levels of 40 ± 10 mg/dl or less, no HDL_{2b} can be detected by this analysis. The regression of HDL_{2b} serum levels on corresponding HDL_3 serum levels (Figure 14b) reveals a small but significant negative correlation ($r = -0.315$, $0.005 > p > 0.001$) whereas the regression of HDL_{2a} serum levels on corresponding HDL_3 serum levels (Figure 14c) shows no significant correlation ($r = 0.105$, p 0.25) and suggests that HDL_{2a} serum levels for both males and females are independent of HDL_3 levels. It should be noted, however, that the range of HDL_3 serum levels (Figure 14d) among the 160 cases of the Modesto Study extends only from 100 mg/dl to 220 mg/dl with a standard deviation of the mean of 30 mg/dl (or 19% of the mean). The standard deviations of the mean HDL_{2b} and HDL_{2a} levels

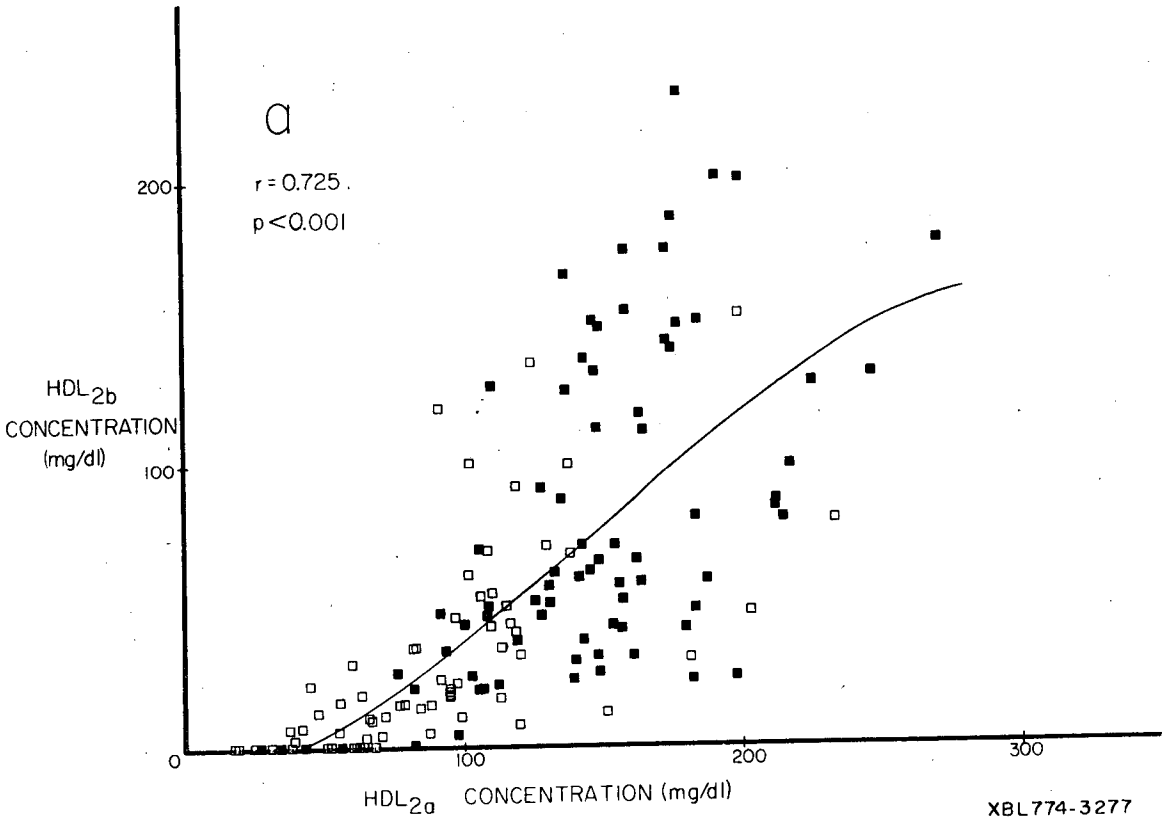

Figure 14a. Regression of HDL_{2b} on HDL_{2a} concentration. For Figs. 14a, 14b, and 14c, the solid squares (■) represent female values and empty squares (□) represent male values, and solid line represents the second degree polynomial regression line. The HDL_{2b}, HDL_{2a}, and HDL_3 components for the eighty male and eighty female subjects in the Modesto Study were compared under the assumption that the values of all three components have a multivariate normal distribution with the same unknown covariance matrix.

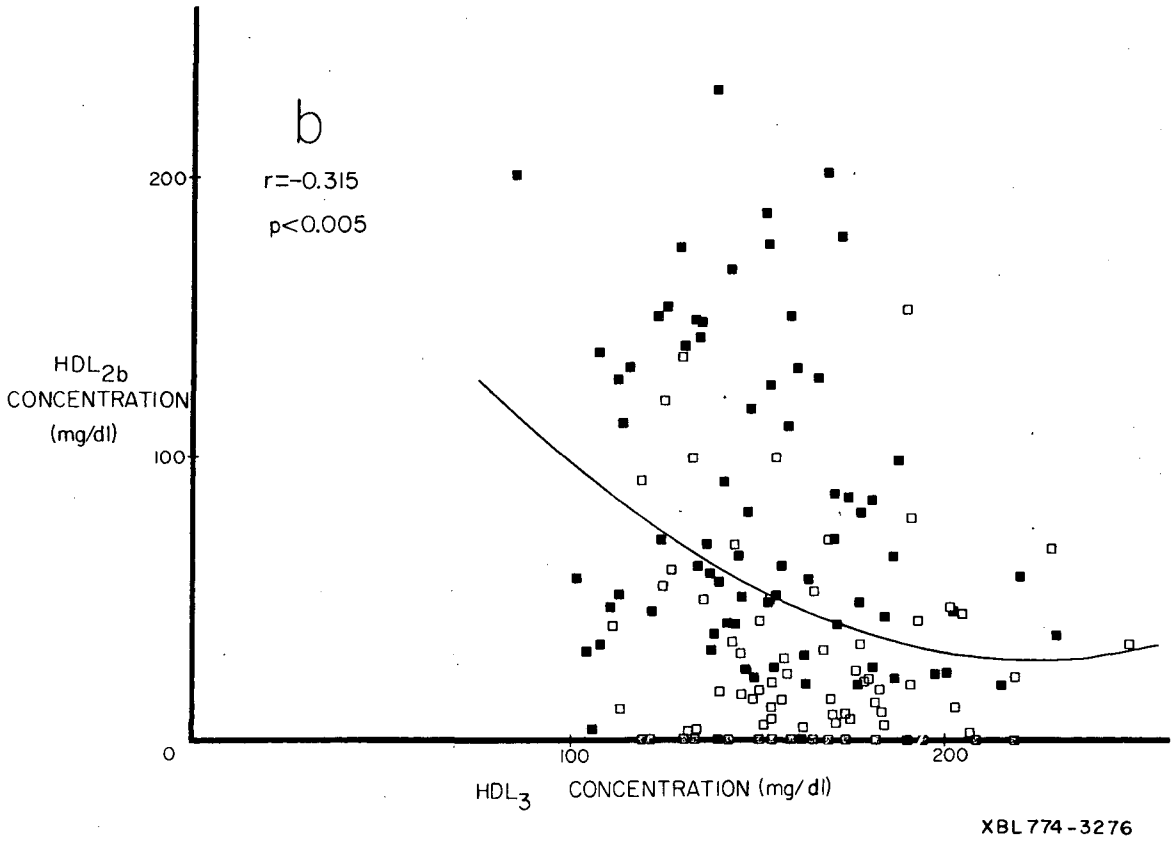

Figure 14b. Regression of HDL_{2b} on HDL_3 concentration.

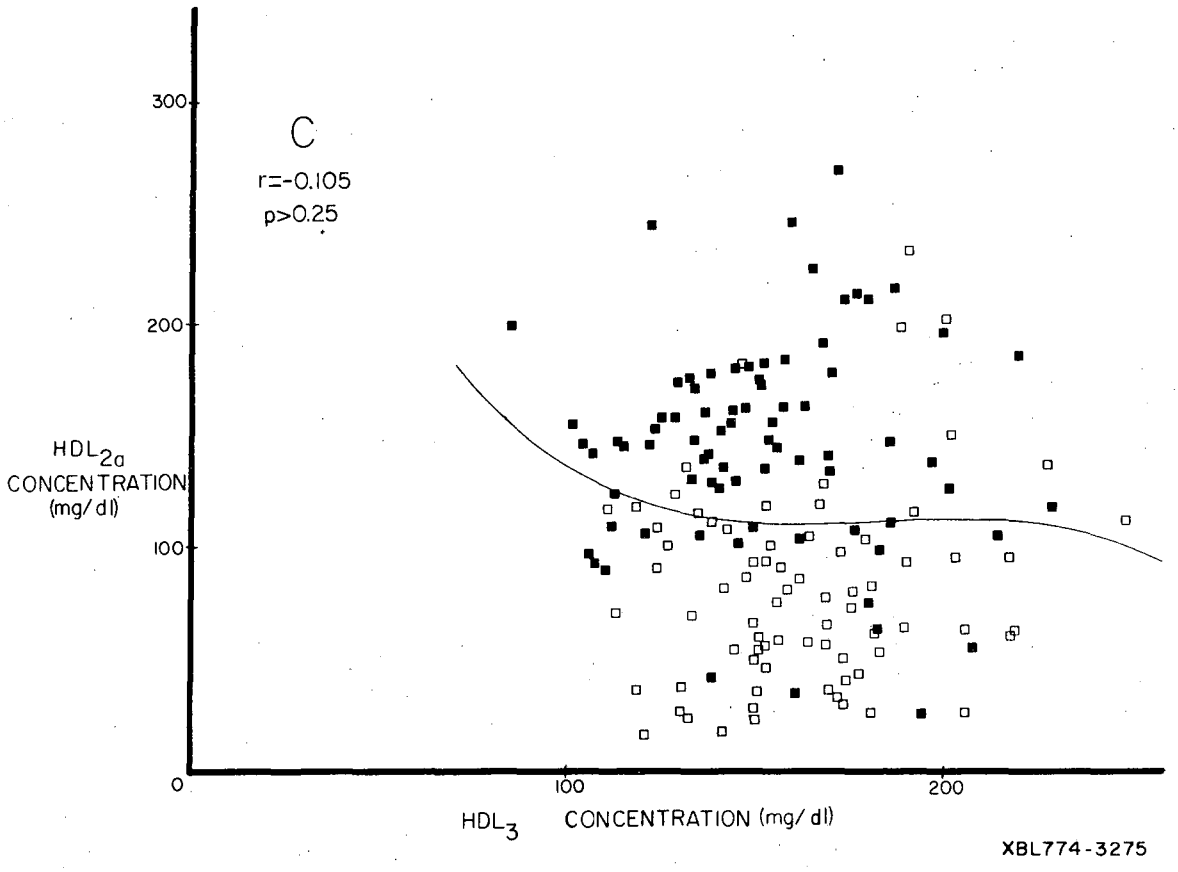

Figure 14c. Regression of HDL_{2a} on HDL_3 concentration.

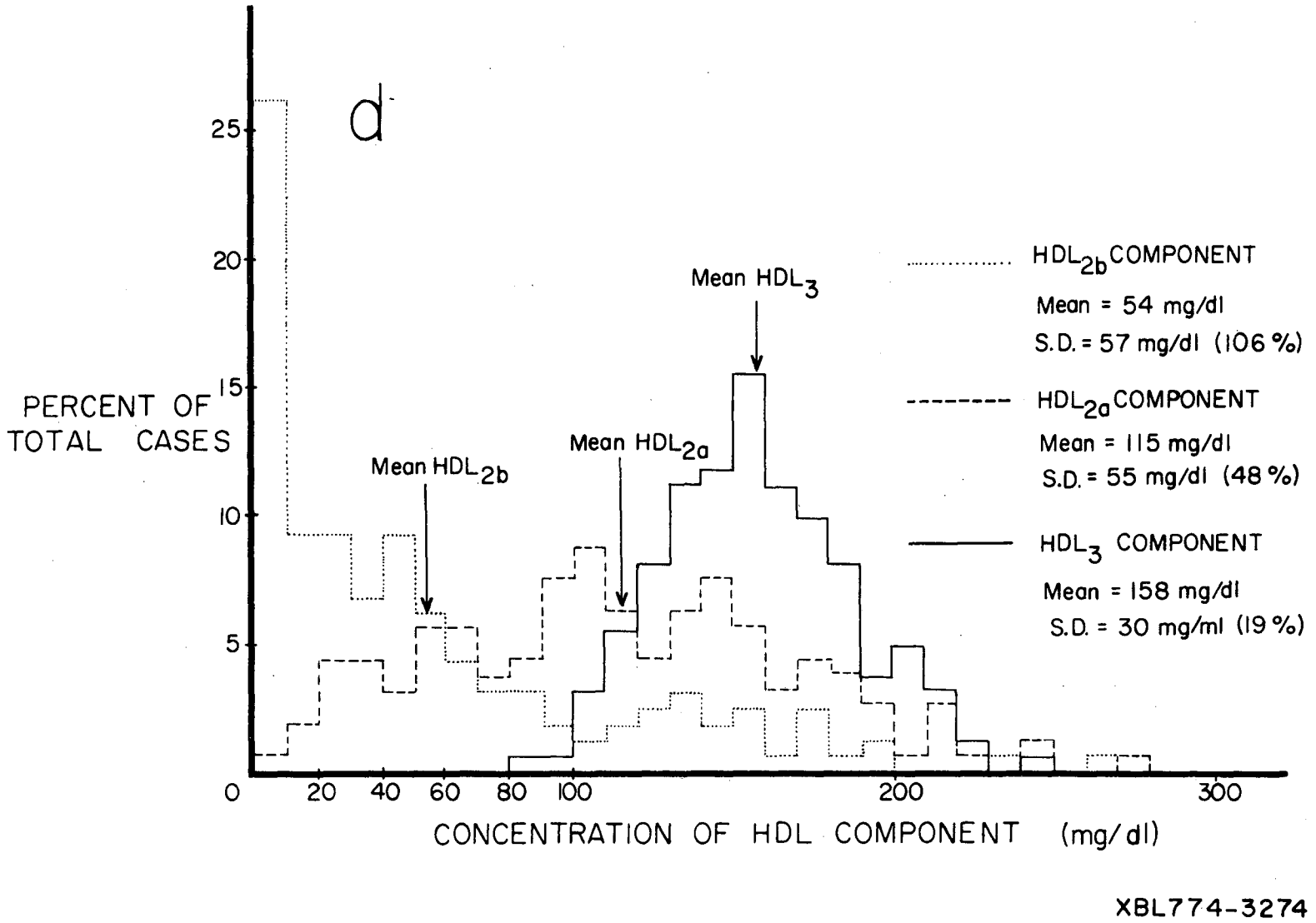

Figure 14d. Distribution of precent of total number of Modesto Study cases within specific concentration ranges of HDL_{2b}, HDL_{2a}, and HDL_3.

(± 57 mg/dl or 106% of the mean for HDL_{2b} and ± 55 mg/dl or 48% of the mean for HDL_{2a}) indicate that both HDL_{2b} and HDL_{2a} component levels exhibit a substantially wider range of biological variation in the Modesto Study population than do HDL_3 component levels.

3. The relationship of serum levels of the HDL_{2b}, HDL_{2a}, and HDL_3 components to total HDL concentration.

Serum levels of both HDL_{2b} and HDL_{2a} show strong positive correlations to total HDL concentration ($r = 0.872$, $p < 0.001$ and $r = 0.926$, $p < 0.001$ for HDL_{2b} and HDL_{2a} in Figure 15a and Figure 15b, respectively). In contrast, the regression curve of HDL_3 serum concentration versus total HDL serum concentration in Figure 15c is essentially flat at an HDL_3 level approximating the mean HDL_3 serum level of the Modesto population (158 mg/dl). The correlation of HDL_3 serum levels on total HDL concentration was low order and not significant ($r = 0.106$, $p > 0.25$).

The regression curves of percent HDL_{2b}, HDL_{2a}, and HDL_3 versus total HDL concentration can be used to predict the minimal total HDL concentrations at which HDL_{2b} and HDL_{2a} can be demonstrated in serum samples from the Modesto population. The regression curve in Figure 15d predicts detection of HDL_{2b} only for those samples in which the total HDL concentration is greater than 200 ± 8 mg/dl. Likewise the regression in Figure 15e predicts measureable HDL_{2a} levels only in samples with total HDL concentrations greater than 100 ± 5 mg/dl. This value agrees closely with that of the total HDL concentration (115 ± 7 mg/dl) at which the regression curve of percent HDL_3 versus total HDL concentration in Figure 15f approaches the 100% HDL_3 value. Based on these regression data (Figures

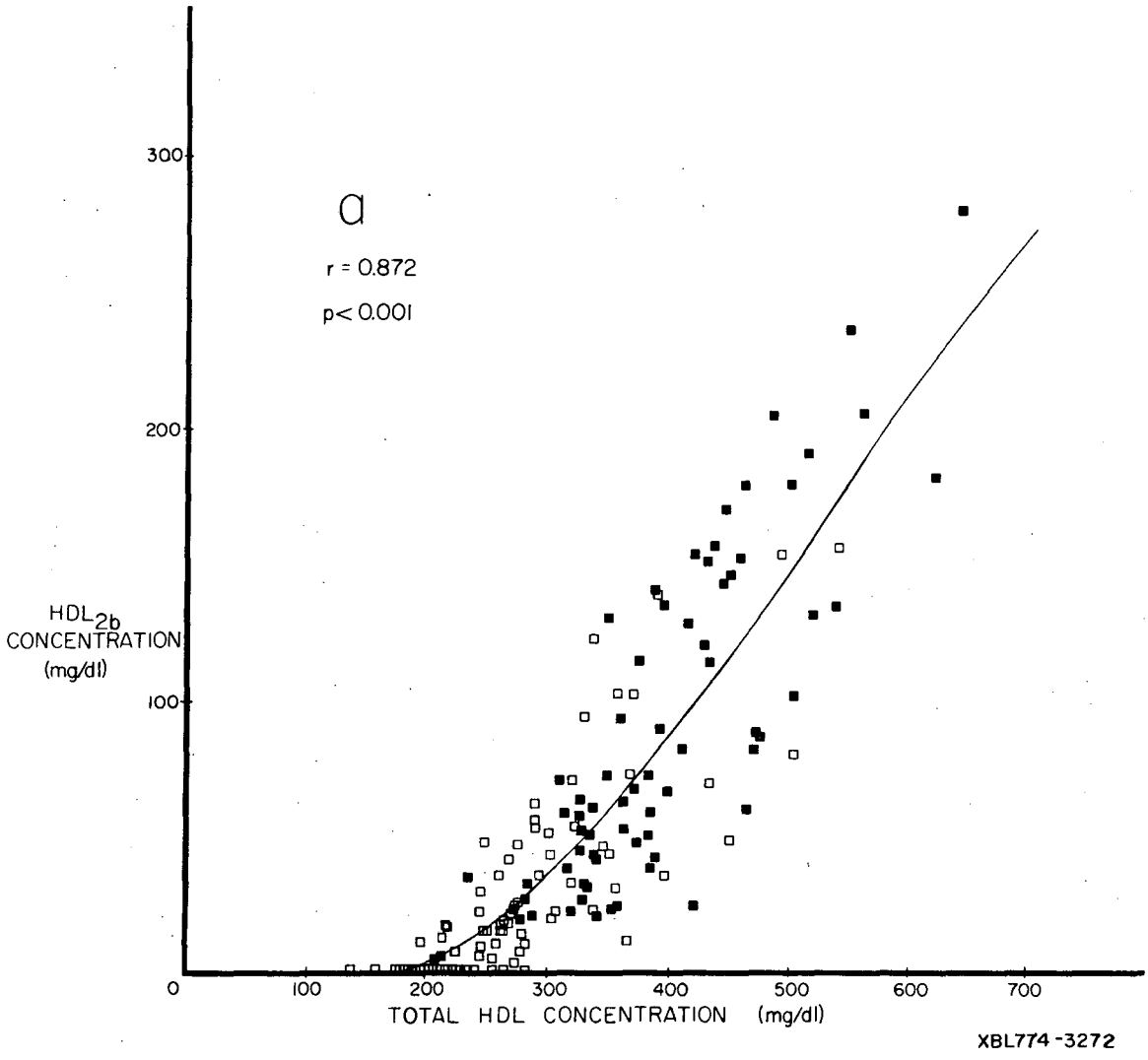

Figure 15a. Regression of HDL_{2b} on total HDL concentration. For Figs. 15a, 15b, 15c, 15d, 15e, and 15f the solid squares (■) represent female values, the empty squares (□) male values, and the solid line represents the second degree polynomial regression line.

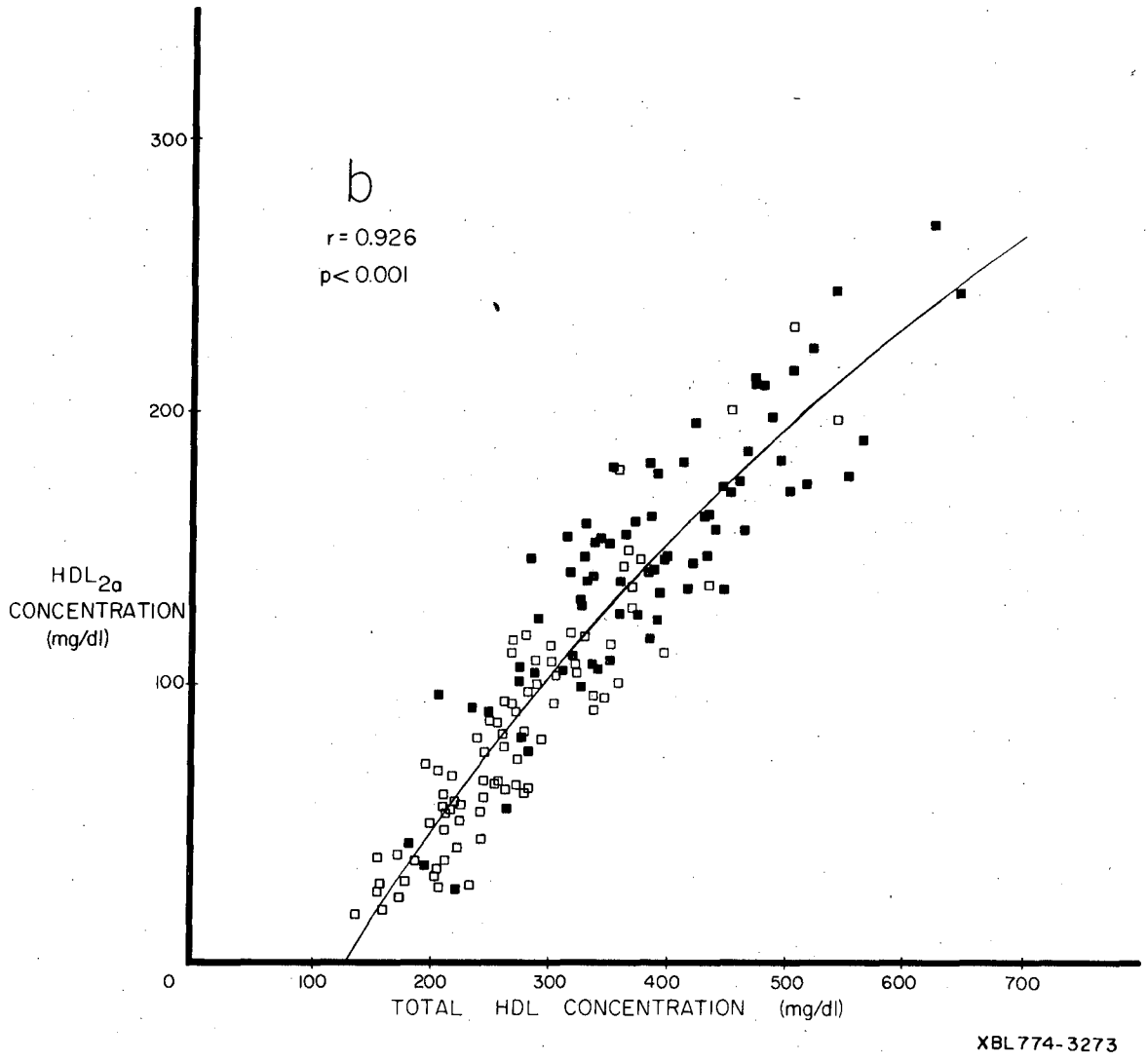

Figure 15b. Regression of HDL_{2a} on total HDL concentration.

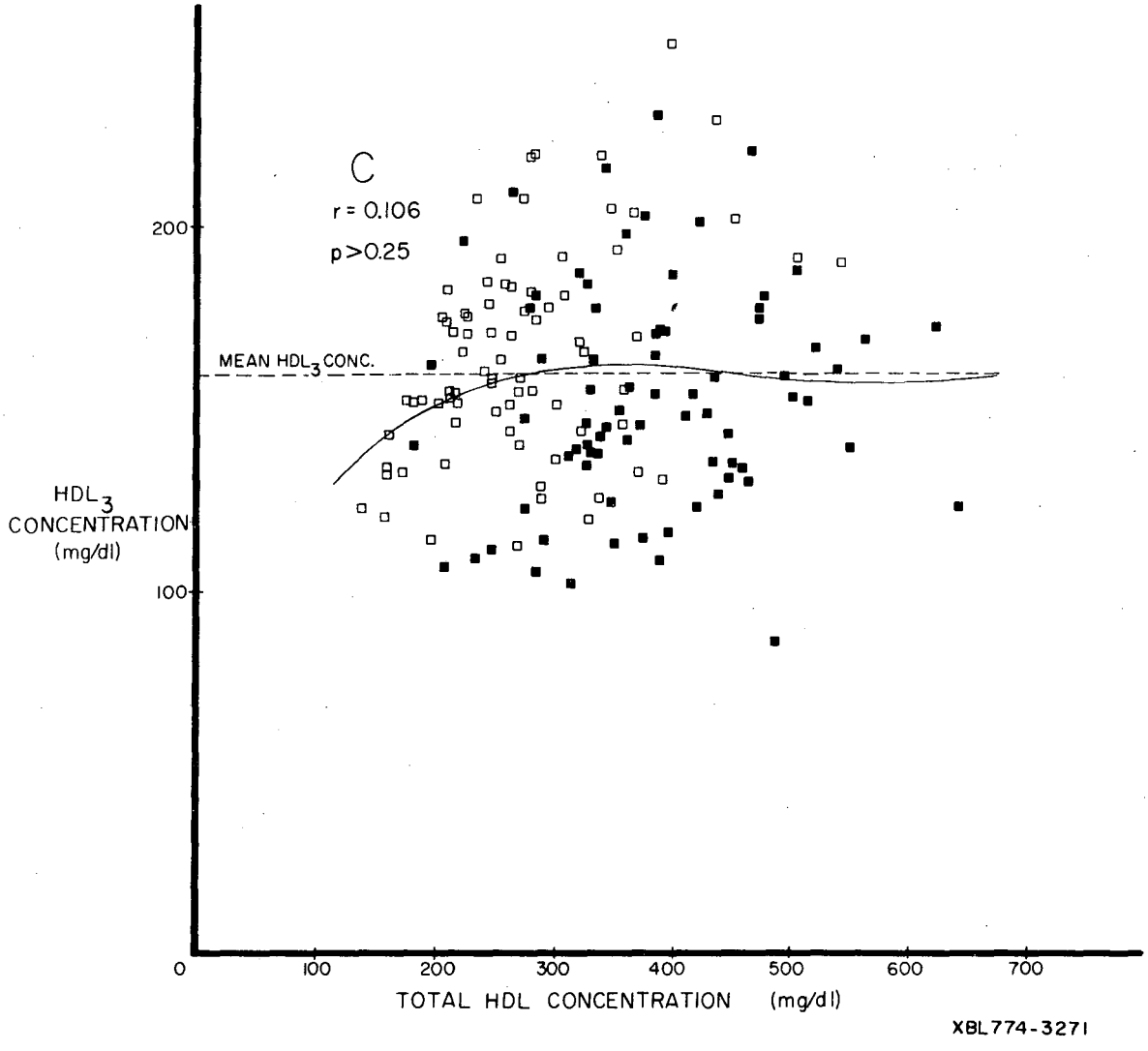

Figure 15c. Regression of HDL_3 on total HDL concentration.

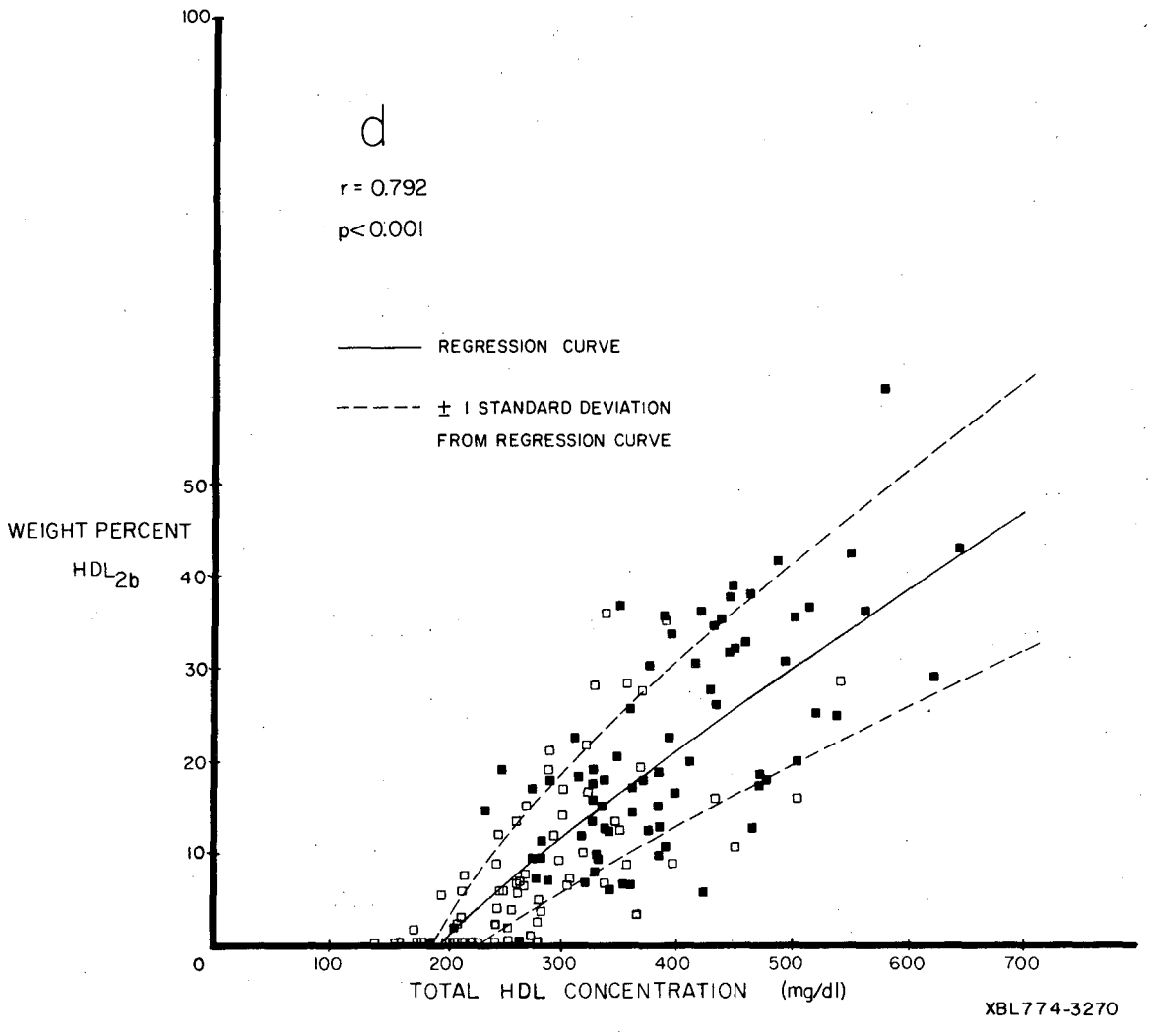

Figure 15d. Regression of weight percent HDL_{2b} on total HDL concentration. For Figs. 15d, 15e, and 15f the standard deviation of the data about the fitted curve was calculated from the standard deviations of the three polynomial coefficients.

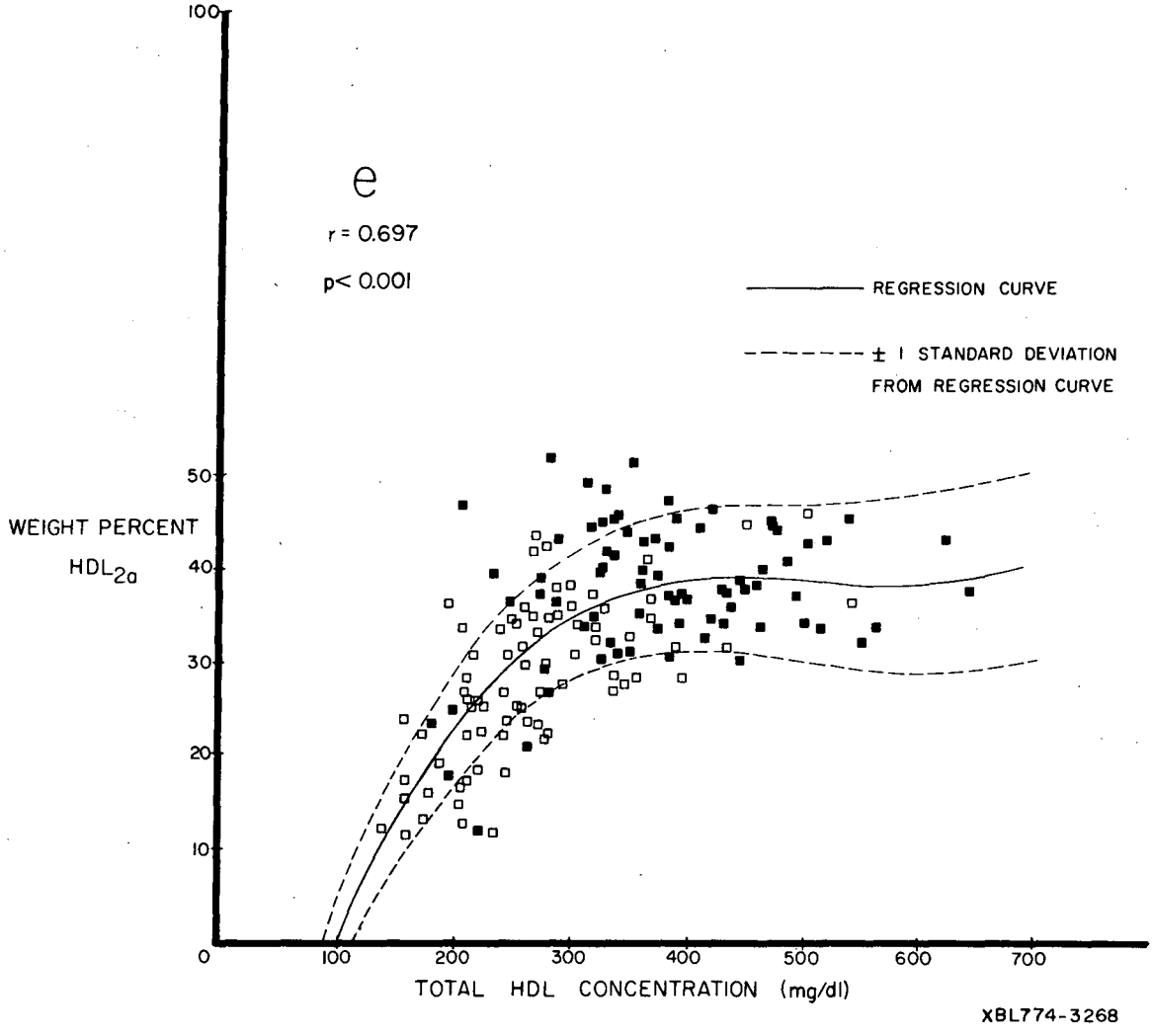

Figure 15e. Regression of weight percent HDL_{2a} on total HDL concentration.

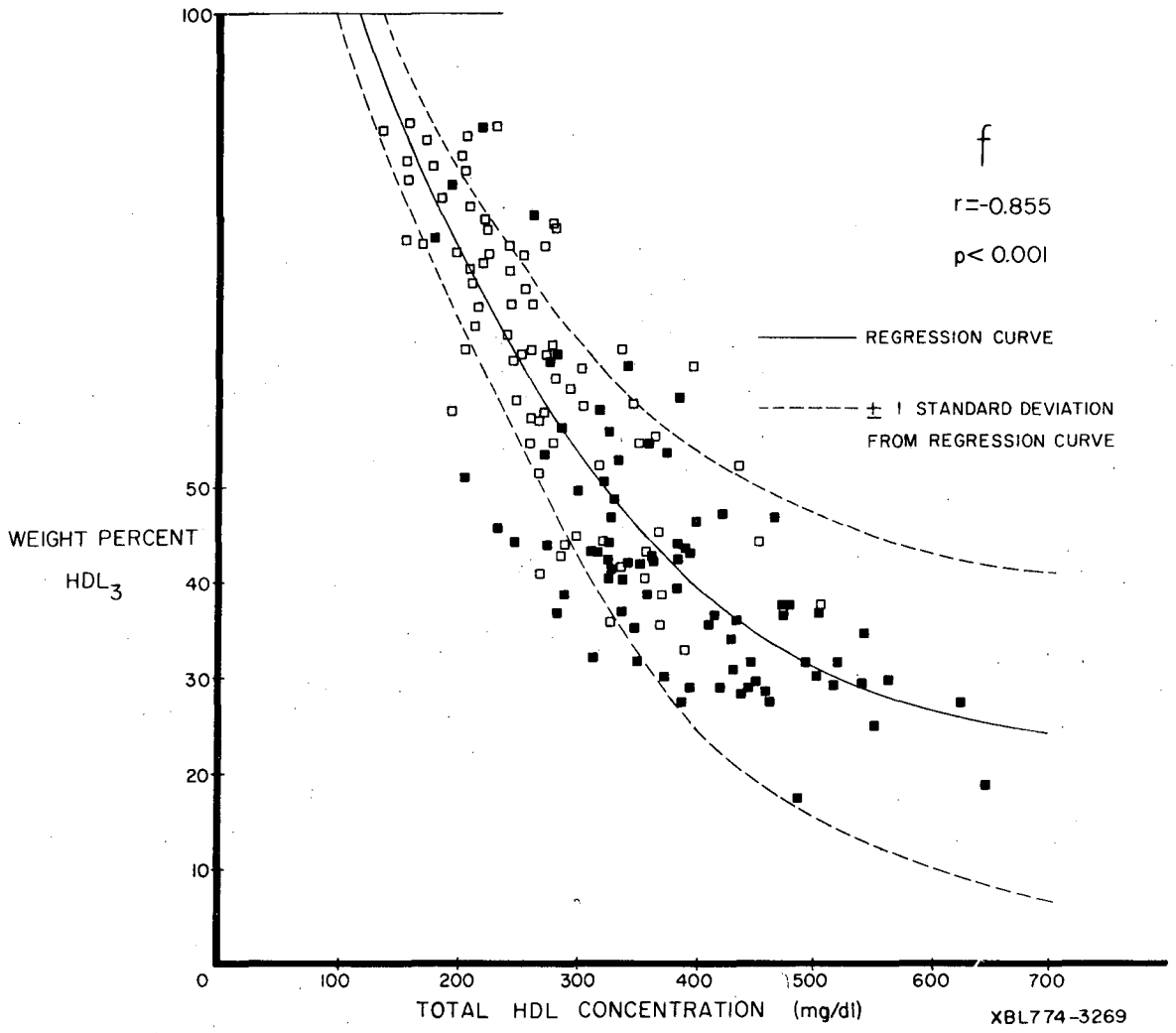

Figure 15f. Regression of weight percent HDL_3 on total HDL concentration.

15d and 15e), samples with total HDL concentrations of less than 100 ± 5 mg/dl would be expected to exhibit negligible levels of both HDL_{2b} and HDL_{2a}.

4. The relationship of lipoprotein composition to total HDL concentration

The lipid and protein compositions of the three reference components HDL_{2b}, HDL_{2a}, and HDL_3 isolated from 8 normolipemic subjects were determined (RESULTS section II.A.) and averaged for each component over the 8 subjects. These mean lipid and mean protein compositions (Table IV) can be used with values of the regression coefficients (Figures 15d, 15e, and 15f) or percent HDL_{2b}, HDL_{2a}, and HDL_3 on total HDL concentration to estimate the variation of each compositional parameter as a function of total HDL concentration (Figure 16). It is assumed that the lipid compositions of each HDL component do not vary with increasing serum levels of these components throughout the Modesto population. This assumption is supported by the recent work of S. Mendoza et al. (64) who found that five familial hyperalphalipoproteinemic women with increased concentrations of HDL_2 (d 1.063-1.125 g/ml fraction) and HDL_3 (d 1.125-1.200 g/ml fraction) showed normal lipid and protein compositions for each fraction. The data in Figure 8 indicate that the relative amounts of protein and cholesteryl ester decrease while that of phospholipid, unesterified cholesterol, and triglyceride increase with increasing total HDL concentration.

TABLE IV.

LIPID AND PROTEIN COMPOSITIONS OF HDL COMPONENTS

Values presented are means and standard deviations for four male samples and four female samples.

	HDL_{2b}	HDL_{2a}	HDL_3
Percent protein*	37.0 ± 2.9	47.7 ± 0.9	54.5 ± 2.0
Percent phospholipid	39.6 ± 4.2	36.6 ± 4.5	23.0 ± 3.1
Percent unesterified cholesterol	6.8 ± 0.7	3.2 ± 0.3	3.0 ± 0.2
Percent cholesteryl ester	14.6 ± 2.0	11.4 ± 0.8	17.9 ± 0.6
Percent triglyceride	2.0 ± 0.2	1.1 ± 0.1	1.6 ± 0.2

* Percent denotes percent of total lipoprotein weight.

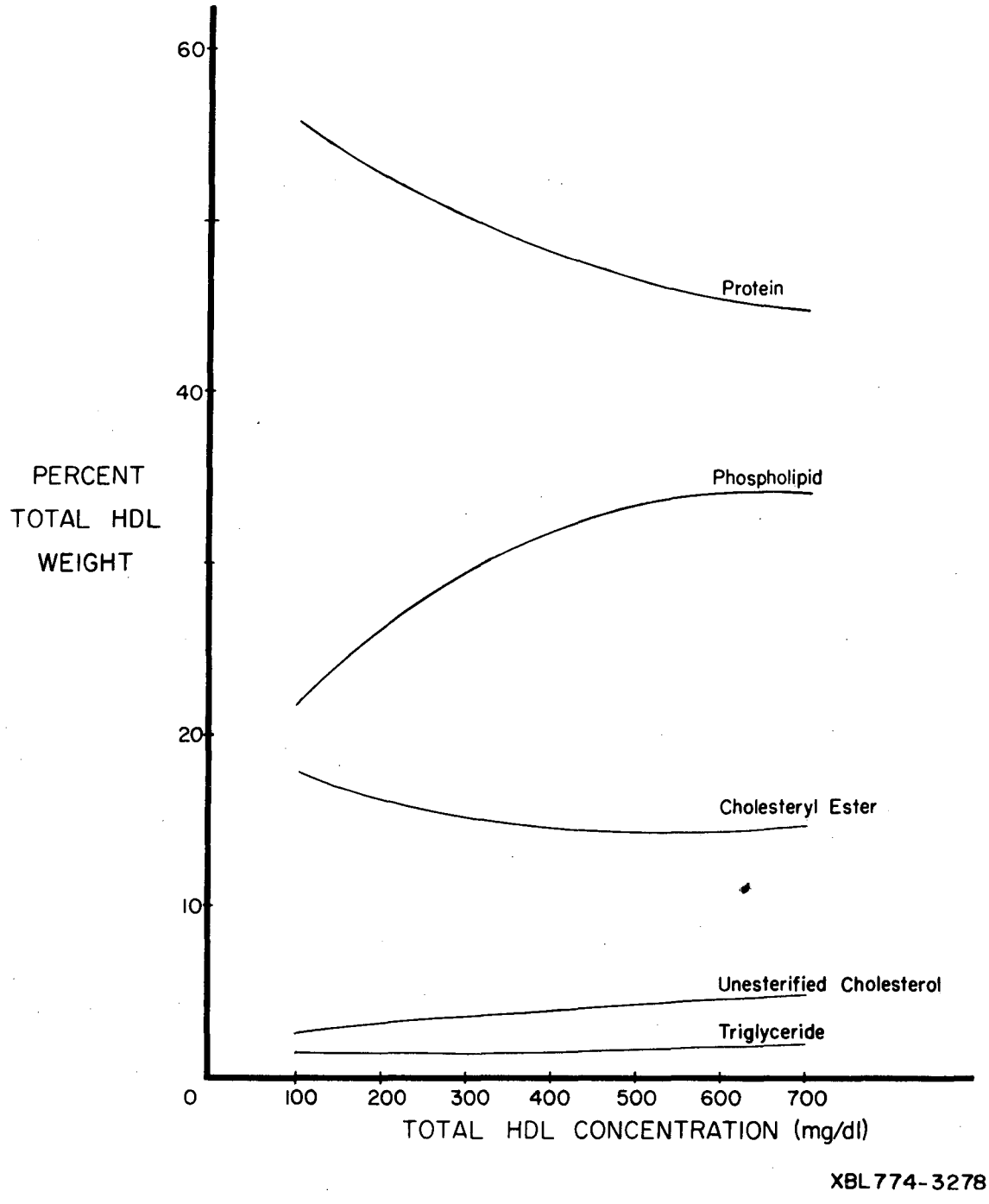

Figure 16. Estimated variation of protein and lipid composition of total HDL with increasing total HDL concentration. Values of the compositional parameters for HDL_{2b}, HDL_{2a}, and HDL_3 (Table IV) were used with the fitted polynomial coefficients from Figs. 15d, 15e, and 15f to calculate these curves.

D. Correlations between HDL component concentrations and serum concentrations of the LDL and VLDL components S_f^o 0-12, 12-20, 0-20, 20-100, 100-400, 20-400, 12-400, and 0-400.

Multiple correlation coefficients for third degree polynomial regressions of HDL component serum levels on LDL and VLDL component serum levels for the 160 cases of the Modesto Study are given in Table V. The LDL (S_f^o 0-12, 12-20, and 0-20), VLDL (S_f^o 20-100, 100-400, and 20-400), and LDL + VLDL (S_f^o 12-400 and 0-400) serum levels were determined elsewhere by analytic ultracentrifugation (48) and made available for this study by Dr. F. T. Lindgren. The magnitude of the correlation coefficients and their corresponding confidence limits indicate that both HDL_{2b} and HDL_{2a} levels display a significant negative correlation with virtually every component of the total low density lipoprotein spectrum. Moreover, in the case of each LDL and VLDL component, the correlation coefficient for the regression of HDL_{2a} levels on LDL and VLDL component levels is consistently greater than that for the regression of HDL_{2b} levels. As described in the INTRODUCTION, section II.B.2., significant negative correlations between serum levels of the HDL_2 density class (d 1.063-1.125 g/ml)and levels of the above LDL and VLDL components have been previously shown (2,15). The magnitude of the correlation coefficients reported in these earlier studies is consistently smaller than that of either the HDL_{2b} or HDL_{2a} regressions on each of the LDL or VLDL levels, however.

Regression of HDL_3 serum levels on LDL and VLDL component serum levels results in positive correlation coefficients of equal magnitude and statistical significance as those described above for the negative correlations of HDL_{2a} levels on LDL and VLDL component levels.

Table V.

Multiple Correlation Coefficients between HDL Component and LDL & VLDL Component Serum Levels

LDL & VLDL versus HDL component levels			Multiple correlation coefficients from the regression of HDL component serum levels on LDL and VLDL component serum levels					
			Serum concentration of HDL_{2b}	Percent[a] HDL_{2b}	Serum concentration of HDL_{2a}	Percent HDL_{2a}	Serum concentration of HDL_3	Percent HDL_3
Serum concentration of LDL components	S_f°	0 - 12	(0.240[b])[c]	(0.260[b])	(0.351)	(0.398)	0.334	0.370
	S_f°	12 - 20	(0.282)	(0.313)	(0.291)	(0.356)	0.382	0.378
	S_f°	0 - 20	(0.238[b])	(0.278)	(0.351)	(0.418)	0.375	0.393
Serum concentration of VLDL components	S_f°	20 - 100	(0.314)	(0.377)	(0.389)	(0.478)	0.314	0.492
	S_f°	100 - 400	(0.209[b])	(0.290)	(0.270)	(0.396)	0.382	0.396
	S_f°	20 - 400	(0.289)	(0.359)	(0.357)	(0.449)	0.338	0.396
Serum concentrations of LDL + VLDL components	S_f°	12 - 400	(0.285)	(0.362)	(0.353)	(0.479)	0.384	0.478
	S_f°	0 - 400	(0.294)	(0.361)	(0.424)	(0.520)	0.418	0.510

[a] Percent of total HDL mass in the given HDL component.

[b] Designates those regressions with $p < 0.05$. For all other regressions, $p < 0.01$.

[c] Those regression coefficients shown in parenthesis represent inverse correlations between HDL component levels and the LDL & VLDL levels.

XBL 774-8437

Such positive correlations have not yet been reported in the literature and are particularly noteworthy in view of the narrow distribution of HDL_3 serum levels described in the RESULTS section III.B.2. (the range of Modesto Study HDL_3 levels is approximately one half that of the HDL_{2b} and HDL_{2a} levels).

In each case, regression of percent HDL_{2b}, HDL_{2a}, and HDL_3 on the particular LDL or VLDL component levels consistently results in a larger multiple correlation coefficient than when the serum concentration of the HDL component is employed. This effect may arise due to a reduction in the magnitude of variation of the HDL_{2b}, HDL_{2a}, and HDL_3 levels when they are expressed as percent of total HDL mass instead of as absolute concentration (mg/dl). On the other hand, since regressions employing HDL component levels expressed as percent of total HDL mass result in increased correlation coefficient values regardless of the HDL component in question, this effect may actually hold some metabolic significance.

E. Modesto study cases designated as hyperalphalipoproteinemic

1. Criteria for designation of hyperalphalipoproteinemia

Familial hyperalphalipoproteinemia (FH alpha), characterized by elevated levels of HDL cholesterol (HDL-C or, according to Glueck et al (65), "alpha-C") and decreased LDL cholesterol levels, has recently been described (65,66) as a disorder transmitted as an autosomal dominant trait. To establish hyperalphalipoproteinemia, Glueck et al. used a cut-point of "alpha-C" levels equal to or greater than the 90th percentile value (70 mg/dl) for 168 free-living controls (mean $\pm$ 1 S.D. "alpha-C"

value was 55 ± 12 mg/dl). By comparison, the Modesto Study mean ± 1 S.D. and 90th percentile HDL-C values are 53 ± 22 mg/dl and 84 mg/dl, respectively. HDL-C values were determined as outlined in MATERIALS AND METHODS section IV. C. Although the mean values from the two studies compare favorably, the standard deviation is much larger for the Modesto Study. This discrepancy may reflect errors in the calibration curve used for conversion of Modesto Study total HDL concentrations to HDL-C levels or possible differences in the cross section of individuals sampled in the two studies. Since hyperalphalipoproteinemia (hyperalpha) was originally established (65) using a cut-point of "alpha-C" levels equal to or greater than 70 mg/dl, for the purpose of this comparison, Modesto Study cases will be designated as hyperalpha on this basis. A value of "alpha-C" of 70 mg/dl corresponds to the 78th percentile of HDL-C levels for the Modesto Study population and therefore 34 cases could be designated as hyperalpha.

2. Characteristics of HDL component distributions for those Modesto Study cases designated as hyperalphalipoproteinemics

The 34 Modesto Study cases of hyperalpha (30 females and 4 males) were divided into two groups on the basis of hormone administration at the time of blood sample collection. Since the administration of various gonadal hormones is known to affect HDL serum levels, such cases will not be represented here. The group of cases with history of gonadal hormone administration at the time of blood sample collection totalled 18 females. The remaining group of hyperalpha cases (12 females and 4 males) could be

divided equally into two subgroups: subgroup-a with total HDL serum concentration between 400 and 475 mg/dl (6 females and 2 males) and subgroup-b with total HDL serum concentrations greater than 475 mg/dl (6 females and 2 males). The cut-point of 475 mg/dl total HDL concentration was chosen because it represents the 90th percentile of total HDL concentration and HDL-C values for the Modesto Study population. The mean total HDL schlieren patterns for the cases in subgroups a and b are shown in Figure 17. As noted for the Modesto population as a whole, in RESULTS section III.B.3., elevated total HDL concentrations are due to increased levels of HDL_{2b} and HDL_{2a} in both subgroups. Indeed, the mean HDL_3 levels of subgroups a and b (159 ± 18 and 149 ± 17, mean ± 1 S.D., respectively) are not significantly different from the mean HDL_3 level of the Modesto population (158 ± 30 mg/dl, mean ± 1 S.D.).

The greatest relative difference in HDL component levels between the mean patterns of subgroups a and b is seen in the concentration of additional components (A.C.). The higher A.C. level in the subgroup-b mean pattern (17 ± 10 (S.D.) mg/dl) than in the subgroup-a mean pattern (1 ± 2 (S.D.) mg/dl) is consistent with the observation made in RESULTS section III. B.1. that A.C. concentrations become apparent only at HDL_{2b} levels above approximately 150 mg/dl. Based on the regression of HDL_{2b} serum levels on total HDL concentration (Figure 15a), 150 mg/dl in HDL_{2b} corresponds to 480 mg/dl total HDL concentration or 86 mg/dl HDL-C. Thus, roughly half of the hyperalpha cases with no history of gonadal hormone administration at the time of blood sample collection display measurable amounts of the A.C. It would be interesting to determine whether HDL-C levels greater than 70 mg/dl or the presence of measurable A.C. concentrations or both could be shown to be transmitted as autosomal dominant traits in the Modesto population.

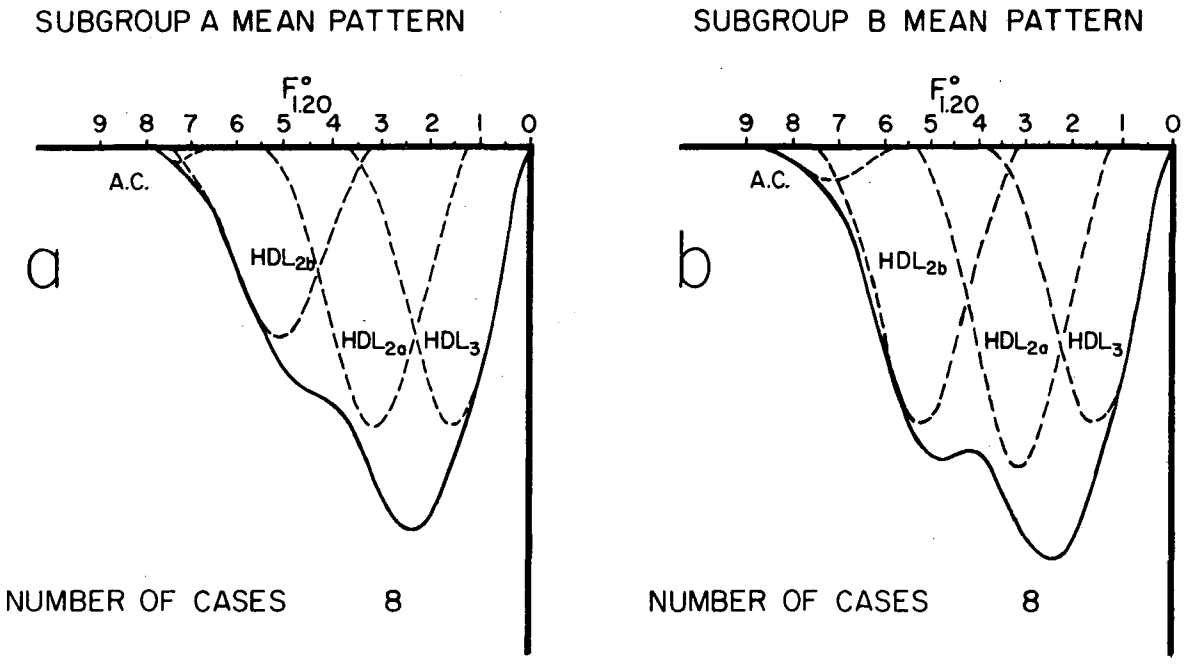

A.C.*	1 ± 2	mg/dl
HDL_{2b}	113 ± 43	"
HDL_{2a}	162 ± 24	"
HDL_3	159 ± 18	"
TOTAL HDL	434± 15	"

A.C.*	17 ± 10	mg/dl
HDL_{2b}	154 ± 37	"
HDL_{2a}	188 ± 23	"
HDL_3	149 ± 17	"
TOTAL HDL	508± 41	"

*ADDITIONAL COMPONENTS (HDL)

XBL774-3323

Figure 17a. Mean total HDL schlieren patterns for Modesto Study cases with total HDL concentrations between 400 and 475 mg/dl.
17b. Mean total HDL schlieren patterns for Modesto Study cases with total HDL concentrations above 475 mg/dl.

DISCUSSION

I. Interrelationships of the Three Major Components in the HDL Particle Distribution

A. Molecular and compositional parameters

The average distributions of percent total HDL mass versus particle hydrated density for four normolipemic males and four normolipemic females were found to display three maxima. By gradient gel electrophoresis, HDL subfractions corresponding to each maximum fell within three distinct particle size ranges. Based on the above, an inverse relationship between particle diameter and banding position density was obtained. This relationship was also observed to hold when particle diameters were determined using electron microscopy and analytic ultracentrifugation. Comparison of the average Stokes' diameter from gradient gel electrophoresis with the diameter (center-to-center distance) from electron microscopy was good, indicating that the particles in each size range are probably spherical.

When HDL subfractions from different normal subjects, both male and female, were analyzed, the compositional parameters of weight percent of protein, phospholipid, unesterified cholesterol, cholesteryl ester, and triglyceride were defined by the subfraction's size range. Such information, relating composition and size range of subfractions from both sexes, is critical when investigating individual differences in serum concentrations of HDL subfractions and their metabolic determinants. Additional studies on HDL from individuals exhibiting a wider spectrum of

levels of HDL in size ranges I, II, and III than in this thesis are required for definitive delineation of the correlation between compositional parameters and particle size.

Significant differences were noted between male and female HDL in the percent total HDL mass in the groups of subfractions 1-3 (size range I material) and subfractions 11-12 (size range III material). The percentage of total mass values for the HDL of the group of subfractions 1-3 is increased in females whereas that for the HDL of the group of subfractions 11-12 is increased in males. The shapes of the total HDL schlieren patterns and the values of the major peak $F^{o}_{1.20}$ rates reflect these male-female differences. Thus, lower peak $F^{o}_{1.20}$ rates are observed in male HDL in association with a greater percentage of total HDL mass in the group of subfractions 11-12.

B. Relationship of HDL from size ranges I, II, and III to both density-defined HDL_2 and HDL_3 and the $F^{o}_{1.20}$ 3.5-9.0 and $F^{o}_{1.20}$ 0-3.5 components

Based on the results presented, preparative ultracentrifugation of HDL for 48 hr at 178,125 x g in a background salt solution density of 1.100 g/ml, which is approximately the density used by Kostner and Alaupovic (23), would yield a top fraction containing HDL material primarily of size range I and an infranatant containing size range II and III material (Figure 12b). In contrast, separation in a solution background density of 1.125 g/ml (21) under the same conditions of ultracentrifugation would yield a top fraction containing both size range I and II material plus some size range III material and an infranatant containing only size range III material.

The relationship of the flotation rate ranges of HDL within each of the three particle size ranges (I, II, and III) to those ranges roughly corresponding (22) to HDL_2 and HDL_3 is of interest (see Figs. 10 and 12a). Material floating in the range $F^o_{1.20}$ 3.5-9.0 includes all of the HDL in size range I and some of the HDL in size range II. Material floating in the $F^o_{1.20}$ 0-3.5 range includes all of the HDL in size range III and some of the HDL in size range II. Thus, HDL_2 and HDL_3 concentrations as currently estimated by analytic ultracentrifugation (22) would reflect primarily material of size range I in the former and material of size range III in the latter, with a contribution to both from material of size range II.

C. Significance of Correlations established among HDL component serum concentrations

In this thesis a scheme for three component (HDL_{2b}, HDL_{2a}, and HDL_3) analysis of analytic ultracentrifugal schlieren patterns of total serum HDL is described. The procedure employs reference schlieren patterns which were obtained by averaging HDL_{2b}, HDL_{2a}, and HDL_3 component patterns from four normolipemic males and four normolipemic females. In the three component analysis scheme the reference patterns are sequentially fitted to the total HDL pattern yielding the serum levels for each component. When this procedure was applied to the analysis of total HDL schlieren patterns from all 160 normal subjects of the Modesto Study, the mean error in fitting all three components was estimated at 9.5% of the total HDL serum concentration. The low value of this error indicates that among normolipemic subjects, the HDL particle distribution can be

determined by the relative levels of at least three components. In cases with HDL_{2b} serum levels greater than 150 mg/dl, a significant amount of schlieren pattern area between $F^{o}_{1.20}$ rates 5.0 and 9.0 is not fitted by the reference HDL_{2b} component, indicating the presence of an additional component or components with greater size and lower weight percent protein than HDL_{2b}.

Evaluation of HDL_{2b}, HDL_{2a}, and HDL_3 serum levels as a function of age for both males and females failed to establish any statisically significant trends, although a tendency of mean total HDL and HDL_3 levels to increase with age was observed (Table III). The most pronounced differences among serum levels of the three components occur between male and female values for all four age decades. HDL_{2b} and HDL_{2a} levels are significantly elevated in females whereas HDL_3 levels are slightly lower than those of males in the same age decade (Table III). Taken together, these results indicate two trends among the serum levels of the three HDL components in the Modesto population sample: 1) The HDL_3 serum levels show little variation with age and only slight variation with sex, with an average increase of 10 mg/dl in the male mean value over the female mean value for each age decade. HDL_3 serum levels show no correlation with HDL_{2a} levels and only a small negative correlation with HDL_{2b} serum levels. 2) The HDL_{2b} and HDL_{2a} serum levels exhibit a wide range of values (0-250 mg/dl). Elevations in mean serum levels of the HDL_{2b} and HDL_{2a} components in female samples account for the differences in mean total HDL levels between females and males.

The results of the three component analysis of total HDL (Figs. 15d, 15e, and 15f) indicate that in cases where the total HDL concentration ranges between 100 mg/dl and 600 mg/dl, the distribution of the total HDL concentration among the three HDL components can be correlated with the total HDL concentration. In cases with total HDL concentrations close to 100 ± 5 mg/dl, over 90% of the total HDL concentration is represented by HDL_3. At higher total HDL concentrations (100 ± 5 mg/dl to 200 mg/dl) the increase in concentration is observed primarily as a build-up in HDL_{2a} level with little change in HDL_3 and no demonstrable HDL_{2b}. At still higher total HDL levels (200 ± 8 mg/dl to 475 ± 20 mg/dl*), the increase in concentration is reflected in further build-up of HDL_{2a}, accompanied with the appearance and build-up of HDL_{2b}, and no change in the mean HDL_3 level. Finally at total HDL concentration of 475 ± 20 mg/dl and above, the increase in concentration includes not only a further build-up of HDL_{2b} and HDL_{2a} levels but also the appearance of additional faster-floating components (Figs. 7a and 7b); HDL_3 levels remain relatively unchanged. The regression curves of percent HDL_{2b}, HDL_{2a}, and HDL_3 (Figs. 15d, 15e, and 15f) can further be used with the lipid and protein compositions of the three HDL components (Table IV) to predict, for the high density lipoproteins as a whole, a progressive increase in mean particle size, weight percent phospholipid, and weight percent unesterified cholesterol with increasing total HDL serum concentration (8). In the same manner, a decrease in the mean particle hydrated density, weight percent

---

*475 ± 20 mg/dl corresponds to the total HDL serum concentration in Fig. 15d at which HDL_{2b} serum levels reach 150 mg/dl.

protein, and weight percent cholesteryl ester is predicted with increasing total serum concentration. It is interesting that the LCAT substrates phospholipid and unesterified cholesterol increase in weight percent whereas the product of LCAT activity, cholesteryl ester, decreases in weight percent with increasing total HDL levels.

Further investigation of HDL_{2b}, HDL_{2a}, and HDL_3 component levels and compositions with increasing total HDL serum concentration in other normal populations is required to determine whether the present observation can be generalized to other populations. Moreover, it will be important to establish if the above distribution of total HDL concentration among the three HDL components is observed when total HDL concentrations are altered in individuals by metabolic and/or environmental factors. Will the interrelationships established in Figs. 15d, 15e, and 15f for the 160 Modesto cases hold in correlating HDL component levels with total HDL concentration for a given normal individual as his total HDL serum level is progressively altered? Do currently known factors which alter total HDL serum levels (environmental and metabolic) affect component levels in a manner consistent with the Modesto population interrelationships? Thus, estrogen administration to human subjects leads to an increase in total HDL concentration and androgen administration results in a considerable decrease in the total HDL concentration (67). Data are not currently available to determine whether these changes in total HDL serum concentration with gonadal hormone administration translate themselves into changes in levels of the HDL_{2b}, HDL_{2a}, and HDL_3 components according to the interrelationships seen in Figs. 15d, 15e, and 15f. If confirmed, such an influence of gonadal hormones on HDL component levels may be one factor influencing their variation in a normal population.

D. Significance of correlations established among HDL component levels and those of VLDL and LDL

The correlations established among HDL component levels and those of VLDL and LDL are in accord with previous studies on the Livermore population (see INTRODUCTION, section II.B.2.). The strong inverse correlations among HDL_{2b} and HDL_{2a} levels and the total low density lipoprotein (VLDL + LDL) levels mirror the direct correlation between HDL_{2b} and HDL_{2a} discussed in the previous section (DISCUSSION section I.C.). The metabolic significance of this inverse correlation between HDL_2 (HDL_{2b} + HDL_{2a}) and VLDL + LDL levels was suggested by Nichols (2) to arise from "possible intrusion of VLDL production on the available HDL pool of protein." Eisenberg demonstrated (7) a net transfer of the C apoproteins between VLDL and HDL during triglyceride clearance in plasma. Havel et al. (8) observed that HDL_2 displays a sizeable increase in phospholipid, triglyceride, and protein content during alimentary lipemia. This work indicates that not only protein but also phospholipid and triglyceride are transferred to HDL (mostly to HDL_2) as a result of VLDL lipolysis. Thus, low levels of HDL_2 may accompany elevated levels of VLDL and LDL when clearance of the latter is defective and transfer of VLDL surface components (protein and phospholipid) to HDL is reduced. Conversely, low levels of VLDL and LDL may reflect effective clearance of these particles leading to a build up in HDL of protein and phospholipid and HDL_2 particle formation. Inasmuch as the serum levels of the VLDL and LDL represent steady state values, changes in synthesis rates must also be considered to potentially give rise to VLDL and LDL level changes.

The direct correlation of HDL_3 levels with VLDL and LDL levels is striking. Such a correlation was not found in the Livermore studies possibly because the existing techniques for resolution of HDL into HDL_2 and HDL_3 did not suitably resolve HDL_{2a} from HDL_3. Put in the context of the possible metabolic relationship of HDL and VLDL + LDL levels mentioned above, the direct relationship of HDL_3 levels to VLDL and LDL levels may provide insight into metabolic interrelationships between HDL_3 and the two HDL_2 components, HDL_{2b} and HDL_{2a}. Thus, higher levels of HDL_3 accompany higher levels of VLDL and LDL. However, as discussed above (DISCUSSION section I. C.), HDL_3 levels do not correlate with HDL_{2a} levels. HDL_3 levels do show a small negative correlation with HDL_{2b} levels and therefore may be involved in increases in the HDL_{2b} component as VLDL levels decrease. The possibility of a precursor-product interrelationship among HDL component levels will be discussed in the following section.

II. Proposed Metabolic Interrelationships among the Three HDL Components

In order to infer interrelationships among the HDL components HDL_{2b}, HDL_{2a}, and HDL_3 in normal lipid metabolism it is critical to ascertain whether or not the trends established in Figs. 15d, 15e, and 15f for the 160 Modesto cases would hold in correlating HDL component levels with total HDL concentration for a given normal individual as his or her total HDL serum level is progressively altered. Although data on the variation of HDL_{2b}, HDL_{2a}, and HDL_3 levels in a given individual are not yet available, work done at the National Heart, Lung, and Blood Institute on individual subjects by Blum et al. (68,69) does bear upon this question. It was found that as total HDL concentration rose (22%) with

nicotinic acid feeding, the concentration ratio of HDL_2:HDL_3, estimated from the $F^{o}_{1.20}$ 3.5-9.0 and $F^{o}_{1.20}$ 0-3.5 components, rose by 335%. Conversely, with carbohydrate feeding, as total HDL levels fell (33%), so did the HDL_2:HDL_3 ratio (78%). These results provide an indication that the interrelationships represented by Figs. 15d, 15e, and 15f may be more than general trends for a normal population sample. They may pertain to interconversions between HDL components which occur due to the specific role of the HDL in lipid transport.

In Figure 18 the polynomial regression curves from Figs. 15a, 15b, and 15c are plotted in terms of the molar concentrations of HDL_{2b}, HDL_{2a}, and HDL_3 versus total HDL concentration. It is important to note that at all but the highest total HDL concentrations (greater than 600 mg/dl), the number of HDL_3 particles in the serum is predicted to be higher than that of either HDL_{2b} or HDL_{2a}. Furthermore, the number of HDL_3 particles remains fairly constant from about 200 mg/dl to greater than 600 mg/dl total HDL concentration. It is proposed that this constant HDL_3 level (approximately 9×10^{-6} moles/l or 158 mg/dl) represents a pool of relatively protein-rich lipoproteins from which the HDL_{2b} and HDL_{2a} components arise as a result of VLDL surface transfer into the HDL and the action of LCAT. Furthermore, it would be the HDL_3 component which would have the greatest avidity for cellular phospholipid and cholesterol due to its high percent protein and low percent phospholipid (see Table IV).

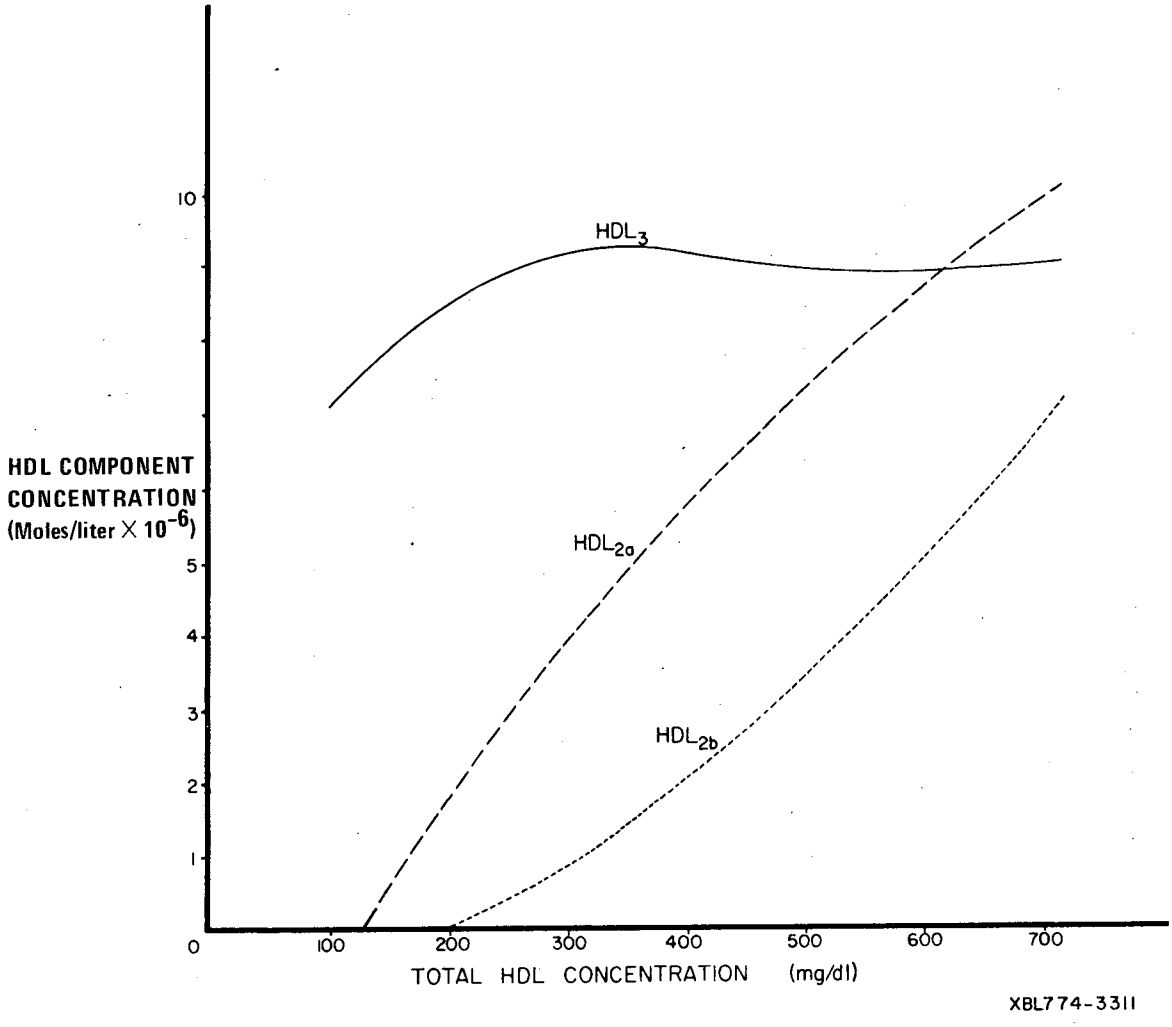

Figure 18. Polynomial regression curves from Figs. 15a (HDL_{2b}), 15b (HDL_{2a}), and 15c (HDL_3) plotted in terms of the molar concentrations of the HDL components versus total HDL concentration.

Scanu and Granda (50) proposed in 1966 that an "HDL cycle" exists in vivo. According to this cycle, HDL_2 would represent an HDL particle secreted by the liver. It would then proceed to lose lipids to tissues, to serum lipoproteins of lower density, and to red blood cells while losing protein to VHDL (HDL particles smaller than HDL_3 with hydrated densities of 1.210-1.25 g/ml). The resultant HDL particle would be HDL_3. The VHDL would then undergo relipidation in the liver to re-emerge as HDL_2.

The progressive build up of HDL_{2a} and HDL_{2b} levels with increasing total HDL concentration noted above in Figure 18 occurs in a direction seemingly opposite to that predicted from the proposed "HDL cycle." In contrast to this cycle, it is proposed in this thesis that the HDL_3 particle arises in the vascular compartment independently of HDL_{2a} and HDL_{2b} by an as yet unknown pathway, possibly from discoidal HDL secreted by the liver (37). Upon interaction with serum lipoproteins of lower density and tissue of the reticuloendothelial system of the body, the HDL_3 gain lipid (phospholipid, cholesterol, and triglyceride) and some protein. The action of LCAT then transforms these lipid-loaded HDL_3 particles into lipoproteins with properties of the HDL_{2a} component. The HDL_{2a}, in turn, interact with the same sources of lipid to become transformed into particles with properties of the HDL_{2b} component. Since such interconversions would take place in accord with mass action considerations, higher levels of HDL_{2b} could be expected to result in the accumulation of additional components of even greater size (see RESULTS section III. B. 1.). The transformations encountered by HDL during lipid metabolism thus are considerably different from those of VLDL and

LDL. While VLDL lose lipid and protein to become increasingly smaller particles, HDL_3 may take up lipid and protein to become increasingly larger particles.

III. A Suggestion for Routine Clinical Characterization of the HDL Distribution

A. HDL level determination in the epidemiology of coronary heart disease

Recently several population studies have demonstrated a significant inverse relationship between serum HDL cholesterol levels and the prevalence of coronary heart disease (42,43). The results presented above indicate that the major differences in serum total HDL as well as in serum HDL cholesterol levels, within a normal population such as the Modesto sample, arise predominantly from differences in serum levels of the HDL_{2a} and HDL_{2b} components (see Figure 19). Hence, it is most likely that the above two HDL subclasses are the major contributors to the inverse correlation of HDL cholesterol with the prevalence of CHD. Since low total HDL levels are associated with the presence primarily of the HDL_3 component, it would appear that, at the concentrations naturally encountered, this component's contribution to any "protective" effect with respect to atherosclerosis is minimal.

B. Total HDL cholesterol corrected for HDL_3 cholesterol: a suggested assay method

In light of the relatively constant levels of HDL_3 in the normal population sample discussed above, it may be possible to subtract out their contribution to the total HDL cholesterol value normally used to monitor HDL levels in large-scale epidemiological studies. The resulting cholesterol value would provide greater relative variability and may lead to statistically stronger correlations. If the mean HDL_3 level for

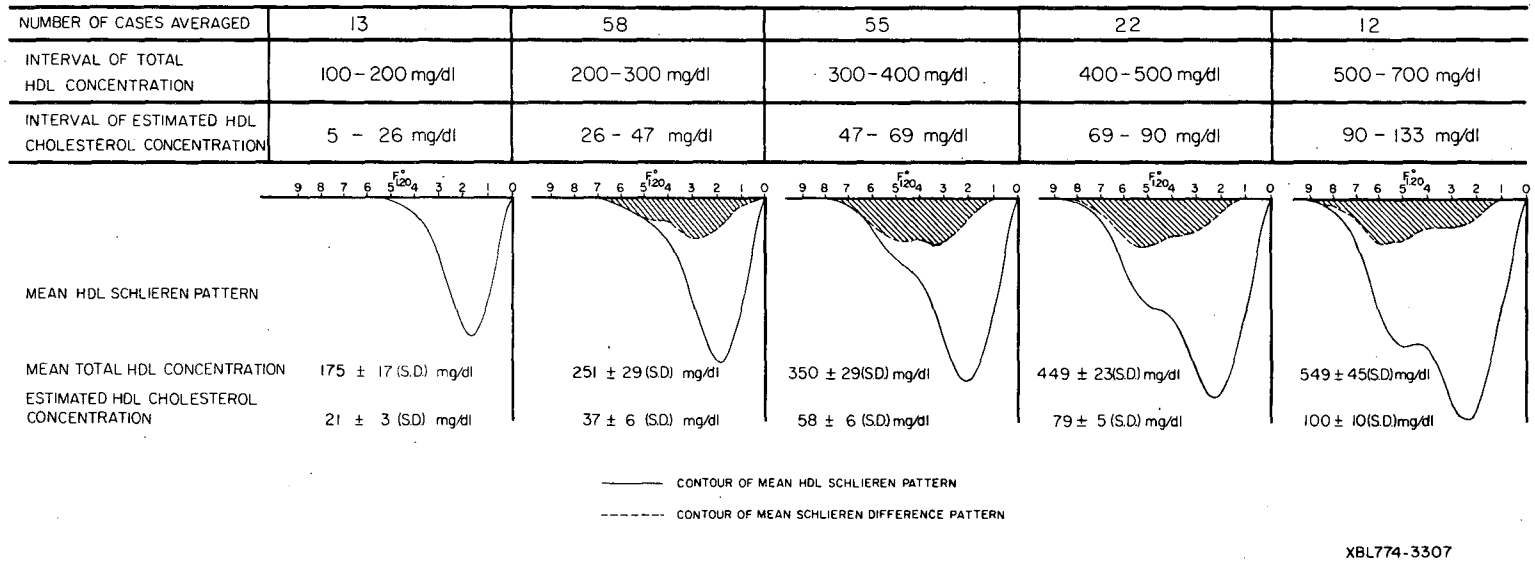

Figure 19. Mean schlieren patterns and associated average HDL cholesterol levels for the five centiles of total HDL concentrations found in the Modesto Study. The shaded area represents the schlieren difference pattern between a given mean pattern and the mean pattern of the next lowest centile of total HDL concentration. For example, the shaded area of the mean schlieren pattern of the 300-400 mg/dl centile represents the schlieren difference pattern obtained by subtracting the 200-300 mg/dl centile pattern from the 300-400 mg/dl centile pattern.

the Modesto Study population is expressed in terms of its cholesterol equivalent (58), a value of 17 ± 3 mg/dl is obtained. To establish whether 17 ± 3 mg/dl HDL_3 cholesterol would be an accurate value for adjusting total HDL cholesterol levels to represent HDL_2 cholesterol levels will require further investigation. Ideally, HDL_3 samples from a normal population study should be isolated via density gradient ultracentrifugation and the HDL_3 cholesterol measured directly.

SUMMARY AND CONCLUSIONS

Density gradient ultracentrifugation of human serum high density lipoproteins from both normolipemic males and females results in a distribution of HDL concentration versus subfraction hydrated density which has three maxima. Gradient gel electrophoresis of total HDL is characterized by three banding maxima, the positions of which suggest the presence of three particle size ranges: I. 10.8-12.0 nm, II. 9.7-10.7 nm, and III. 8.5-9.6 nm. Gradient gel electrophoresis of density gradient subfractions established an inverse relationship between particle size and particle hydrated density which was corroborated by electron microscopy and analytic ultracentrifugation. Comparison of male HDL from size ranges I, II, and III with female HDL from the same size ranges showed only small differences in the mean values of the peak $F^{o}_{1.20}$ rate, size, molecular weight, protein weight percent, and weight percents of phospholipid, unesterified cholesterol, cholesteryl ester and triglyceride. Major differences between males and females were seen in the relative amounts of HDL in density gradient subfractions 1-3 (size range I material) and 11-12 (size range III material); the percent total HDL in the group of subfractions 1-3 was greatly increased in female HDL while that of the group of subfractions 11-12 was increased in the male HDL. These studies indicate the presence of at least three major components in HDL instead of two (HDL_2 and HDL_3) and that peak $F^{o}_{1.20}$ rate differences in HDL schlieren patterns between males and females are a function of the relative levels of these three components.

Since the particle hydrated density ranges for HDL from size range I (d 1.063-1.100 g/ml) and from size range II (d 1.100-1.125 g/ml) comprise the HDL_2 particle density range (d 1.063-1.125 g/ml), these two components are designated in this thesis as HDL components HDL_{2b} (HDL from size range I) and HDL_{2a} (HDL from size range II). The particle hydrated density range of HDL from size range III (d 1.125-1.200 g/ml) is identical to that of HDL_3.

By determining reference schlieren patterns for each of the three HDL components it was possible to computer-fit each reference pattern to the total HDL schlieren patterns of 160 clinically-screened subjects from a normal population sample. In this manner, the serum concentrations of HDL_{2b}, HDL_{2a}, and HDL_3 could be determined for each case. The mean error of fitting all three reference patterns was low ($9 \pm 8\%$ (S.D.) of total area). Mean serum levels of HDL_{2b} and HDL_{2a} were significantly higher in females than in males for each of the four age decades surveyed (27-36, 37-46, 47-56, and 57-66 years). Mean HDL_3 serum levels were slightly higher in males than in females for the population as a whole. Regression of HDL_{2b}, HDL_{2a}, and HDL_3 levels on each other and on total HDL serum concentration revealed two sex-independent trends: (1) HDL_3 levels are negatively correlated ($r = -0.315$) with HDL_{2b} levels, uncorrelated with HDL_{2a} levels, and are relatively constant (mean level 158 ± 30 mg/dl (S.D.)); (2) HDL_{2b} and HDL_{2a} levels are highly correlated ($r = 0.725$) and display a progressive build up with increasing total HDL levels.

Regression of both HDL_{2b} and HDL_{2a} on VLDL and LDL levels showed significant inverse correlations which agreed with other studies. The regression of HDL_3 levels on VLDL and LDL levels revealed a significant direct correlation, however. This is the first direct correlation observed between HDL and VLDL or LDL levels. Interrelationships between levels of the three HDL components as noted above and the correlations of HDL_{2b} or HDL_{2a} and HDL_3 with VLDL or LDL levels provide insight into possible metabolic interrelationships among the three HDL components.

It would appear that HDL_3 serum levels are relatively constant throughout a normal population sample such as the Modesto Study. These particles may thus represent a pool of relatively protein-rich lipoproteins from which the HDL_{2a} and HDL_{2b} components may arise. Such an interconversion might also involve transfer of VLDL surface components into the HDL and the action of LCAT. With increased HDL_3 production, HDL_{2a} and HDL_{2b} components would exhibit a progressive build up leading to an increase in total HDL concentration. At high serum levels of HDL_{2b}, additional HDL components of larger size may become apparent. Thus, approximately 50% of all cases designated as hyperalphalipoproteinemic (total HDL cholesterol estimated to be equal to or greater than 70 mg/dl) displayed measureable amounts of the additional components.

The determination of total HDL cholesterol levels in large population samples has been used in recent studies to establish a significant inverse relationship between HDL cholesterol and the prevalence of coronary heart disease. The results presented in this thesis indicate that the major differences in serum total HDL as well as in serum HDL

cholesterol levels arise predominantly from differences in serum levels of the HDL_{2a} and HDL_{2b} components. Since low total HDL levels are associated with the presence primarily of the HDL_3 component, it would appear that, at the concentrations naturally encountered, this component's contribution to any "protective" effect with respect to atherosclerosis is minimal. Based on the relative constancy of HDL_3 levels in a population such as Modesto, it should be possible to subtract out the contribution of HDL_3 serum cholesterol to the total HDL cholesterol value. The resulting HDL cholesterol value could provide a greater relative discriminatory power and lead to statistically stronger correlations in large-scale epidimiological studies.

ACKNOWLEDGMENTS

I wish to express my appreciation to the research group of Dr. Alex Nichols, Elaine Gong, Pat Blanche, and Charlie Mae Fuller for sharing with me their insight into scientific research and for instructing me in methodology. I have never enjoyed the role of the student more. I also wish to gratefully acknowledge the advice and cooperation of Jerry Adamson, Suzanne Pan, Robert Wills, and Virgina Obie in the course of my work.

Dr. Trudy Forte and Bob Nordhausen have contributed greatly to my work by providing the stimulation to develop a means of better resolving the HDL particle distribution. I also wish to acknowledge the electron micrographs which they provided for this thesis.

The entire second half of this thesis was made possible by Dr. Frank Lindgren's permission to analyze data he collected in the Modesto Study. I am deeply grateful to him for this contribution and for the insights into lipoprotein separations which he has shared with me.

The role of Dr. Alex Nichols in the development of my research at Donner Laboratory is fondly acknowledged as intense, demanding and extremely fulfilling.

This work was supported in part by USPHS Training Grant 5 T01 GM00829 from the NIGMS, and by the U. S. Energy Research and Development Administration.

BIBLIOGRAPHY

1. Lindgren, F. T., and Nichols, A. V. (1960) in The Plasma Proteins (Putnam, F. W., ed), Vol. 2, pp 1-58, Academic Press, New York.

2. Nichols, A. V. (1967) in Advances in Biological and Medical Physics (Lawrence, J. H. and Gofman, J. W., eds), Vol. 11, pp 110-156, Academic Press, New York.

3. Schumaker, V. N., and Adams, G. H. (1969) in Annual Reviews of Biochemistry, Vol. 38, pp 113-136.

4. LaRosa, J. C., Levy, R. I., Windmueller, H. G., and Fredrickson, D. S. (1972) J. Lipid Res. 13, 356-363.

5. Boberg, J., Augustin, J., Baginsky, M., Tejada, P., and Brown, V. W. (1974) Circulation (Suppl. III), 21.

6. Nestel, P. J. (1964) J. Clin. Invest. 43, 943-949.

7. Eisenberg, S. (1976) in Atherosclerosis Reviews (Paoletti, R., and Gotto, A. M., Jr., eds), Vol. 1, pp 23-60, Raven Press, New York.

8. Havel, R. J., Kane, J. P., Kashyap, M. L. (1973) J. Clin. Invest. 52, 32-37.

9. Kane, J. P., Sata, T., Hamilton, R. L., and Havel, R. J. (1975) J. Clin. Invest. 56, 1622-1634.

10. Laggner, P., Muller, K., Kratky, O., Kostner, G., and Holasek, A. (1973) FEBS Letters 33, 77-81.

11. Mateu, L., Tardieu, A., Luzzati, V., Aggerbeck, L., and Scanu, A. M. (1972) J. Mol. Biol. 70, 105-116.

12. Forte, T., and Nichols, A. V. (1972) in Advances in Lipid Research (Paoletti, R. and Kritchevsky, D., eds), Vol. 10, pp 1-41, Academic Press, New York.

13. Skipski, V. P. (1972) in Blood Lipids and Lipoproteins: Quantitation, Composition, and Metabolism (Nelson, G. J., ed), pp. 471-583, Wiley-Interscience, New York.

14. Bilheimer, D. W., Eisenberg, S., and Levy, R. I. (1971) J. Clin. Invest. 50, 81a.

15. Gofman, J. W., Young, W., and Tandy, R. (1966) Circulation 34, 679-697.

16. Scanu, A. M., Lim. C. T., and Edelstein, C. (1972) J. Biol. Chem. 247, 5850-5856.

17. Fredrickson, D. S. (1973) Harvey Lect. 68, 185-237.

18. Glomset, J. A. (1968) J. Lipid Res. 9, 155-167.

19. Fielding, C. J., Shore, V. G., and Fielding, P. E. (1972) Biochem. Biophys. Res. Commun. 46, 1493-1498.

20. Soutar, A., Garner, C., Baker, H. N., Sparrow, J. T., Jackson, R. L., Gotto, A. M., Smith, L. C. (1975) Biochemistry 14, 3057-3064.

21. DeLalla, O., and Gofman, J. W. (1954) in Methods of Biochemical Analysis (Glick, D., ed), Vol. 1, pp. 459-478, Interscience, New York.

22. Lindgren, F. T., Jensen, L. C., and Hatch, F. T. (1972) in Blood Lipids and Lipoproteins: Quantitation, Composition, and Metabolism (Nelson, G. J., ed), pp. 181-274, Wiley-Interscience, New York.

23. Kostner, G., and Alaupovic, P. (1972) Biochemistry 11, 3419-3428.

24. Havel, R. J., Eder, H. A., and Bragdon, J. H. (1955) J. Clin. Invest. 34, 1345-1353.

25. Scanu, A. M., and Ritter, M. C. (1973) in Advances in Clinical Chemistry (Bodansky, O. and Latmer, A. L., eds), Vol. 16, pp. 112-152, Academic Press, New York.

26. Oncley, J. L., and Allerton, S. E. (1961) Vox. Sang. 6, 201.

27. Camejo G., Munoz, V. and Avila, E. (1971) in Protides of the Biological Fluids (Peeters, H., ed), Vol. 19, pp. 41-47, Pergamon Press, Oxford.

28. DeLalla, O. F., Elliott, H. A., and Gofman, J. W. (1954) Am. J. Physiol. 179, 333-340.

29. Barclay, M., Barclay, R. K., and Skipski, V. P. (1963) Nature (Lond.) 200, 362-363.

30. Lewis, L. A., Green, A. A., and Page, I. H. (1952) Am. J. Physiol. 171, 391-396.

31. Russ, E. M., Eder, H. A., and Barr, D. P. (1951) Am. J. Med. 11, 468-479.

32. Barr, D. P., Russ, E. M., and Eder, H. A. (1951) Am. J. Med. 11, 480-496.

33. Miller, G. J., and Miller, N. E. (1975) Lancet 1, 16-19.

34. Glomset, J. A. (1968) J. Lipid Res. 9, 155-167.

35. Carew, T. E., Koschinsky, T., Hayes, S. B., and Steinberg, D. (1976) Lancet 1, 1315-1317.

36. Hamilton, R. L. (1972) Advances in Experimental and Medical Biology, Vol. 26, pp. 7-24.

37. Hamilton, R. L., Williams, M. C., Fielding, C. J., and Havel, R. J. (1976) J. Clin. Invest. 58, 667-680.

38. Glomset, J. A. (1972) in Blood Lipids and Lipoproteins: Quantitation, Composition, and Metabolism (Nelson, G. J., ed), pp 745-787, Wiley-Interscience, New York.

39. Fredrickson, D. S., Gotto, A. M., and Levy, R. I. (1972) in The Metabolic Basis of Inherited Disease, 3rd edition (Standbury, J., Wyngarten, J. B., and Fredrickson, D. S., eds), pp 493-530, McGraw-Hill, New York.

40. Constantinides, P. (1965) Experimental Atherosclerosis, pp 49-56, Elsevier, Amsterdam.

41. Hulley, S. B. - private communication.

42. Rhoads, G. G., Gulbrandsen, C. L., and Kagan, A. (1976) New Eng. J. Med. 294, 293-301.

43. Castelli, W. P., Doyle, J. T., Gordon, T., Hames, C., Hulley, S. B., Kagan, A., McGee, D., Vicic, W. J., and Zukel, W. J. (1975) Circulation II-52, 97.

44. Berg, K., Borresen, A., and Dahlen, C. (1976) Lancet 1, 499-501.

45. Bachorik, P. S., Wood, P. D., Albers, J. J., Steiner, P., Dempsey, M., Kuba, K., Warnick, R., and Karlsson, L. (1976) Clin. Chem. 22, 1828-1834.

46. Hatch, F. T., Lindgren, F. T., Adamson, G. L., Jensen, L. C., Wong, A. W., and Levy, R. I. (1973) J. Lab. Clin. Med. 81, 946-960.

47. Lindgren, F. T. (1975) in Analysis of Lipids and Lipoproteins (Perkins, E. G., ed), pp 204-224, American Oil Chemists' Society Champaign.

48. Lindgren, F. T. (1974) in Fundamentals of Lipid Chemistry (Burton, R. M. and Guerra, F. C., eds), pp 475-510, BI-Science Publications Division, Webster Grove.

49. Levy, R. I., and Fredrickson, D. S. (1965) J. Clin. Invest. 44, 426-441.

50. Scanu, A. M., and Granda, J. L. (1966) Biochemistry 5, 446-455.

51. Fainaru, M., Glangeaud, M. C., and Eisenberg, S. (1975) Biochim. Biophys. Acta 386, 432-443.

52. Ewing, A. M., Freeman, N. K., and Lindgren, F. T. (1965) in Advances in Lipid Research (Paoletti, R. and Kritchevsky, D., eds), Vol. 3, pp 25-61, Academic Press, New York.

53. Smith, H. N. (1970) in C. R. C. Handbook of Biochemistry (Sober, H. A., ed), pp C10-C17, Chemical Rubber Co., Cleveland.

54. Cheng, P. Y., and Schachman, H. K. (1955) J. Polymer Sci. 16, 19-26.

55. Rodbard, D., Kapadia, G., and Chramback, A. (1971) Anal. Biochem. 40, 135-157.

56. Hatch, F. T., Freeman, N. K., Jensen, L. C., Stevens, G. R., and Lindgren, F. T. (1967) Lipids 2, 183-189.

57. Bartlett, G. R. (1959) J. Biol. Chem. 234, 466-472.

58. Lindgren, F. T., Silvers, A., Jutagir, R., Layshot, L., and Bradley, D. D. (1977) Lipids 12, 278-284.

59. Lindgren, F. T., Adamson, G. L., Jensen, L. C., and Wood, P. D. (1975) Lipids 10, 750-754.

60. Williams, E. J. (1959) Regression Analysis, John Wiley & Sons, New York.

61. Ito, K., and Schull, W. J. (1964) Biometrika 51, 71.

62. Fisher, W. R., Granade, M. E., and Mauldin, J. L. (1971) Biochemistry 10, 1622-1629.

63. Hazelwood, R. N. (1958) J. Am. Chem. Soc. 80, 2152-2160.

64. Mendoza, S., Lutmer, R. F., Glueck, C. J., Chen, C-Y., Steiner, P. M., Fallat, R. W., and Kashyap, M. L. (1976) Atherosclerosis 25, 131-138.

65. Glueck, C. J., Fallat, R. W., Millett, F., Gartside, P., Elston, R. C., and Go, R. C. P. (1975) Metabolism 24, 1243-1249.

66. Glueck, C. J., Fallat, R. W., Millett, F., and Steiner, P. M. (1975) Arch. Intern. Med. 135, 1025-1030.

67. Furman, R. H., Alaupovic, P., and Howard, R. P. (1967) in Progress in Biochemical Pharmacology (Kritchevsky, D., Paoletti, R., and Steinberg, D., eds), Vol. 2, pp 215-249, Karger, Basel.

68. Blum, C. B., Levy, R. I., Eisenberg, S., Hall, M., and Berman, M. (1975) Circulation 52, Supp. II, 38.

69. Blum, C. B., Levy, R. I., Hall, M., Goebel, R., and Berman, M. (1976) Circulation 54, Supp. II, 97.

This report was done with support from the Department of Energy. Any conclusions or opinions expressed in this report represent solely those of the author(s) and not necessarily those of The Regents of the University of California, the Lawrence Berkeley Laboratory or the Department of Energy.

TECHNICAL INFORMATION DEPARTMENT
LAWRENCE BERKELEY LABORATORY
UNIVERSITY OF CALIFORNIA
BERKELEY, CALIFORNIA 94720